HYDRAULIC MODELING OF LARGE DISTRICT COOLING SYSTEMS FOR MASTER PLANNING PURPOSES

A Thesis

by

CHEN XU

Submitted to the Office of Graduate Studies of
Texas A&M University
in partial fulfillment of the requirements for the degree of

MASTER OF SCIENCE

May 2006

Major Subject: Mechanical Engineering

HYDRAULIC MODELING OF LARGE DISTRICT COOLING SYSTEMS FOR MASTER PLANNING PURPOSES

A Thesis

by

CHEN XU

Submitted to the Office of Graduate Studies of
Texas A&M University
in partial fulfillment of the requirements for the degree of

MASTER OF SCIENCE

Approved by:

Chair of Committee,	David E. Claridge
Committee Members,	W. Dan Turner
	Charles Culp
Head of Department,	Dennis O'Neal

May 2006

Major Subject: Mechanical Engineering

ABSTRACT

Hydraulic Modeling of Large District Cooling Systems for Master Planning Purposes.

(May 2006)

Chen Xu, B.S., Shanghai Jiaotong University, Shanghai, China

Chair of Advisory Committee: Dr. David E. Claridge

District Cooling Systems (DCS) have been widely applied in large institutions such as universities, government facilities, commercial districts, airports, etc. The hydraulic system of a large DCS can be complicated. They often stem from an original design that has had extensive additions and deletions over time. Expanding or retrofitting such a system involves large capital investment. Consideration of future expansion is often required. Therefore, a thorough study of the whole system at the planning phase is crucial. An effective hydraulic model for the existing DCS will become a powerful analysis tool for this purpose. Engineers can use the model to explore alternative system configurations to find an optimal way of accommodating the DCS hydraulic system to the planned future unit.

This thesis presents the first complete procedure for the use of commercial simulation software to construct the hydraulic model for a large District Cooling System (DCS). A model for one of the largest DCS hydraulic systems in the United States has been developed based on this procedure and has been successfully utilized to assist its master planning study.

ACKNOWLEDGEMENTS

I would like to express my sincere gratitude to my advisor, Dr. David Claridge, for his great guidance, stimulating discussions, support and encouragement throughout this research work. I also would like to acknowledge my committee members Dr. Turner and Dr. Culp for their thorough reading of my thesis and their valuable comments.

I am especially grateful to Mr. Song Deng and Dr. Qiang Chen. Without Song's advice and help the research would not have been possible. Qiang Chen is the person with whom I worked most closely. We spent a lot of time together in the underground tunnel all over the campus collecting information, investigating, measuring, so that such a complicated model could be built. Without good team work, this project could not have been finished.

Appreciation is extended to all my friends and colleagues in the Energy system laboratory for their continuous support, invaluable discussions, and well wishes.

At last I would like to especially thank my wife, Rong Hu, who has always encouraged me and supported me under any situation.

TABLE OF CONTENTS

Page

CHAPTER Page

LIST OF FIGURES

FIGURE Page

FIGURE Page

FIGURE Page

LIST OF TABLES

TABLE Page

CHAPTER I

INTRODUCTION

1.1 Background

In the United States, District Cooling Systems (DCSs) have been widely applied in large institutions such as universities, government facilities, commercial districts, airports etc. The largest DCS in universities can have 44,000 tons of cooling capacity and the total linear pipe length (supply and return) can approach 17 miles in length (IDEA 2002).

The hydraulic systems of large DCSs can be very complicated. They often stem from an original design that has had extensive additions and deletions over time. A DCS is usually continuously expanding as the campus grows. When new buildings are to be built on campus, chilled water piping will be added to connect them with the existing DCS. The existing DCS hydraulic system may need to be modified to accommodate the new buildings. Accordingly, the total cooling capacity may need to be enlarged by installing new chillers in the existing central plant or possibly new satellite plants will need to be built or enlarged. Expanding or retrofitting such a system involves large capital investment (ASHRAE. 2000). On the other hand, once the piping infrastructure is built underground, it will stay there and serve for many years to come. Consideration of future expansion is often required. Therefore, a thorough study of the whole system at the planning phase is crucial. An effective hydraulic model for the existing DCS will become a powerful analysis tool for this purpose (Walski et al. 2001; Chen et al. 2002).

This thesis follows the style of *ASHRAE Journal*.

The DCS hydraulic system model can be used to answer important decision-making questions like: if buildings will be built at specific locations on the campus, could the current distribution system send enough chilled water to these buildings even if the cooling capacity in the plant is sufficient? If not, what are the other opportunities? If the hydraulic system needs to be retrofitted or expanded to satisfy added cooling demand, what is the best solution? If the current plant has no place to put new chillers and a new satellite plant needs to be established, where is the best location? With the DCS hydraulic system model, engineers can explore various alternatives of system configuration to find an optimal way of accommodating the DCS hydraulic system to the planned future. Also, the DCS hydraulic model can serve as an analysis tool for the Continuous Commissioning® (CC®)[1] of the DCS. Eventually, the DCS hydraulic model can be seen as an asset to the facility owner and needs to be continuously maintained and updated so that it can help people make master planning decisions to guide system operation in an efficient way.

1.2 Objective

Research work has been conducted on modeling of the DCS hydraulic system of Texas A&M University (TAMU) for its master planning purposes. A practical way of modeling such large scale DCS hydraulic systems, especially for large university campuses, will be generalized in this thesis. This thesis will address several topics, such as the basic modeling approach, a detailed procedure to construct and calibrate the model, and how to use the model to assist decision makings in master planning studies.

[1] Continuous Commissioning and CC are registered trademarks of the Texas Engineering Experiment Station (TEES), the Texas A&M University System, College Station, Texas.

CHAPTER II

LITERATURE REVIEW

Basically there are no papers that provide a complete study of DCS hydraulic modeling. However several areas of research are related to the thesis topic. The hydraulic modeling method for Domestic Water Systems (DWSs) has been well developed and may apply to the DCS hydraulic system with appropriate modifications (ASHRAE 2001). Energy modeling methods for individual commercial buildings have been widely discussed. Research on energy modeling of the DCS or District Heating System (DHS) also has been reported. Several research projects and industrial applications have studied the relationship of the building cooling load, chilled water flow, and the building differential temperature. These topics are all related to the modeling of the DCS hydraulic system and hence are addressed in the following literature review.

2.1 Introduction of Domestic Water System (DWS) Modeling Technology

The pipe network modeling technologies have been developed primarily for domestic water distribution systems (ASHRAE 2001). Walski (1984) have summarized the complete pipe network hydraulic theory by providing a series of mathematical equations. The pipe network analysis is based on three basic principles of fluid mechanics: (1) conservation of mass, (2) conservation of energy, and (3) the relation between fluid friction and energy dissipation (Larock et al. 2001). Basic principles, when applied to specific pipe network problems, generate a system of governing equations, most of which are nonlinear equations. The Hardy Cross method, linear theory method, and the Newton-Raphson method are the commonly used numerical techniques to solve

these equations (Walski. 1984). However, the Newton-Raphson method, which converges to the solution using the derivative of each of the equations to speed convergence, has proven to be superior in solving the nonlinear equations over the past quarter century, and is especially effective for large scale pipe networks. The more physically-based Darcy-Weisbach formula and the more empirically-based Hazen-Williams formula are the most commonly used equations for the modeling of pipe friction losses. Head losses at valves, tees, bends, reducers, and other appurtenances in the pipe network are typically called minor losses but can be comparable to the major loss contributor – piping. For DWS, minor losses are generally much smaller than the head losses due to pipe friction, and are thus frequently neglected except in some special cases such as pump stations or valve manifolds where there may be more fittings and higher velocities. In these instances, a minor loss coefficient will be multiplied. Pumps are usually modeled as a power function as follows (Walski et al. 2001):

$$h_p = h_0 - c Q_p^m$$

Where h_p = pump head

h_0 = cutoff (shutoff) head (pump head at zero flow)

Q_p = pump discharge flow

c, m = coefficients describing pump curve shape

The general DWS modeling procedure has been generalized by Walski et al. (2001) in Figure 1.

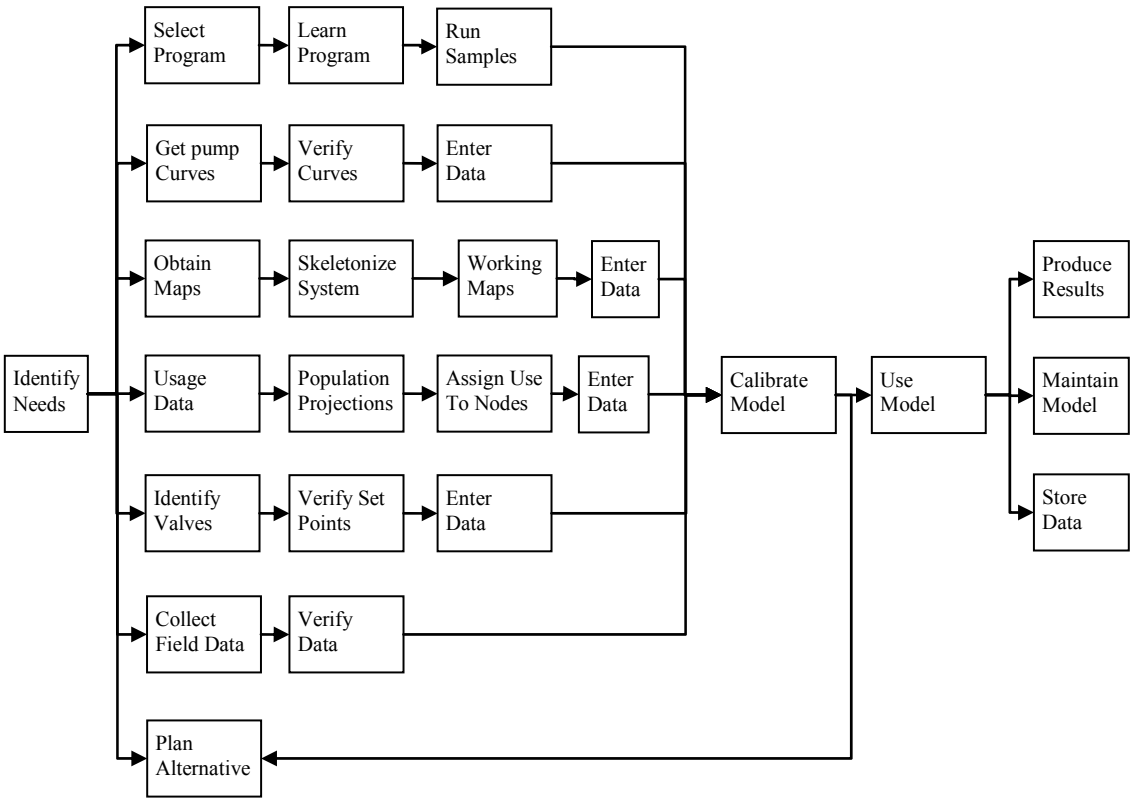

Figure 1 General DWS Modeling Process (Walski et al. 2001)

The DWS modeling process consists of two major parts, physical modeling and demand modeling. The physical model includes fixed information such as the pipe network topological structure, and information on pipes, reservoirs, tanks, junctions, control valves, and pumps. Once the physical model is built, it should represent the real or planned physical structure of the piping system. A large number of commercial software programs are available on the market for the modeling of pipe networks. Engineers can even visually build the physical model through these computer programs. First, all information such as utility maps, pump curves, valves etc. is collected. Then the

information is entered into the selected computer program. During the construction of the physical model, a certain level of skeletonization needs to be considered - that is, to what level the model can be simplified without significantly losing accuracy (Eggener and Polkowski 1976). This can significantly reduce modeling cost. Larock et al. (2001) suggested a three-level skeletonization strategy. The strategy starts from a few pipes that are considered vital to the proper operation of the system to a level of pipe structure that covers more system detail. An engineer should begin with the simplest level. Then more detailed analysis may be conducted to the most complex level as the adequacy of the model is verified. Walski et al. (2001) pointed out that the level of skeletonization used depends on the intended use of the model. For energy operation studies or regional water studies, a broader level of skeletonization will typically suffice. However, for detailed design work or water quality studies, much more of the system needs to be included to accurately model the real-world system.

The demand model includes variable parameters such as the water usage in residential buildings, which fluctuates in seasonal and diurnal cycles. Before starting the modeling procedure, various information needs to be collected such as system operational records, customer meters, and billing records or pre-existing compiled data, etc. Then a baseline demand needs to be determined by spatially allocating the total water consumption rate to individual nodes. The most common allocation method is the unit loading method, which counts the number of the fixture units that the node serves and multiplies by corresponding unit demand. Another approach to determine the baseline demand for individual costumers involves the use of metered data or billing

records. However, a system seldom has enough recorded information to directly define all aspects of customer usage; this is also true for DCS chilled water systems. Therefore, two approaches for filling the gaps between the total water production and the partially recorded customer usage have been developed, called Top-down and Bottom-up (also known as Aggregate and Disaggregate) approaches (Walski et al. 2001). The Top-down demand determination starts from the water production side, and works down to the nodal demands. With known demand for the metered individual water customers, the remainder of the demand is disaggregated among the rest of the customers. The Bottom-up demand determination is exactly the opposite. The total water consumption rate at modeled nodes or water sources is calculated by summing up individual customer's metered readings. After the baseline model is established, a demand multiplier will be assigned to each node to represent different demand conditions, such as average day demand, peak hour demand, maximum day of record time-varying demands, etc.

2.2 Building Cooling Energy Estimation and Modeling Methods

Compared to DWS, the chilled water flow demand characteristic of a DCS is much more complex as it involves multiple factors. The building cooling load is certainly a major factor that should be considered. Many building cooling energy estimation methods and tools have been developed. Basically they can be divided into three basic approaches: (1) Forward modeling, (2) Inverse modeling, and (3) Hybrid modeling that contains both forward and inverse methods.

Forward modeling utilizes the detailed physical description of the building system to predict the energy consumption based on sound engineering principles. The forward

modeling approach has widespread acceptance and use in major public domain simulation codes (e.g., BLAST and DOE-2). However, forward modeling requires input of detailed building parameters and a time-consuming simulation procedure. Performing load modeling for a large number of buildings on district-wide systems, applying the forward approach will be costly.

Inverse modeling uses empirical data to identify building energy behavior through statistical analysis. The outside air dry-bulb temperature is usually the dominant factor that affects the building cooling load (Fels 1986, Kissock et al. 1993, Katipamula et al. 1994, Reddy et al. 1997). The simplest steady state inverse model can be developed by performing a regression analysis on utility consumption data against outside air temperature. For a more sophisticated model, one or more change points can be applied to separate multiple regions with different slopes. Two, three, four (Ruch and Claridge 1991) and five parameter change point models (Fels. 1986) have been developed. An inverse bin method has also been proposed to handle more than four change points (Thamilseran and Haberl 1995). The advantage of the steady-state inverse models is that they can be easily applied to large numbers of buildings wherever the utility billing data and outside air temperature data are available. It has been widely applied to estimate the performance of existing buildings under future weather and occupancy conditions. The disadvantages of the steady-state inverse model are that it can not reflect the dynamic effects and is insensitive to non-outside air temperature parameters. Also, of course, it can not be used for buildings without any recorded data.

2.3 Energy Modeling of DHS and DCS

The modeling of DHS and DCS with an emphasis on energy study has been widely discussed. The literature review below introduces several topics of the DHS and DCS modeling that can be related to the DCS distribution system hydraulic simulation study.

Pálsson et al. (1999) introduced an equivalent modeling method that lumps the DHS buildings together with minimum loss of dynamic thermal and hydraulic effects, so that researchers can model the interaction between the thermal plant and the lumped buildings from a system point of view, e.g., plant return temperature. Since their research was focused on a system-wide study, the building heating load is simply allocated from the plant total production weighted by the building's annual heating load billing data.

Dotzauer (2002) provided a simple approach for the DHS load forecasting. Besides the dominant effect of the outside air temperature, the model also included the social component factor. The load model is defined as the summation of two dependent parts, the temperature part and the social component part. The temperature-dependent part is theoretically the same as the Single Variable Regression Analysis and is extended to nine parameters, four temperature change points and five slopes. By comparing the temperature-dependent portion of the model with the measured input data, the residual leads to the social component part. Finally, a target function is generated by defining the difference of the metered data and the sum of these two dependent parts. An optimization algorithm is applied to search for the minimum value of this target function

to determine these parameters. The predictions were comparable with those of other more sophisticated methods.

Yik et al. (2001a) conducted research on DCS building energy estimation. They separated the buildings on a commercial DCS into major categories - offices, retail shops, restaurants, and hotel guestrooms. For each category, the detailed building physical description was summarized to generate a typical building for that category. Then they conducted simulation for these typical buildings by using forward modeling programs. The modeled cooling load profiles were normalized into load intensities (kW/m^2). Finally, the load intensity data in the models were statistically generalized to be able to represent the "average" cooling load intensities of the corresponding types of buildings. This method provides a quick and easy approach to estimate building energy profiles for groups of buildings. Also, this method provides the opportunity to estimate the cooling load of DCS buildings without empirical data, for which inverse modeling can not be applied. Based on this method, Chow et al. (2004) used the genetic algorithm (GA) to find the optimum combination of load profiles for district cooling systems. The basic assumption behind their research is that substantial savings are possible when the fluctuations in thermal load can be leveled out by serving a mix of building types with appropriate differences in cooling-load patterns.

2.4 Load, Flow, and Temperature

Unlike the DWS, in which the flow rate in houses fluctuates diurnally, the DCS buildings' chilled water flow rate, entering/leaving temperature, and their cooling load

are coupled together. The behavior of the buildings' chilled water flow rate is not apparent.

ASHRAE (2000) provides a series of equations to physically describe the air cooling and dehumidification coils, which could be used to forward model the cooling load, chilled water flow, and the differential temperatures across the cooling coils. These equations, like other forward modeling techniques, require very detailed physical information for each cooling coil. Phetteplace (1995) discussed the optimal design for a DHS. In part of his work, he developed a simple model for the normal radiator by using an explicit solvable approximation to the logarithmic mean temperature method that requires numerical solutions. He compared two alternative approximations (arithmetic mean temperature and geometric mean temperature), and proved that the geometric mean temperature method is a better approximation to the logarithmic mean temperature method. Based on this model, the hot water flow through the radiators can be modeled. Phetteplace's idea is a good approach to simplify the modeling of cooling coils. However, it still requires detailed information about the specific cooling coil. Given the large number of buildings on a DCS, each of which may have multiple Air Handling Units (AHUs), obtaining the detailed cooling coil information for each building is almost impossible.

Pálsson et al. (1999) applied the logarithmic mean temperature method to model the simple plate heat exchangers and used the Newton-Raphson method to solve the nonlinear equations to obtain the main return temperature. The predicted total heat load was distributed among the connected houses in proportion to the annual heat load in

each house. All the buildings were considered to have the same supply and return temperature, which means the flow rate for each building will be proportional to its heat load.

Yik et al. (2001b) conducted a study on the energy performance of water cooled air conditioning systems in Hong Kong. The DCS model they developed during their research assumed a fixed chilled water differential temperature and it let the flow rate fluctuate proportionally to the building's cooling load.

Chen et al. (2002) conducted retrofit design for the DCS chilled water distribution system expansion of the University of Texas at San Antonio (UTSA). A baseline model was built through commercial software. Field measurement data was used to determine the chilled water flow for existing buildings and design flow was used for the proposed new building. Six scenarios of pipeline arrangement were then studied. The most economical scenario was selected as the recommended design. If the metered data is well validated and justified, using actual metered flow as the model input is a quick and easy way to determine the flow demand.

Due to energy conservation requirements, variable flow (two-way valve systems) has been widely applied to DCS chilled water systems. Constant temperature differential and flow proportional to cooling load is expected. However, many systems do not perform as anticipated and are reported as having "low ΔT disease," especially for older and larger systems that have been converted from three-way valve to two-way valve systems. The DCS chilled water ΔT becomes a critical factor for the DCS performance and operation.

It is considered as the performance index for the DCS chilled water system and building performance by the CC® engineers (Deng 2002).

Sauer (1989) conducted a study on diagnosing the low temperature differential for chilled water systems. According to his study, the chilled water ΔT should actually rise from the design temperature differential as the cooling load decreases, which is generally opposite to what occurs in large chilled water systems. He summarized seven major reasons to explain why cooling coils produce less than design ΔT at design and partial load conditions. These reasons are: (1) Controls out of calibration and/or leaving air temperature set point too low; (2) Cooling coil control valve sizing; (3) Cooling coil selection; (4) Low air flow; (5) Air bypass or leaks around cooling coils; (6) Poor water treatment; and (7) Dirty coils. Accordingly, solutions were proposed as: (1) Proper selection of cooling coils for new systems and good maintenance; (2) Recalibrate the existing systems' pneumatic controls to ensure well-controlled cooling coil leaving air temperature. Direct Digital Control (DDC) is recommended; (3) Proper cooling coil valve sizing; and (4) Provide good water treatment and air filter maintenance.

Fiorino (1999) summarized 25 "best practices" to achieve high chilled water differential temperatures based on successfully implemented industrial applications. The 25 "best practices" range from component selection criteria to distribution system configuration guidelines and are applicable to new installations as well as retrofit projects. One important point he made is that chilled water ΔTs are determined by the terminal cooling loads and not by the central plant.

2.5 Conclusions

Both the DWS and DCS hydraulic systems are pipe networks and most of their hydraulic components are the same. Hence, the hydraulic principles of the DWS and DCS are the same. Therefore the physical modeling method for the DWS (Walski et al. 2001) will be adopted with certain modifications for DCS hydraulic systems.

However, their consumption behavior is significantly different; thus the demand model method is expected to be different. For a large scale DCS, it is not practical to model the cooling load for buildings one by one using forward modeling methods. And it is difficult to model cooling loads for all the individual buildings using the inverse modeling technique as most large DCSs do not have complete metering that covers all of their buildings. The building categorization based modeling method for a large number of DCS buildings (Yik et al. 2001a, Yik et al. 2001b, and Chow et al. 2004) is an applicable way and will be adopted. Inverse modeling technique using pre-existing data can be adopted to model those metered buildings and the chilled water consumption for those un-metered buildings can be estimated from the metered buildings of the same type. In order to determine the differential temperatures for specific buildings, the studies of low differential temperature syndrome (Sauer 1989, and Fiorino 1999) in DCS buildings provide a good indication of where building HVAC systems need to be inspected. Finally, the Top-down and/or Bottom-up approaches (Walski et al. 2001) will be adopted to allocate the chilled water flow to individual buildings or a group of buildings.

CHAPTER III

UNDERSTANDING LARGE DCS HYDRAULIC SYSTEMS

3.1 Introduction

Large DCSs are usually applied in university campuses, airports, government facilities, and commercial districts, where the cooling load density is high and the annual cooling load factor is high. The largest DCS can have over 44,000 tons chilling capacity, span over one square mile of area and cover more than 100 hundred buildings. Although these systems could be initially designed and built this large from the beginning, Systems of this scale usually start from smaller ones and growing over years of expansion. Piping is added to the existing system when new buildings are built. The existing piping infrastructure may be modified to accommodate the new buildings. Satellite plants may be established to reach the remote areas of the system expansion. Their hydraulic systems may become very complicated.

Before developing the modeling methodology for DCS hydraulic systems, a thorough understanding of the DCS system from a hydraulic point of view is necessary. This chapter is intended to summarize the characteristics of large DCS hydraulic systems. First, the characteristics of a large DCS hydraulic system will be described from different aspects. Second, the typical structure of a large DCS hydraulic system will be will be introduced in detail. Third, the differences between DWSs and large DCS hydraulic systems are compared. The purpose of the comparison is for the development of the modeling method for large DCS hydraulic systems, which will be discussed in the following chapters. At the end of this chapter, the TAMU main campus (MC) DCS will

be introduced as an example. It also provides background information as the hydraulic modeling of this system will be used as case studies through out this thesis.

3.2 General Description of Large DCS Hydraulic Systems

This section is intended to describe a large DCS hydraulic system from various points of view.

1. From the consumption point of view, water systems can be either once-through or re-circulating systems. DCS hydraulic systems are re-circulating systems, in which a fixed amount of water continuously circulates within the system instead of flowing out of the system.
2. Water systems can be either open or closed systems. A closed water system is defined as having no more than one point of interface with a compressible gas or surface. The major differences in hydraulics between open systems (such as cooling tower systems) and closed systems are: (1) flow can not be driven by static head differences, (2) pumps do not provide static lift, and (3) the entire piping system is always filled with water. DCS hydraulic systems belong to closed water systems (ASHRAE, 2000).
3. From the distribution point of view, load distribution circuits generally can be divided into two types: series piping and parallel piping. Parallel piping networks are the most commonly used in large DCS hydraulic systems as they provide the same chilled water temperature to all consumers.
4. From the water flow point of view, DCS hydraulic systems can be categorized as constant flow systems or variable flow systems. Variable flow is most commonly

used for large DCS hydraulic systems, as it can reduce energy use and expand the capacity of the distribution system piping by using diversity.

5. From the pumping point of view, DCS hydraulic systems can be categorized into three major pumping configurations: (1) source distributed pumping, where source system pumping provides the total system pumping. This type of pumping configuration is only applied where the distribution system pressure drops are minimal and the distribution system is relatively short-coupled (3,000 ft or less). (2) Distributed pumping, in contrast, uses local pumps, i.e. building pumps to provide all pumping for the DCS. (3) Combination of these two types of pumping configuration. This is the most commonly applied pumping configuration for large DCS hydraulic systems.

3.3 Anatomy of a Large DCS Hydraulic System

Large DCS hydraulic systems consist of three sub-systems: the source system, the distribution system, and the load system, i.e. the in-building system. Figure 2 illustrates a typical system structure for large DCS hydraulic systems. The heat flows into the DCS from the consumer systems, then is transported via the distribution network and finally is rejected to the atmosphere at the source system.

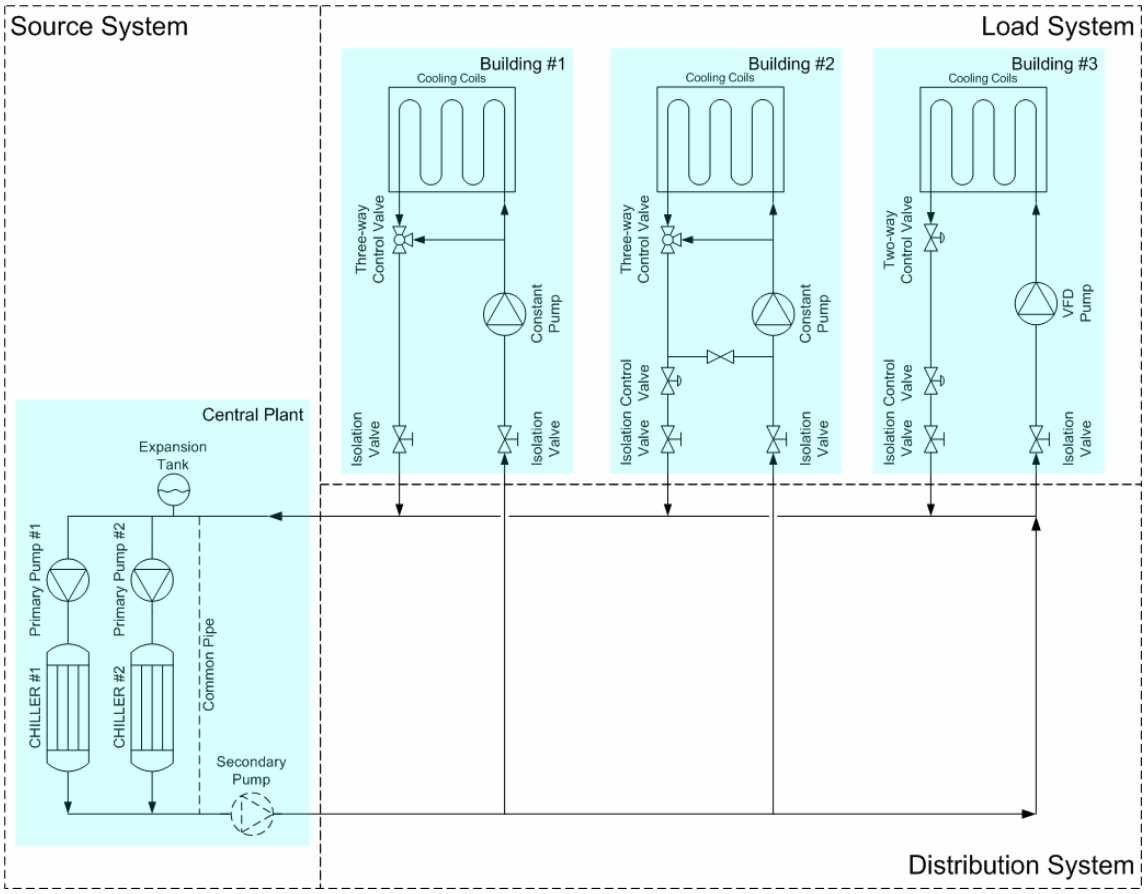

Figure 2 System Components of DCS Hydraulic System

3.3.1 Source System

In District Energy Systems (DES), the central plant may include equipment to provide heating, cooling, both heating and cooling, or combine any of these three options with electric power generation to become a co-generation system. A large DCS plant system is often part of a co-generation system. In addition to the central plant, satellite plants are sometimes used in situations where buildings are located in areas that the central plant is not able to cover (from the thermal capacity and/or hydraulic

distribution capacity point of view). The DCS plant system usually includes the following hydraulic components:

1. *Chillers*. They are used to extract heat from the chilled water returned from the buildings through a refrigeration cycle and reject it to the atmosphere through cooling towers. They may be single stage or double stage absorption chillers using steam as the energy source. They also may be vapor-compression chillers driven by electricity, turbines (steam or combustion), or internal combustion engines. Chillers in large DCS plants are usually arranged in parallel.
2. *Pumps*. Centrifugal pumps are often used to provide sufficient pressure head to the primary equipment i.e. chillers and to the secondary system. For large DCS plants, the secondary pumps are usually VFD controlled.
3. *Expansion tank and water make-up*. The expansion tank serves both thermal and hydraulic purposes. As a thermal device, the expansion tank provides a space so that the chilled water can expand or contract as it undergoes volumetric changes with changes in temperature. As a hydraulic device, the expansion tank serves as the reference pressure point in the system, analogous to a ground in an electrical system (Lockhart and Carlson 1953). An entire DCS hydraulic system can have only one expansion tank. On large chilled water systems, a makeup water pump generally is used to make up water loss. The pump is typically controlled from level switches on the expansion tank or from a desired pump suction pressure.
4. *Piping*. Piping is to connect individual components to form an integrated chilled water system. The piping in a large DCS plant is usually arranged in the form of

headers, so that chillers and pumps can transmit water through uniform places. For Figure 3 as an example, primary pumps and chillers are arranged in parallel and connected to the headers. Primary pumps supply the chilled water to the common header instead of individual chillers. Chillers receive the chilled water from the common header instead of individual pumps. This type of arrangement provides better operational flexibility. Piping for a large DCS plant can be very complicated, especially where multiple chillers and pumps are involved.

5. *Control valve*. Control valves are used to automatically maintain the flow, pressure, and temperature at their set-points.

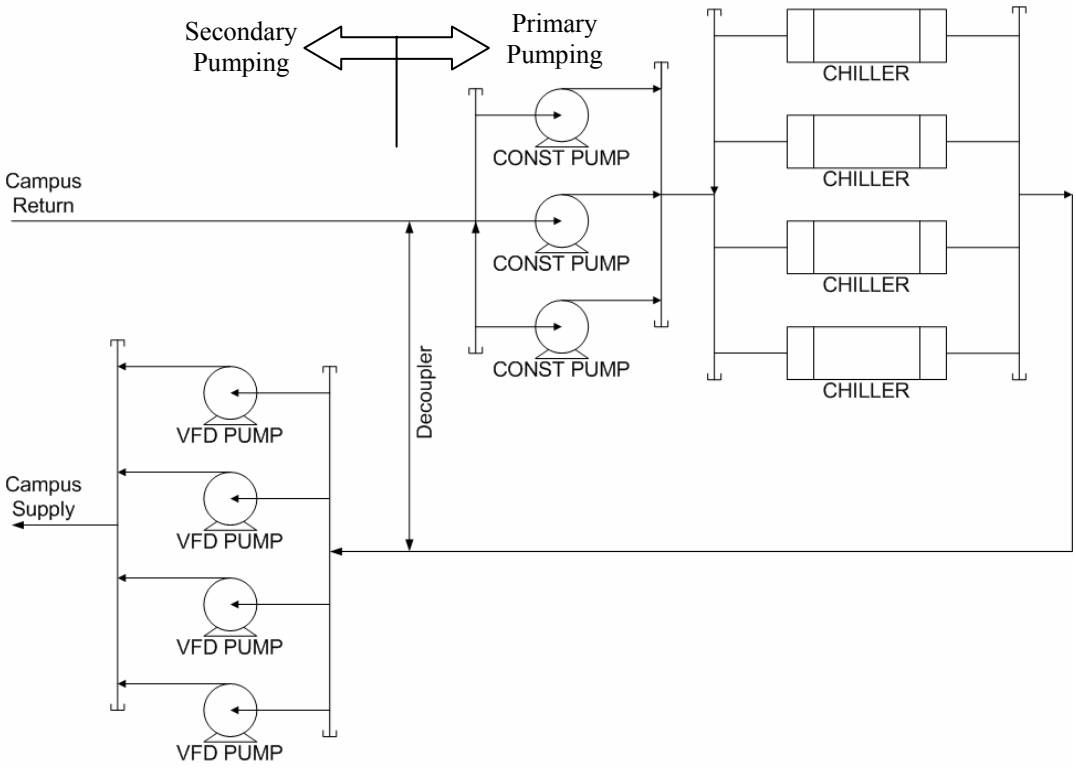

Figure 3 Schematic Layout of TAMU South Satellite Plant Chilled Water System

Large DCS hydraulic systems are usually variable flow systems, which can lower energy use and expand the capacity of the distribution network piping by using diversity. However, conventional chillers can only sustain a narrow range of chilled water flow variation. To provide variable flow while maintaining a relatively constant flow to individual chillers, DCS plants usually employ compound pumping, also known as a primary-secondary system. As shown in Figure 3, a common pipe (decoupler) isolates the primary and the secondary systems. While the chilled water flow is varying at the distribution network, individual chillers can obtain a constant flow by bypassing part of the chilled water through the common pipe. Therefore the impact of variation of the secondary system flow on the primary system is minimized. However this type of system structure has its disadvantages. Pumping energy will be wasted during partial load conditions. And chiller efficiency will decrease as well. When the cooling load decreases, if the chilled water flow through the chiller is maintained constant, and when maintaining the same chilled water temperature set-point, the chilled water return temperature will decrease and hence the overall refrigerant temperature in the evaporator will decrease. According to the Carnot Cycle, the efficiency of the chiller will decrease. As energy economics have become an increasing concern, more and more large DCS plants have turned to pure variable flow systems. Large DCS plants are often equipped with multiple chillers that can be staged on and off to meet the varying loads. Newer chillers can sustain variable chilled water flow while maintaining a reliable and consistent performance. Therefore, the DCS plant can remove or shut off the common pipe to save the pumping energy during the partial load condition.

Large DCS plant systems are usually controlled by modulating control valves or the speed of VFD pumps to maintain a set-point value of secondary system loop differential pressure. The set-point can be a reset schedule based on the ambient temperature.

3.3.2 Distribution System

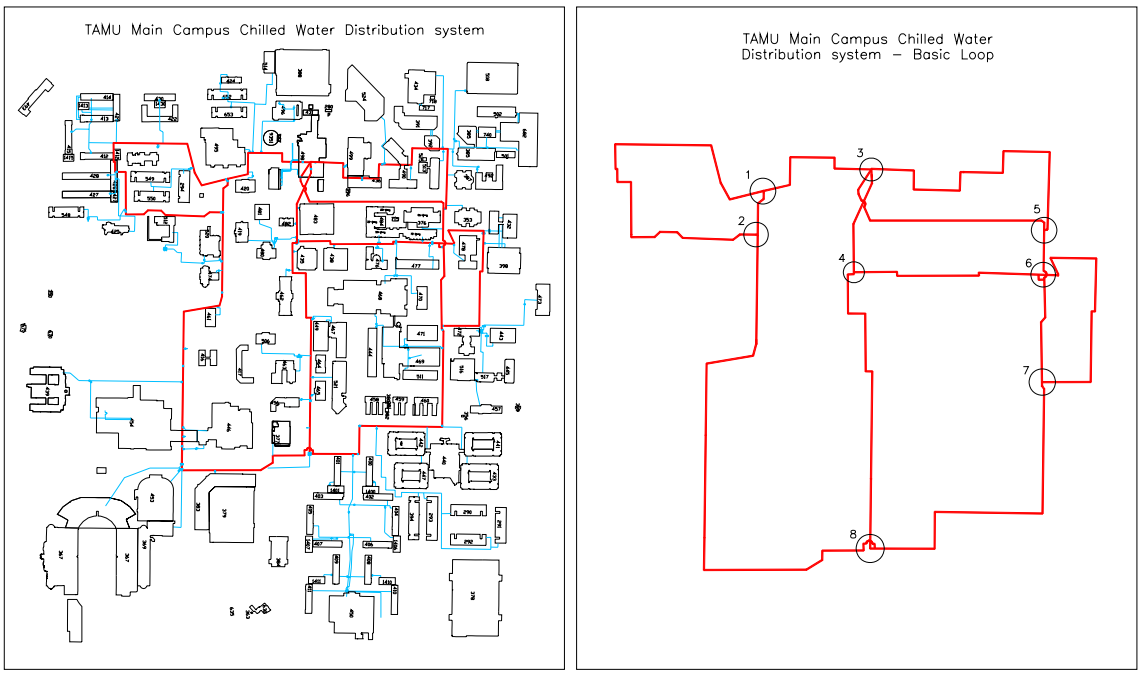

Figure 4 TAMU Main Campus DCS Distribution Network

The distribution system is the pipe network that connects the source system and individual consumers, i.e. buildings. Piping networks can be categorized into tree-shaped and loop-shaped structures. Large DCS distribution networks often employ the looped structure on their main circuits, i.e. basic loops. A tree-shaped structure is often used to distribute the chilled water from main circuits to a group or sub-division of buildings.

Supply and return piping are usually laid in parallel, either through a utilities tunnel or directly buried under ground.

Walski (1984) introduced the concept of independent loops. Independent loops represent the basic topological structure of the pipe network. The rules for determining the number of independent loops, L is:

$$L = P - J + 1$$

Where

L = number of independent loops
P = number of pipes
J = number of nodes

The left part of Figure 4 is the Geographic Information System (GIS) drawing of the TAMU main campus DCS distribution network. The basic loop structure, which does not include tree-shaped branches is embossed in red and displaced in the right part of Figure 4. It shows that the TAMU main campus DCS distribution network has 13 – 8 + 1 = 5 independent loops. The basic loops represent the critical topological structure of the DCS pipe network.

3.3.3 Load System

The load system is composed of individual in-building chilled water systems. The final cooling devices in buildings are cooling coils, fan-coil units, induction unit coils, radiant cooling panels, and water-to-water heat exchangers. These cooling devices, as well as building control valves, building pumps, and the piping that connects these components together form each building chilled water system in the load system. In-building systems can be mainly categorized into constant flow systems and variable flow

systems. The water side capacity control of these devices is realized by modulating the chilled water flow through two-way or three-way control valves. The water side control of the in-building chilled water systems is usually realized by modulating the pump speed (if it is VFD pump) and/or the position of the building control valve to maintain a certain set-point of building differential pressure (ΔP) or loop return temperature or differential temperature (ΔT). Detailed study of in-building systems is as follows:

Types of In-building Systems

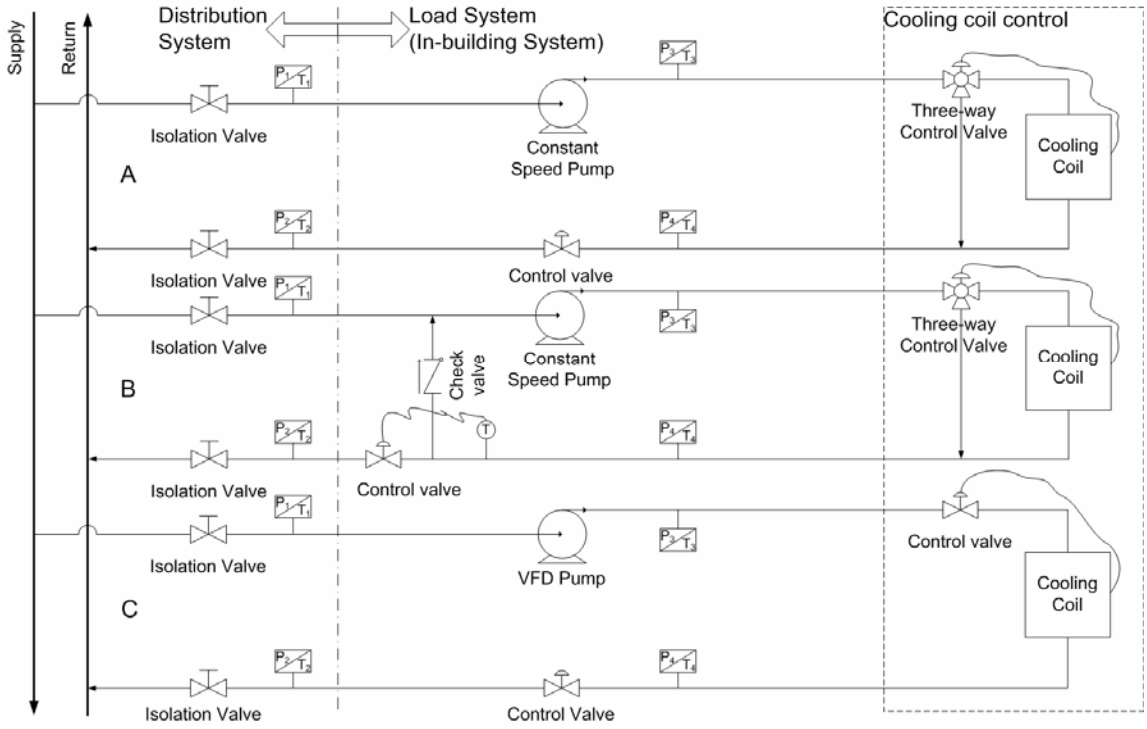

Figure 5 Schematic Layout of Typical In-building Systems

Figure 5 demonstrates three typical load system configurations. The dashed line defines the boundary between the distribution system and the load system. Pressures and temperatures measured on the distribution system side (see P_1/T_1 and P_2/T_2 in Figure 5) are usually called primary or loop pressures/temperatures. Pressures and temperatures measured after the building pumps and before the building return control valve (see P_3/T_3 and P_4/T_4 in Figure 5) are secondary or building pressures/temperatures.

Type A: As shown in Figure 5, Type A systems have constant primary flow, constant secondary flow and three-way valve controlled cooling coil flow. This is typical of a traditional in-building system. The constant speed pump supplies the chilled water to cooling coils at a relatively constant flow rate (if the pump is sized correctly). The cooling coil receives a variable flow by modulating the three-way valve to bypass some of the chilled water to the return line. Pumps are simply controlled through on and off switches, either automatically or manually. The control valve on the building return line may be used to maintain a set-point of the building ΔP ($P_3 - P_4$ in Figure 5). If the loop ΔP ($P_1 - P_2$ in Figure 5) is higher than the building ΔP set-point, the pump will be shut off.

For a type A in-building system configuration, the distribution system sees a constant chilled water flow. Figure 6 illustrates the daily chilled water consumption for a TAMU DCS building with a type A in-building system. Due to the constant speed pump, the chilled water flow demonstrates a flat pattern with small variation and does not correlate with the chilled water energy consumption. This type of load system configuration wastes pumping energy during partial load conditions.

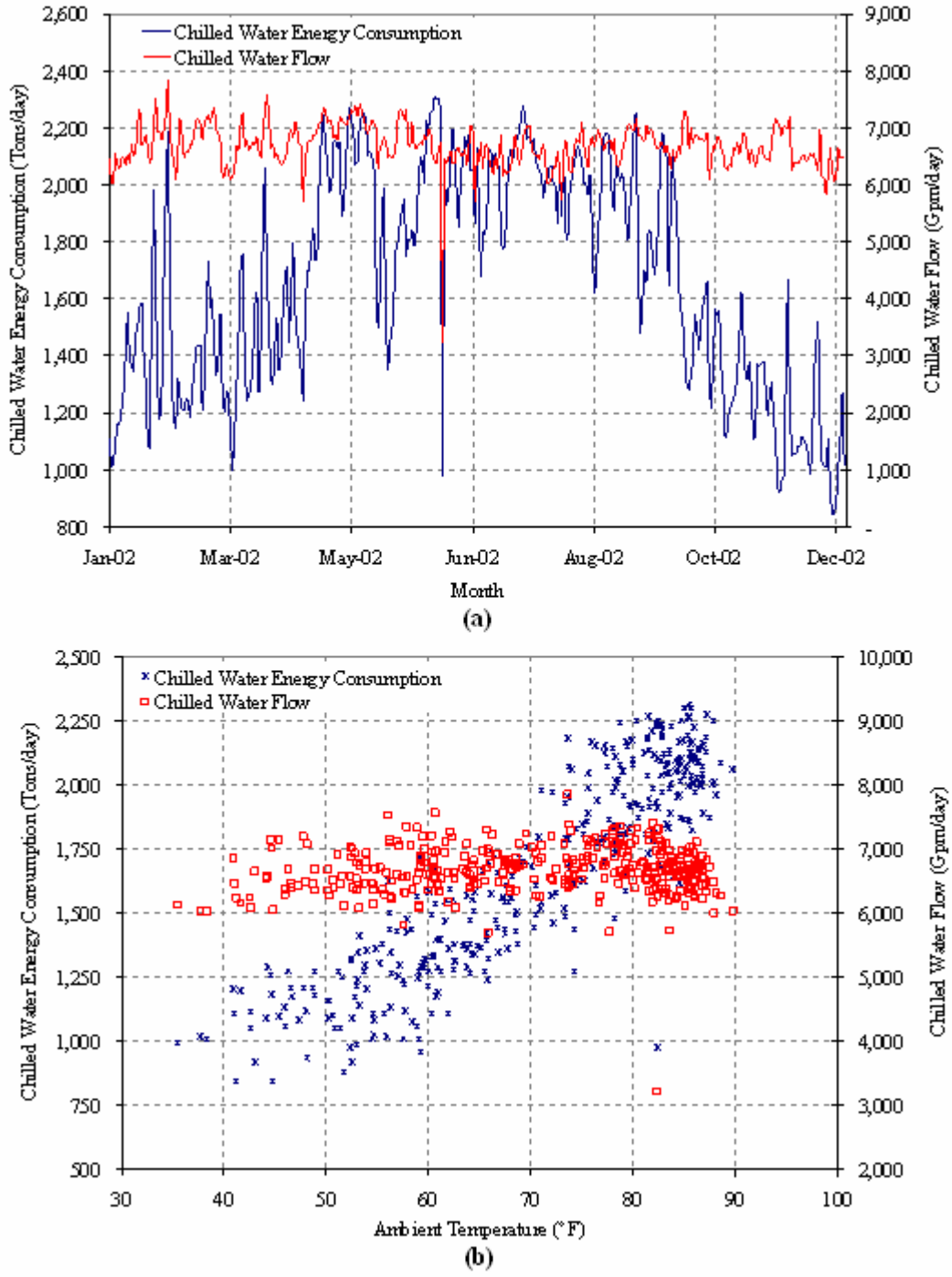

Figure 6 (a) Time Series and (b) Scatter Plots of Daily Chilled Water Consumption for Type A I-building Aystems (TAMU Bldg. #492)

Type B: As shown in Figure 5, the type B system has variable primary flow, constant secondary flow, and three-way valve controlled cooling coil flow. This type of in-building system has the same type of cooling coil control valve as a type A system, but introduces a common pipe to isolate the distribution system and the load system.

With the constant speed pump running, a control valve is used to modulate the chilled water flow to meet the building chilled water return temperature set-point. Mean while some of the building return water mixes with the building supply water. Therefore, while the chilled water in the building secondary system circulates at a relatively constant flow rate, the distribution system sees a variable flow. This type of in-building system results in an almost fixed loop ΔT if the plant sends out the chilled water at a fixed temperature. Figure 7 illustrates the daily chilled water consumption for a selected TAMU DCS building, which belongs to type B in-building systems. It clearly demonstrates that the chilled water flow follows the trend of chilled water energy consumption closely. The well followed patterns of chilled water flow and chilled water energy consumption indicate about 2.3 gpm/ton. Different set-point temperatures will result in different gpm/ton values.

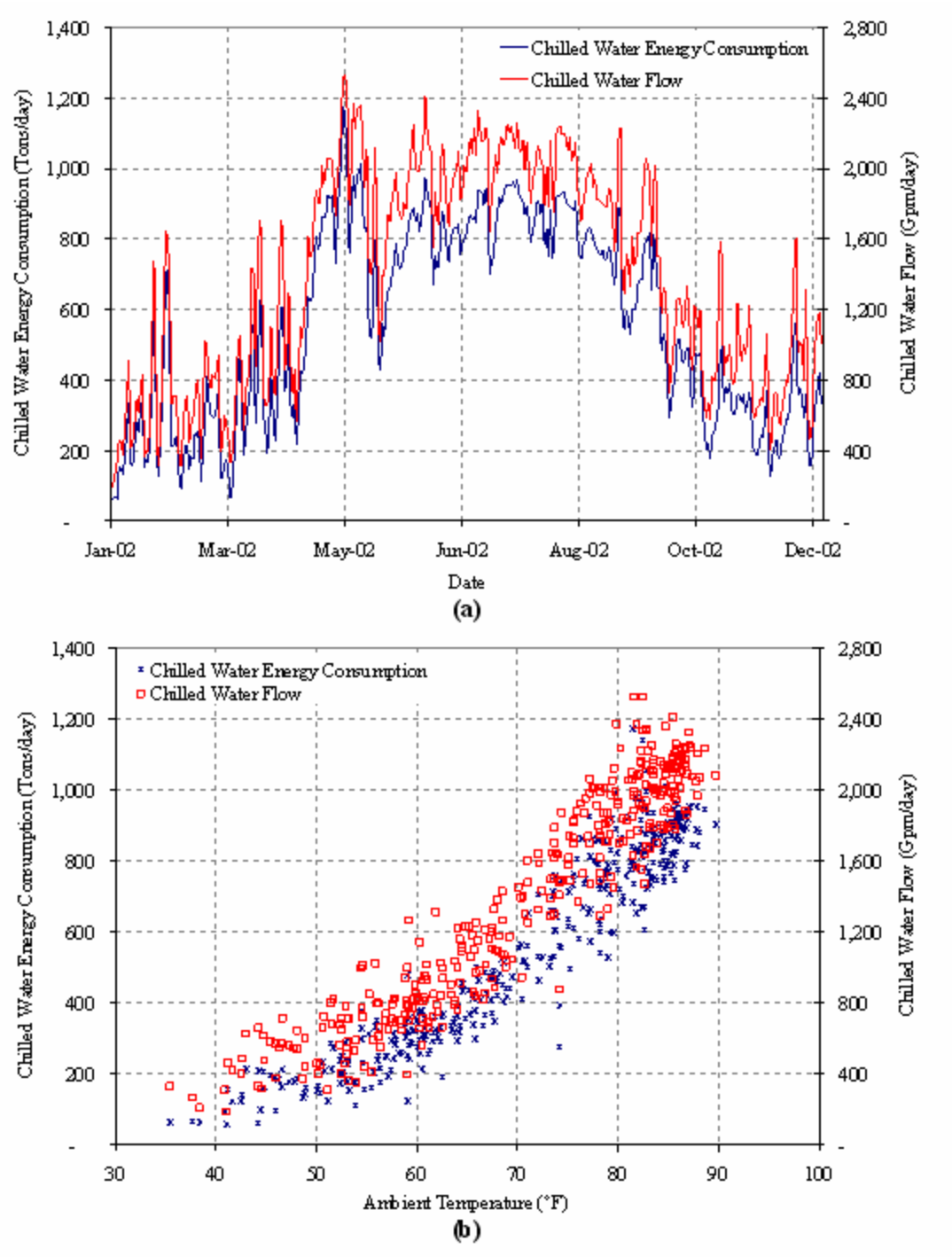

Figure 7 Plots (a) Time Series and (b) Scatter of Daily Chilled Water Consumption for Type B of In-building System (TAMU Bldg. #478)

Type C: In Figure 5, the type C system has variable primary flow, variable secondary flow and a two-way valve controlling cooling coil flow. VFD pumps are used to vary the chilled water flow through the building during partial load condition, so that the chilled water flow can track the building cooling load and, therefore, pumping energy can be saved. The VFD pump speed is often varied to maintain the building ΔP at its set-point. From the building pressure transmitter, the building DP is calculated in the Energy Management and Control System (EMCS) and compared with the set-point. Then the control signal is sent to the local controller to drive the VFD pump speed. When loop ΔP is higher than the building ΔP set-point, VFD pumps will be turned off automatically and the control valve will maintain the building DP at its set-point.

The building ΔP set-point is usually on a reset schedule based on the chilled water flow rate or the ambient temperature or cooling coil valve positions. On the other hand, the VFD pump speed can also be varied to maintain the loop ΔT or loop return temperature at its set-point. For this type of in-building system, the distribution network sees a varied chilled water flow. Figure 8 illustrates the daily chilled water consumption for a TAMU DCS building, which has a type C in-building system. In this case, the speed of the building pump is controlled to maintain the set-point of the building loop ΔP modulated for the ambient temperature. As demonstrated in Figure 8, the chilled water flow of this building generally follows the trend of the chilled water energy consumption.

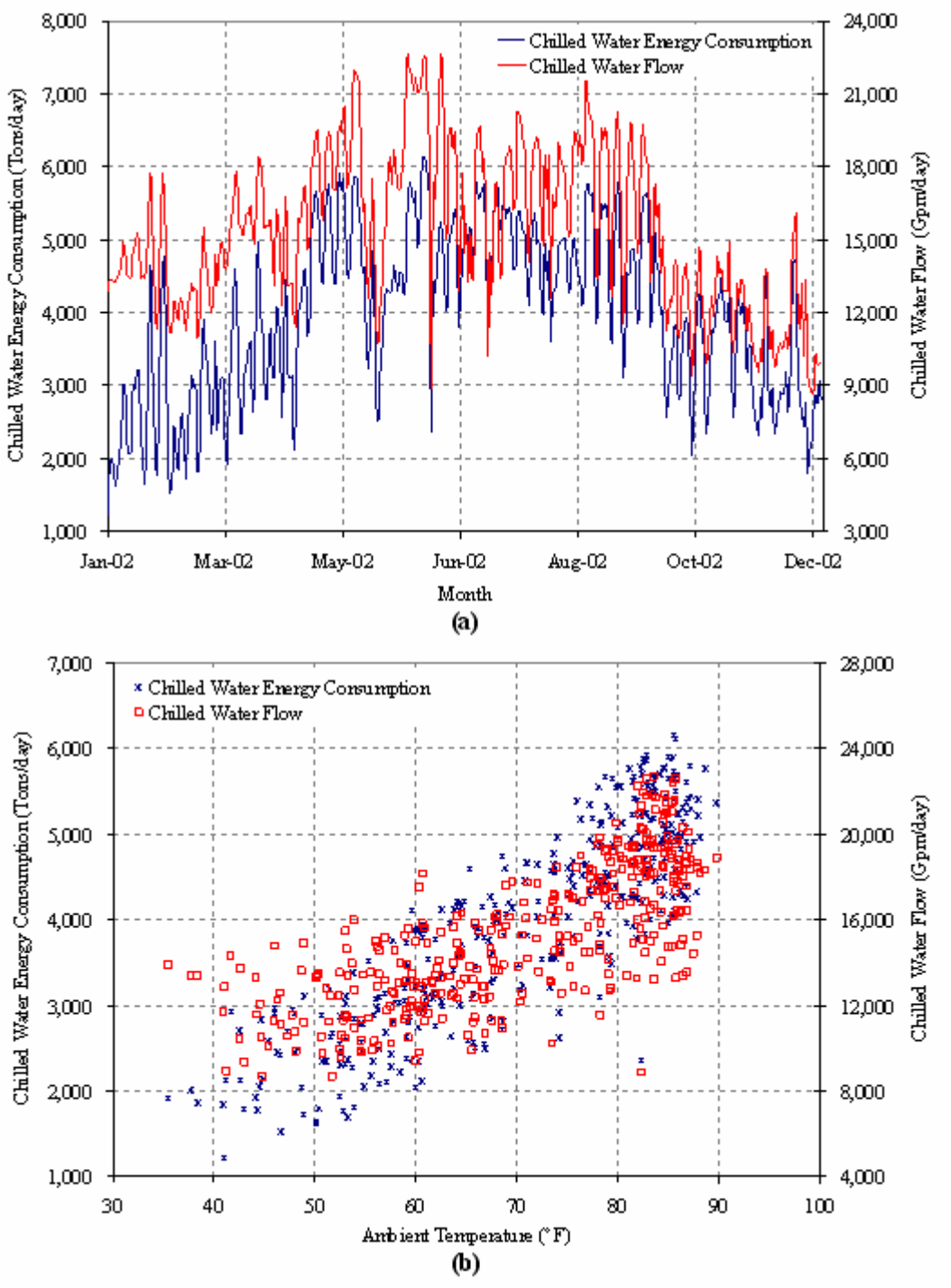

Figure 8 Plots (a) Time Series and (b) Scatter of Daily Chilled Water Consumption for Type C of In-building System (TAMU Bldg. #524)

Relationship of Cooling Load, Flow, and Temperature

In the load system, the building chilled water flow rate is indirectly determined by the cooling load, and the differential temperature of the chilled water entering and leaving the building. The basic relationship of the chilled water flow rate Q_w (gpm), differential temperature ΔT (°F), and the cooling load q_w (tons) is:

$$q_w = \frac{Q_w \cdot \Delta T}{24}$$

In this equation, the cooling load q_w depends on the following factors: (1) weather conditions, (2) internal heat gain, (3) building's physical structure, and (4) performance of the building's HVAC system.

The chilled water differential temperature ΔT is the other parameter in the above equation. In practice, the chilled water temperature has a limited range. Building Air Handler Units (AHU) usually maintain the room temperature at approximately 75 °F and 50% relative humidity. Accordingly, the dew-point temperature is 55 °F, which sets the maximum return water temperature near 55 °F (60 °F maximum). On the other hand, considering the freezing point of water, the lowest practical temperature for water distribution systems is about 40 °F. This temperature spread then sets constraints for a chilled water system. Buildings are usually designed at 12 °F temperature difference (ΔT) for their chilled water system. Newer buildings or buildings designed to achieve higher energy efficiency may have higher chilled water ΔT. These result in a flow rate of 2 gpm/ton of refrigeration or even lower values. Optimization of the ΔT is critical to successful operation of the DCS.

The factors that affect the building's chilled water differential temperature have been introduced in the literature review. For large DCS hydraulic systems, the pump control of the in-building chilled water system becomes the dominant factor.

3.4 Comparison between DWS and DCS Hydraulic Systems

Although both of DWS and DCS hydraulic systems are pipe networks, they are different in many ways:

1. The major difference between DWS and DCS hydraulic systems is what is consumed at their end users. DWSs are once-through systems. The water is sent out from the plant, flows through the distribution system and finally is consumed at the end users. DCS hydraulic systems are re-circulating systems with supply and return piping. Through the distribution system, water cooled at the plant is sent to end users, i.e. buildings. Instead of consuming water, thermal energy is added to the chilled water by building HVAC systems. Then the heated water is re-circulated back to the plant. This difference results in totally different flow demand patterns. For a DWS, the water flow of a house relies on diurnal human behavior, such as taking a shower in the morning and doing kitchen work around 6 o'clock in the evening. The pattern is more predictable. However, the flow demand behavior for a DCS building is more complicated as it involves the building's cooling load and its chilled water differential temperature.
2. DWSs are open loop pipe networks. The absolute discharge pressure at end users is affected by the elevation of junctions. DCS hydraulic systems are closed loop pipe

networks. Supply and return pipes are usually laid in parallel. The pressure loss built up by the effect of elevation on the supply side will be canceled out at the return side.

3.5 Introduction of TAMU Main Campus DCS Hydraulic System

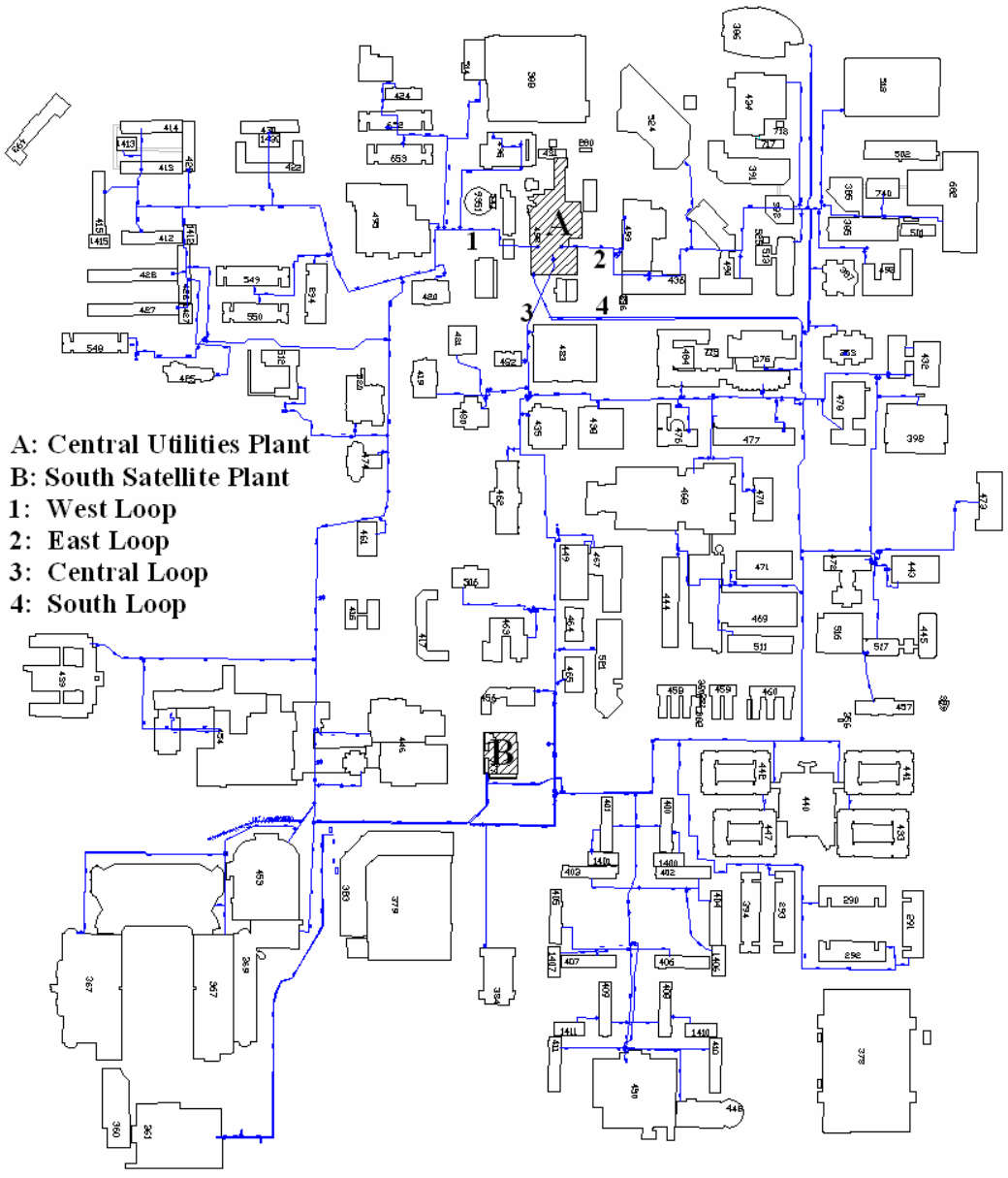

Figure 9 Simplified System Map of TAMU MC DCS Distribution System

This section is intended to give an example of a large DCS hydraulic system, i.e. the TAMU main campus DCS hydraulic system. The modeling of this system will be used as case studies through out this thesis in different chapters. TAMU located in College Station, Texas, has a 5,200-acre campus, among the largest in the nation. With more than 150 buildings and 18.5 million square feet of gross building space, the university serves over 45,000 students, 2,400 faculty and more than 5,000 staff members. TAMU at College Station is divided into two campuses, the main campus and the west campus. Each campus has its own DCS.

The TAMU main campus has an extensive and sophisticated chilled water distribution system. As the university expanded over the decades, the main campus alone has grown to 12.5 million square feet of building space and is still expanding. The current TAMU Main Campus chilled water system includes more than 16 miles of piping and reaches out to 117 buildings with a total of more than 9 million square feet of conditioned space. The 117 DCS buildings are composed of offices, classrooms, laboratories, dormitories, dining facilities, sports facilities and combinations of these uses. These buildings vary in ages ranging from those built late in the 19th century to some built in recent years. The type and condition of in-building chilled water systems differ as well. Some old buildings have a constant flow system with constant speed pumps and three-way valve controlled air handler units (type A of in-building system). Other buildings have variable flow systems with types B and C in-building systems. Continuous Commissioning® has been implemented in the majority of the buildings over the last decade and is still on going. For these commissioned buildings, the HVAC

system water side control sequences may be more optimal. A lot of old buildings have had their chilled water in-building system converted from a constant flow system to a variable flow system. Due to these on-going changes, the current chilled water consumption may be different from the original designs values.

All these buildings receive chilled water from two utilities plants: the Central Utilities Plant (CUP) and the South Satellite Plant (SS3). With installed cooling capacity of 21,400 tons, the CUP sends out chilled water through four loops: West, East, South, and Central. All these loops are interconnected through supply and return common headers in the CUP and pipe connections over the campus. The SS3 is a complementary plant with installed cooling capacity of 4,700 tons, connected to the South loop about 2/3 of the way from the CUP.

As shown in Figure 9, the distribution system of the TAMU MC DCS hydraulic system is a very complicated system. It is a parallel system with supply and return lines connected with each other (supply and return lines are shown as single lines in this simplified system map). It consists of four major loops: east, west, central and south loops, as well as some other small loops. Branches extend from a main loop to each individual building.

Such a large DCS is still expanding. According to the university's 30-year master plan, 5.9 million square feet of new building space is planned and 0.9 million square feet of building space is scheduled to be demolished. The very sophisticated DCS hydraulic system will have to be expanded and modified accordingly. Because the implementation cost is high, it is very important to have a thorough analysis of the impact of the planned

expansion/demolition on the existing system. Therefore, the DCS hydraulic system model is a very useful tool to help decision making.

3.6 Summary

In this chapter, the characteristics of large district cooling systems are summarized from a hydraulic point of view. A general description of large DCS hydraulic systems is first introduced. Then the major components of the system i.e. three sub-systems: source system, distribution system, and load system are introduced. Based on the study, the differences between large DCS hydraulic systems and DWSs are compared. The major difference lies in the flow demand behavior. The DWS is a mass consumption system, whereas DCSs are energy consumption systems that when considering the hydraulic behavior of such as system, must considers temperature as an important parameter. At the end of this chapter, an example of a large DCS hydraulic system is given to show what a large DCS hydraulic system looks like. It also provides background information for the modeling case studies in the following chapters.

CHAPTER IV

GENERALIZED MODELING PROCESS

4.1 Introduction

This chapter describes the overall procedure of modeling a large DCS hydraulic system. As introduced in Chapter II, the methodology has been maturely developed for DWS modeling and is documented in the published literature. Many hydraulic modeling software packages are available on the market. As summarized in Chapter III, DCS hydraulic systems and DWS are both pipe networks. Theories and methodologies developed for DWS modeling can generally be applied to DCS hydraulic system modeling. However, significant differences exist between DCS hydraulic systems and DWSs, which result in different modeling methodologies.

Taking the modeling procedure for DWSs as a reference, and summarizing actual modeling experience with one of the largest DCSs in the United States, a generalized modeling process for the DCS hydraulic system modeling is developed. A brief explanation of this process is given. The following chapters will follow the procedure and discuss it in detail.

4.2 Overall Modeling Process

Figure 10 illustrates the overall DCS hydraulic system modeling process. Just like the way to complete any large project, the modeling work is broken down to components and work through each step. Some tasks can be done in parallel while other must be done in series. As shown in Figure 10, the DCS hydraulic modeling process follows four major steps:

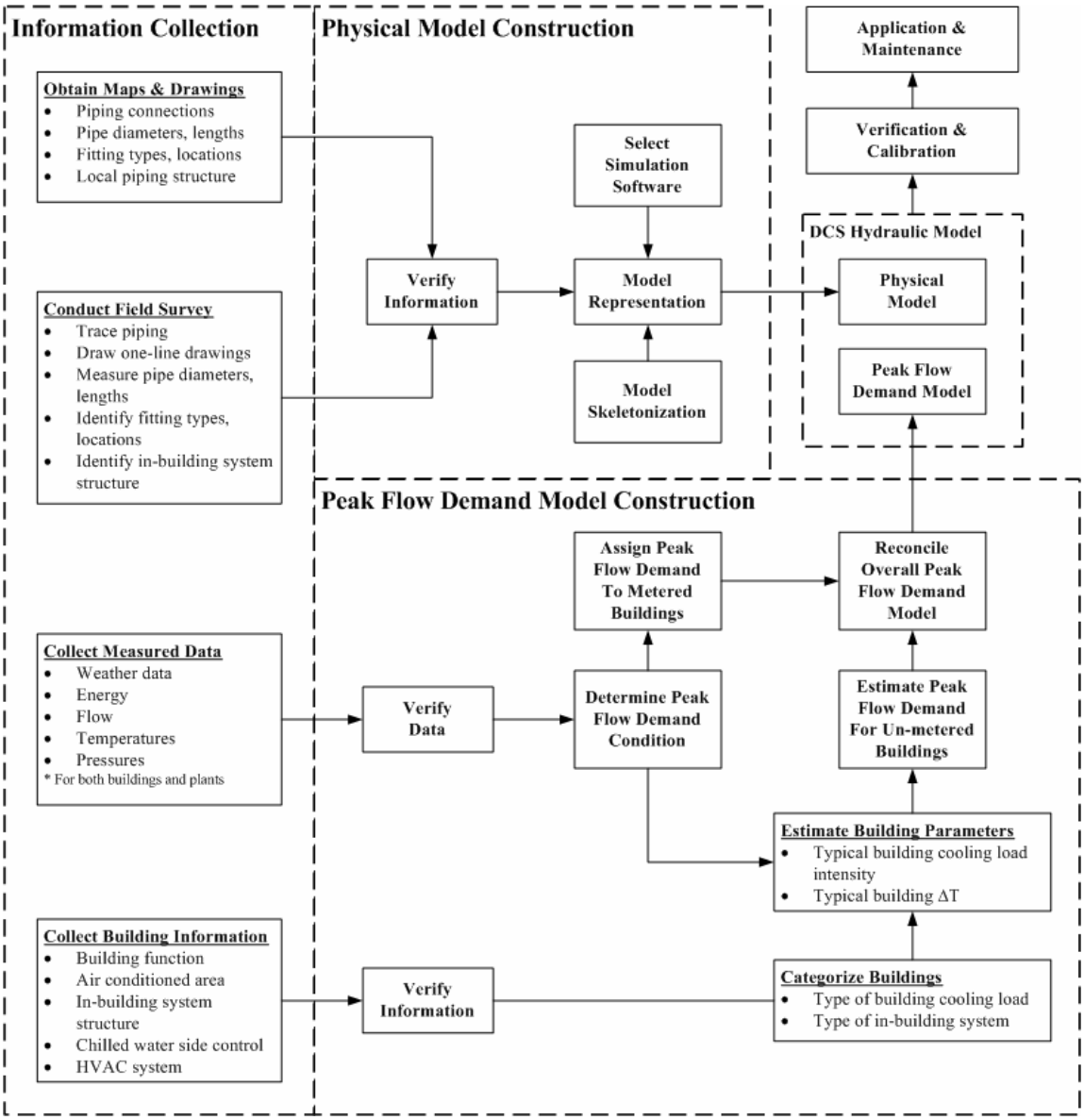

Figure 10 Generalized DCS Hydraulic Modeling Procedure

1. The first step is to collect a tremendous amount of information and data. Drawings and maps are to be collected. Data will be collected through the utilities' metering system or building metering systems. Operation and maintenance records will be collected. A field survey will be conducted and

measurement data will be conducted. During the information and data collection step, multiple departments will be involved to coordinate the field work, and provide the information and data requested. The collected information and data are then verified and summarized in a convenient format for the modeler to process to the following steps. Details about the information to collect and how to collect it will be discussed in chapter VI and chapter VII.

2. The second step consists of two parts; the physical model construction and the peak flow demand model construction. The physical model is the part of the model that represents the physical structure of the real system, such as piping layout, fittings, pumps, etc. The physical model is built on a selected simulation software package. There are many hydraulic simulation software packages available. Chapter V introduces the simulation software that is used for the DCS hydraulic system modeling work in this thesis. Chapter VI discusses the physical modeling in detail. The flow demand model reflects the water usage at the end consumers under certain condition. Basically it is a set of flow numbers assigned to the modeled nodes that represent the end consumer i.e. buildings in the physical model. The peak flow demand model is the flow demand model under the peak flow condition. Detailed peak flow demand modeling will be discussed in chapter VII. The processes of developing the peak flow demand model and the physical model can be conducted in parallel.
3. The third step is to verify and calibrate the DCS hydraulic model after the physical model and peak flow demand model are constructed. Simulation can be

conducted and the hydraulic model can be verified with actual measured data. Calibration is then conducted to match the simulated results to the measured results. The entire modeling effort is an iterative process. At any moment, the modeler may go back to request new information, refine the model, and/or conduct additional field investigation, until the calibrated model is ready to use. The verification and calibration methodology and procedure will be discussed in chapter VIII.

4. After the overall DCS hydraulic model is verified and calibrated, it can be used for master planning purposes. Chapter IX demonstrates how to use the model to assist decision making in master planning through a case study.

CHAPTER V

INTRODUCTION OF AFT FATHOM

5.1 Introduction

As introduced in chapter IV, The entire hydraulic model is built on a selected simulation software platform. This chapter is intended to introduce AFT Fathom, a commercial software package that is used through out the modeling process in this research.

AFT Fathom was developed by Applied Flow Technology Corporation. It provides incompressible pipe flow analysis and system modeling capabilities combined with visualized model building features. AFT Fathom is based on the following fundamental fluid mechanics assumptions: (1) incompressible flow, (2) steady-State conditions, (3) one dimensional flow, and (4) no chemical reactions. AFT Fathom employs proven matrix methods to solve the governing equations of pipe networks. Addressing open and closed loop systems, AFT Fathom includes a built-in library of fluids and fittings, variable model configurations, pump and control valve modeling, etc. Detailed modeling methodology and operation instructions are well documented in the AFT Fathom™ User's Guide (Applied Flow Technology, 2004). The following sections of this chapter briefly summarize the methodology applied in AFT Fathom and the use of this simulation software for the hydraulic simulation of pipe networks.

5.2 Pipe Network Solution Methodology

AFT Fathom makes use of standard matrix solution techniques (Jeppson 1976). The method is known as the H-Equation method, where H, the piezometric head, is

determined at each junction by forcing continuity of flow through each connecting pipe. Simultaneously, the head loss across each pipe is updated based on the flow balance information. The flow rate and head are solved in an inner-outer loop algorithm, where the flow is guessed, the head loss is calculated consistent with that guess, and the flow is updated according to the new pressure drop information. The Newton-Raphson method is employed to refine each successive solution, resulting in a sparse square matrix that is solved during each solution pass.

The concepts of pressure and hydraulic grade line (HGL, also called piezometric head) are related but use different frameworks for considering pipe system behavior. The HGL includes both the static and elevational effects of pressure. The relationship between the two is:

$$HGL = \frac{P}{\rho g} + Z \qquad 1$$

Where:

Z = elevation

P = Pressure, static

ρ = Density

g = Gravitational constant

The solution technique makes use of the continuity and one-dimensional momentum equations. In the following discussion, subscripts denote values at junctions. Thus, P_i represents the pressure at junction *i*. Double subscripts denote values along pipes

connecting two junctions, thus, $\dot{m}_{ij}$ represents the mass flow rate in the pipe connecting junctions *i* and *j*. Application of the law of mass conservation to each junction yields:

$$\sum_{j=1}^{n} \dot{m}_{ij} = 0 \qquad 2$$

where *n* is the number of pipes connected to junction *i*. This equation states that the net mass flow rate into each junction must sum to zero.

The basic equation for pipe pressure drop due to friction can be expressed with the Darcy-Weisbach equation:

$$\Delta P_f = f \frac{L}{D}\left(\frac{1}{2}\rho V^2\right) \qquad 3$$

where ΔP_f is the frictional pressure loss. The total pressure change between junctions is given by the momentum equation in the form of the Bernoulli equation:

$$P_1 + \frac{1}{2}\rho V_1^2 + \rho g Z_1 = P_2 + \frac{1}{2}\rho V_2^2 + \rho g Z_2 + \Delta P_f \qquad 4$$

Solving for the frictional pressure drop for a constant area pipe yields:

$$\rho g\left(HGL_i - HGL_j\right) = \Delta P_f \qquad 5$$

where *i* and *j* denote upstream and downstream junction values. The definition of mass flow rate is:

$$\dot{m} = \rho A V \qquad 6$$

Combining equation 3 and equation 5 and substituting for velocity (*V*), using equation 6 gives the mass flow for each pipe:

$$\left(\frac{HGL_i - HGL_j}{R_{ij}}\right)^{\frac{1}{2}} = \dot{m}_{ij} \tag{7}$$

where R_{ij} is the effective flow resistance in the pipe and the subscript *ij* refers to the pipe connecting junctions *i* and *j*.

$$R_{ij} = \left(\frac{f_{ij} L_{ij}}{D_{ij}}\right) \frac{1}{2g\rho^2 A_{ij}^2} \tag{8}$$

Substituting equation 7 into equation 2 results in the equation to be applied to each junction i:

$$\sum_{j=1}^{n} \left(\frac{HGL_i - HGL_j}{R_{ij}}\right)^{\frac{1}{2}} = 0 \tag{9}$$

where *n* is the number of pipes connected to junction *i*. To be completely general, equation 9 should be written for junction *i*:

$$\sum_{j=1}^{n} \left(\frac{HGL_i - HGL_j}{R_{ij}}\right)^{\frac{1}{2}} = \dot{m}_{i,boundary} \tag{10}$$

Equation 10 as applied to each junction in the network represents the system of equations that need to be solved to determine the piezometric head at each junction. To solve this system of equations, AFT Fathom employs the Newton-Raphson method. In the Newton-Raphson method, new values for each unknown are calculated based on the previous value and a correction that uses the first derivative of the function. In this instance the function would be of the form:

$$F_i = \sum_{j=1}^{n} \left(\frac{HGL_i - HGL_j}{R_{ij}} \right)^{\frac{1}{2}} - \dot{m}_{i,boundary} \qquad 11$$

The method involves finding all the junction piezometric head values (HGL_i), that cause all of the F_i to be zero, thus satisfying equation 10 at all junctions. When applied to a system of equations, the Jacobian matrix contains all the required derivative information to employ the Newton-Raphson technique. The Jacobian J_F is given by:

$$J_F = \begin{bmatrix} \frac{\partial F_1}{\partial H_1} & \frac{\partial F_1}{\partial H_2} & \cdots & \frac{\partial F_1}{\partial H_n} \\ \frac{\partial F_2}{\partial H_1} & \frac{\partial F_2}{\partial H_2} & \cdots & \frac{\partial F_2}{\partial H_n} \\ \vdots & \vdots & \ddots & \vdots \\ \frac{\partial F_n}{\partial H_1} & \frac{\partial F_n}{\partial H_2} & \cdots & \frac{\partial F_n}{\partial H_n} \end{bmatrix} \qquad 12$$

The column matrix $\vec{H}$ contains the piezometric head at each junction, and column matrix $\vec{F}$ contains the F values at each junction. The updated solutions for $\vec{H}$ are obtained from the following Newton-Raphson equation:

$$\vec{H}_{new} = \vec{H}_{old} - J_F^{-1} \times \vec{F} \qquad 13$$

5.3 Irrecoverable Loss Models

AFT Fathom provides a flexible approach to selecting standard, handbook loss models for pipes and other junction types, such as tees/wyes, area changes, valves, pumps, etc. (Applied Flow Technology, 2004). Table 1 lists references of junction loss models used in AFT Fathom. Model details are well documented in AFT Fathom™ User's Guide (Applied Flow Technology, 2004).

Table 1 Loss Model References Used in AFT Fathom (Applied Flow Technology 2004)

Junction Type	References
Bend	Crane 1998
Area Change	Crane 1998 and Idelchik 1994
Tee/Wye	Idelchik 1994 and Miller 1990
Valve	Crane 1998, Idelchik 1994 and Miller 1990
Orifice	Idelchik 1994
Screen	Idelchik 1994

AFT Fathom also provides flexible approaches to select friction loss models for pipes. The user can select an appropriate loss model for the specific modeling situation. The loss models that AFT Fathom employs for modeling of water flowing through a pipe are listed below:

1. Absolute roughness – AFT Fathom's default method is to specify the roughness as an absolute average roughness height. Values of pipe roughness can be found in many pipe handbooks or from manufacturer's data. This uses the Darcy-Weisbach method.
2. Relative roughness – Some pipe roughness specifications are given as a relative roughness. In this case, the roughness height is divided by the pipe diameter. This uses the Darcy-Weisbach method.
3. Hazen-Williams – The Hazen-Williams method uses an empirical factor to relate the flow rate to the pressure drop in the pipe. This method is still in common use in the field of water distribution.

4. Explicit Friction factor – If the friction factor for the pipe is known, it can be entered explicitly.
5. Hydraulically smooth –A pipe can also be specified as hydraulically smooth. Modeling a pipe as hydraulically smooth implies that its roughness is negligible. However, having a small roughness is not the same as being frictionless. Rather, the pipe friction factor follows the hydraulically smooth curve in the turbulent region of a standard Moody diagram.
6. Frictionless – For modeling purposes, it is occasionally useful to model a pipe as having no friction.

Besides the standard pipe and junction loss models, AFT Fathom also provides a mechanism to model friction losses for a general hydraulic component according to the following equation:

$$\Delta P_f = K\left(\frac{1}{2}\rho V^2\right) \qquad 14$$

where K is commonly referred to as the loss factor.

5.4 Using AFT Fathom

This section briefly introduces how to use AFT Fathom to construct the physical model of a hydraulic system. AFT Fathom provides a graphical interface so that users can drag and drop pre-encapsulated component modules such as pipes and fittings to the work space (see Figure 11). Users can move the components in the work space to connect them according to the system map and drawings. By clicking through each component, users can specify the parameters for that component, such as pipe length,

type of valves, etc. Users can also globally set some parameters that are common for a type of component, for example, globally set the design factors for all the pipes to 1.2.

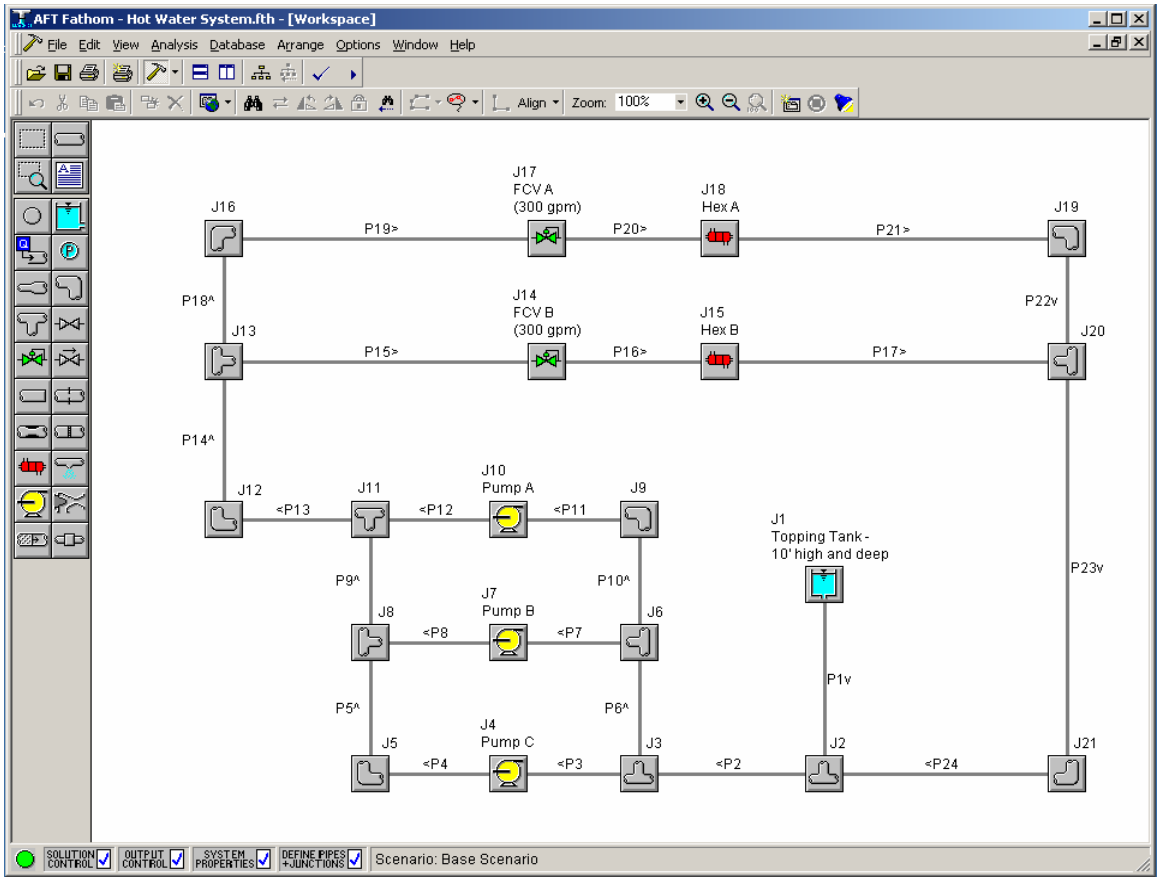

Figure 11 Graphical Interface of AFT Fathom – Workspace Window

Besides visually adjusting the components parameters in the workspace window, users can also directly adjust the components through the Model Data window (see Figure 12).

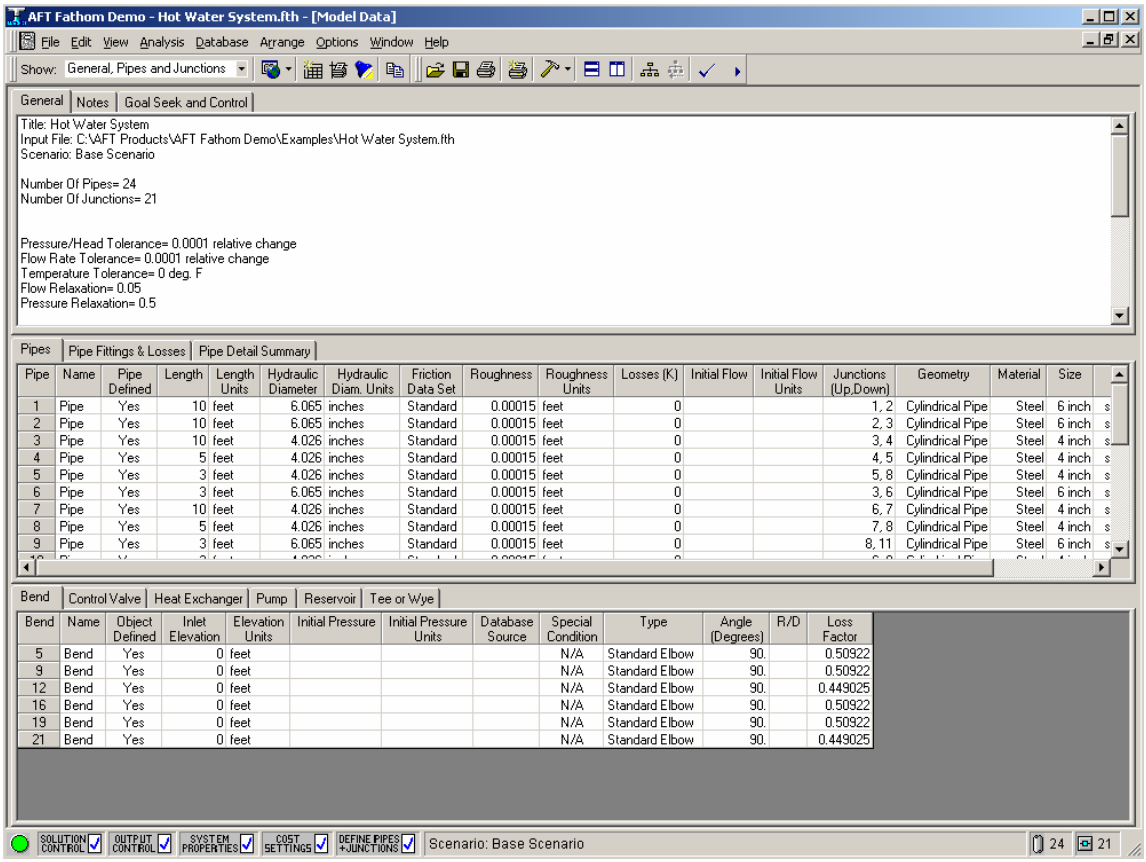

Figure 12 Graphical Interface of AFT Fathom - Model Data Window

After all the information is input into AFT Fathom and software settings are properly set, users can start to run the model. Once the simulation converges, the results are shown in the Output Window (see Figure 13) and users can copy selected results to other programs such as Microsoft Excel for further analysis.

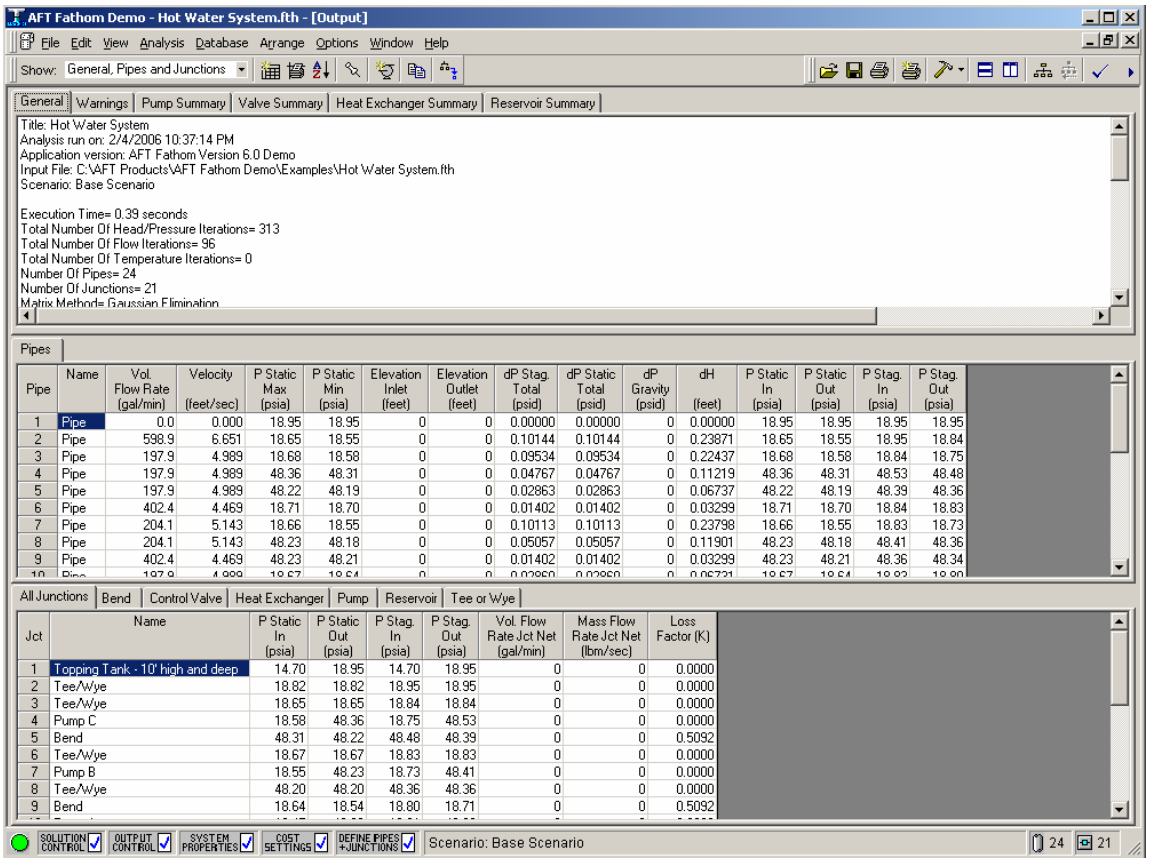

Pipe	Name	Vol. Flow Rate (gal/min)	Velocity (feet/sec)	P Static Max (psia)	P Static Min (psia)	Elevation Inlet (feet)	Elevation Outlet (feet)	dP Stag. Total (psid)	dP Static Total (psid)	dP Gravity (psid)	dH (feet)	P Static In (psia)	P Static Out (psia)	P Stag. In (psia)	P Stag. Out (psia)
1	Pipe	0.0	0.000	18.95	18.95	0	0	0.00000	0.00000	0	0.00000	18.95	18.95	18.95	18.95
2	Pipe	598.9	6.651	18.65	18.55	0	0	0.10144	0.10144	0	0.23871	18.65	18.55	18.95	18.84
3	Pipe	197.9	4.989	18.68	18.58	0	0	0.09534	0.09534	0	0.22437	18.68	18.58	18.84	18.75
4	Pipe	197.9	4.989	48.36	48.31	0	0	0.04767	0.04767	0	0.11219	48.36	48.31	48.53	48.48
5	Pipe	197.9	4.989	48.22	48.19	0	0	0.02863	0.02863	0	0.06737	48.22	48.19	48.39	48.36
6	Pipe	402.4	4.469	18.71	18.70	0	0	0.01402	0.01402	0	0.03299	18.71	18.70	18.84	18.83
7	Pipe	204.1	5.143	18.66	18.55	0	0	0.10113	0.10113	0	0.23798	18.66	18.55	18.83	18.73
8	Pipe	204.1	5.143	48.23	48.18	0	0	0.05057	0.05057	0	0.11901	48.23	48.18	48.41	48.36
9	Pipe	402.4	4.469	48.23	48.21	0	0	0.01402	0.01402	0	0.03299	48.23	48.21	48.36	48.34

Jct	Name	P Static In (psia)	P Static Out (psia)	P Stag. In (psia)	P Stag. Out (psia)	Vol. Flow Rate Jct Net (gal/min)	Mass Flow Rate Jct Net (lbm/sec)	Loss Factor (K)
1	Topping Tank - 10' high and deep	14.70	18.95	14.70	18.95	0	0	0.0000
2	Tee/Wye	18.82	18.82	18.95	18.95	0	0	0.0000
3	Tee/Wye	18.65	18.65	18.84	18.84	0	0	0.0000
4	Pump C	18.58	48.36	18.75	48.53	0	0	0.0000
5	Bend	48.31	48.22	48.48	48.39	0	0	0.5092
6	Tee/Wye	18.67	18.67	18.83	18.83	0	0	0.0000
7	Pump B	18.55	48.23	18.73	48.41	0	0	0.0000
8	Tee/Wye	48.20	48.20	48.36	48.36	0	0	0.0000
9	Bend	18.64	18.54	18.80	18.71	0	0	0.5092

Figure 13 Graphical Interface of AFT Fathom - Output Window

5.5 Summary

This chapter briefly introduces a pipe network hydraulic simulation software package, i.e. AFT Fathom, which is used through out the research of this thesis. Detailed operation instructions have been well documented in the user's guide. This chapter emphasizes background information on how AFT Fathom works and how to use it.

CHAPTER VI

PHYSICAL MODEL

6.1 Introduction

The physical model is the model that represents the physical structure of a real system. Following the general modeling process introduced in chapter IV, this chapter discusses in detail about the procedure and considerations when constructing the physical model by using a commercial hydraulic simulation software package, e.g. AFT Fathom. What kind of information should be collected and how to collect the information is discussed first. Second, the skeletonization, i.e. the selection for inclusion in the model only the parts of the hydraulic network that have a significant impact on a large DCS hydraulic system for master planning purposes is discussed. Third, how to represent the real DCS hydraulic system into the selected simulation software by using appropriate model components is discussed. The network elements of a typical DCS hydraulic system are introduced, and modeling considerations for the individual system components are discussed. At the end of this chapter, a case study is introduced to demonstrate physical modeling process.

6.2 Information Collection

Modeling of a large DCS hydraulic system requires a tremendous amount of information be collected. The information needed to generate the physical model of a DCS hydraulic system includes: (1) pipe alignment, connectivity, material, size, length, etc.; (2) the locations and types of other system components, such as valves, tees/wyes, bends, area changes, heat exchangers, pumps, storage tanks, etc.; and (3) elevations of

junctions (optional). The information can be collected from various sources, such as system maps, as-built drawings, and electronic data files, and even field survey information.

6.2.1 Maps and Records

Systems maps are the most useful documents for gaining an overall understanding of the DCS hydraulic system, since they illustrate a wide variety of valuable system characteristics. In addition to the information that must be collected to build the physical model, system maps may include other information for better understanding the background of a DCS hydraulic system, such as: (1) miscellaneous notes regarding detailed records that may help the modeling process; (2) the locations of roadways, streams, planning zones, etc.; and (3) other utility lines, such as domestic water, steam, heating hot water, electricity, etc.

For a large DCS, years of changes often result in differences between original design plans and the actual system as constructed. System maps may be outdated in part. As-built drawings that document the system exactly as it was built are the other important sources for updated information at a detail level such as pipe lengths, fitting types and locations, and so forth.

Today, maps and records are usually stored in some electronic format such as a database, Computer Aided Drafting (CAD) drawings, and/or a Geographic Information System (GIS). A GIS is a computer-based tool for mapping and analyzing objects and events that happen on earth. To reflect the most recent changes in a DCS hydraulic system, it is a common practice to routinely update the information in the GIS. Therefore,

a GIS is often a good source of the system information needed to construct the physical model.

6.2.2 Field Survey

Although maps are generally good sources of information, there are situations that require caution. Maps may be unclear on some piping connections or outdated due to changes. As-built drawings may be hard to find or out-dated. These problems are especially common with a large and old DCS. Where utilities tunnels are available, a field survey becomes an alternative way to supplement or cross check the collected information. A field survey usually involves the following actions: (1) trace the piping; (2) draw one line drawings for the piping infrastructure; (3) measure the size and length of pipe sections; (4) identify the locations and types of fittings such as valves, area changes, tees/wyes, etc. Some part of the chilled water piping of the DCS may be directly buried. In this case, the accuracy of the physical model will largely depend on the accuracy of the map.

6.2.3 Information Verification

To ensure the physical model to reflect the up-to-date and accurate piping infrastructure, before starting the construction of the physical model, the information obtained from the field investigation should be used to verify and cross-check with the drawings and maps. If some part of the map or drawing does not agree with the field investigated result, it indicates that the map or draw may not be accurate or out-dated.

For this part of piping infrastructure, the field investigated results should be used to construct the physical model.

For example, if a drawing shows the diameter of a pipe is 10 inches whereas the field measured diameter of this pipe is 12 inches, the drawing may be not accurate or the information has been out-dated. The field measured diameter of this pipe should be used in the physical model.

6.3 Model Skeletonization

As introduced in chapter III, DCS hydraulic systems can be divided into three sub-systems: the source system, the distribution system, and the load system. The source system starts at the individual chillers and goes to the plant entrance. The load system starts from each building's entrance and goes to the individual cooling coils. The distribution system lies between the source system and the load system. For a large DCS, each of the three sub-systems can be very complicated. Having a complete DCS hydraulic model with every detail of each of these sub-systems is ideal. It could be easily realized for a small DCS with several buildings and a simple plant. However, for a large DCS with hundreds of buildings and multiple thermal utilities plants, trying to include each individual pipe, valve, pump, and every other component of a large system in a model could be a huge work load and make no significant impact on the model results. Capturing every feature of a system would also involve tremendous amounts of data, which make the model error-prone (Walski et al. 2001).

Skeletonization is a term that used in DWS modeling. It is the process of selecting for inclusion in the model only the parts of the hydraulic network that have a significant

impact on the behavior of the system (Walski et al. 2001). However, skeletonization does not mean omission of data. The portions of the system that are not included in the model during the skeletonization process are not discarded. Their effects are taken into account within the parts of the system that are included in the model. This section discusses the skeletonization for a large DCS hydraulic system model, i.e. the level of detail that the physical model should include if it will be used for master planning purposes.

Basically, two types of skeletonization are used in DWS modeling: (1) loop reformation, which will affect the model accuracy; (2) branch simplification, which will not affect the model accuracy. The following two sub-sections will discuss these two types of skeletonization for the specific situation of DCS hydraulic system modeling for master planning.

6.3.1 Loop Reformation

Loop reformation involves removing some un-important pipes in pipe loops, so that the loop structure of the system is changed and the physical model is simplified. This kind of skeletonization will result in model inaccuracy. However, Eggener and Polkowski (1976) found that they could remove a significant number of un-important pipes in a DWS model, and still have it yield results of acceptable accuracy.

As introduced in chapter III, the topological structure of a large DCS hydraulic system usually does not include as many loops as a DWS. Even a very large DCS pipe network, such as that on the TAMU main campus, consists of only five independent

loops (see Chapter III). Therefore this kind of skeletonization is not necessary to simplify the physical structure of a DCS hydraulic system.

6.3.2 Branch Simplification

The other type of skeletonization simplifies one or more branches into one or more nodal components when the hydraulic parameters such as pressure or flow are known at the branch entrances. Meanwhile, the basic loop structure of the pipe network does not change. For example, a 12-inch branch connects four downstream buildings to the main loop. Each building is connected to the branch with a 4-inch pipe and has 100 GPM of flow demand. The entire branch can be represented as a junction node connecting to the main loop with total of 400 GPM flowing through it. This type of skeletonization is widely applied for DWS modeling to aggregate individual houses to one junction node, or even to aggregate a cluster of houses to district level junction nodes. When the boundary condition and the flow demand at the modeled junction nodes are determined, the simulation software will automatically calculate the pressure at the modeled junction nodes iteratively. Therefore, the aggregation of the demands does not affect the model accuracy. However, the modeler will not be able to determine how pressure and flows vary within the aggregated subdivisions.

6.3.3 Physical Model Skeletonization of a Large DCS Hydraulic System

The extent of skeletonization depends on the intended use of the model (Walski et al. 2001). The objective of the large DCS hydraulic system model used for master planning is to predict the impact of newly planned buildings on the existing system. From the

planning point of view, the predicted differential pressure distribution is the key result needed from the model and detailed hydraulic behavior within the plant and in-building systems is not the focus of master planning. Therefore, if the hydraulic parameters at the plant and building entrances are known, the plant and in-building systems can be simplified as nodal components without sacrificing the model accuracy.

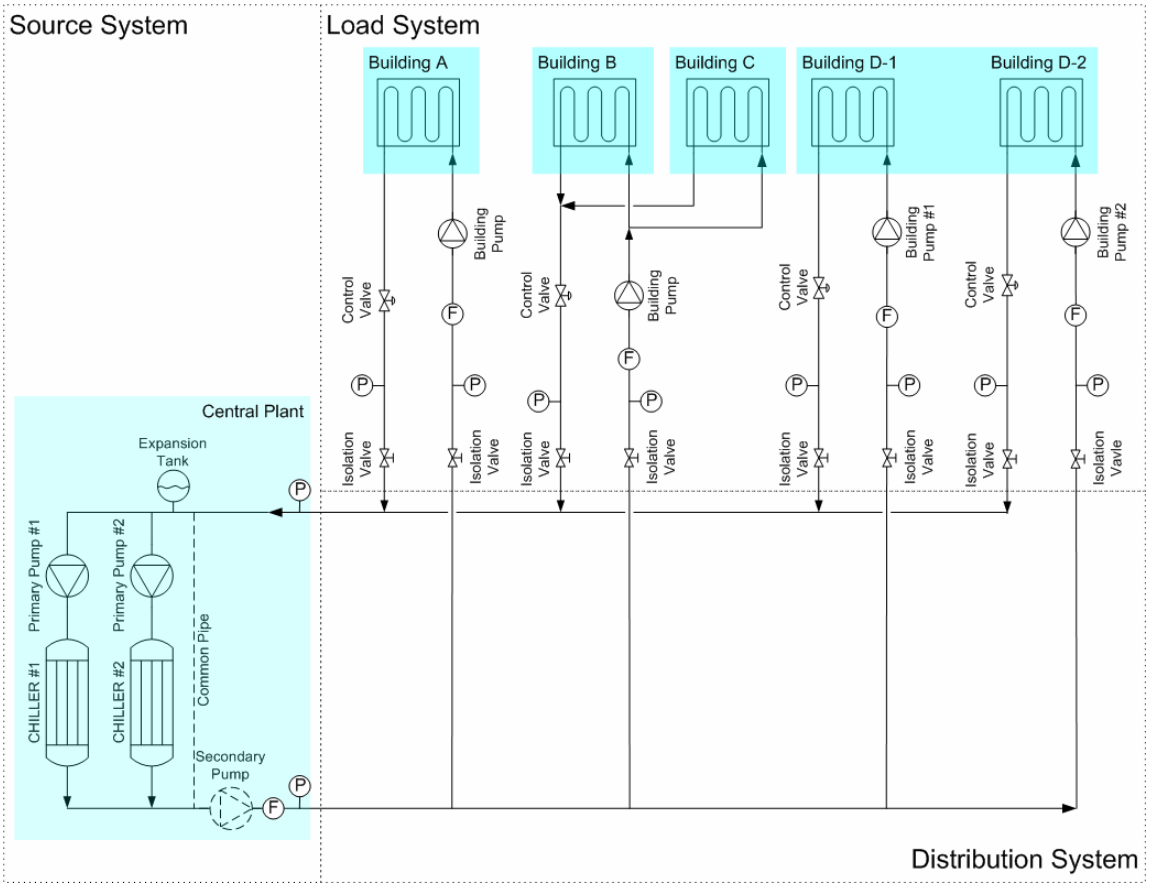

Figure 14 Original Representation of a Large DCS Hydraulic System

For example, the Figure 14 is a schematic layout of a large DCS hydraulic system. Usually the chilled water flow, and supply/return pressures and temperatures are

measured at plant entrances and building entrances (An “F” in a circle means flow meter and a “P” in a circle means pressure meter). As shown in Figure 14, a flow meter and two pressure meters are installed at the plant entrances. There are four buildings shown in Figure 14, buildings A, B, C and D. Building A is connected to the distribution system through one set of supply/return piping. The flow meter (shown as “F” in a circle) is installed at the building entrance. Buildings B and C are connected to the distribution system through one set of supply/return piping. And the flow meter is installed so that it measures the total flow of buildings B and C. Building D is connected to the distribution system through two sets of supply and return piping with each set serving one portion of the building.

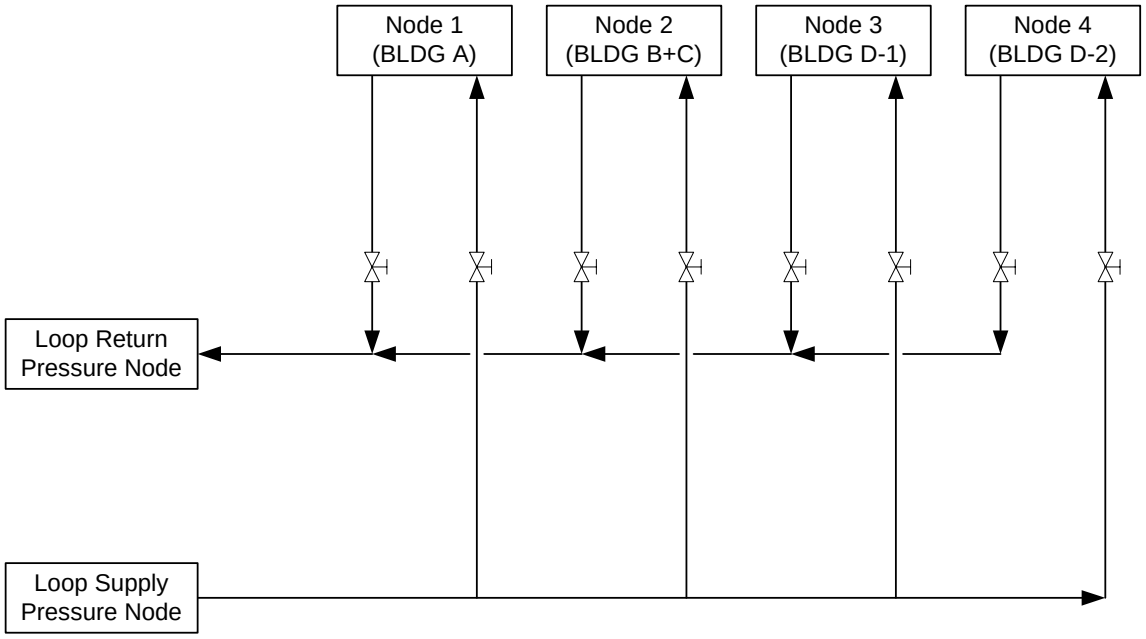

Figure 15 Skeletonized Representation of a Large DCS Hydraulic System

On the source system side, the entire plant can be simplified into two pressure nodes or one flow node with metered pressures or flow. On the load system side, the entire in-building chilled water piping can be simplified into one flow node with metered flow. For example, Figure 15 is the skeletonized system layout of Figure 14. Buildings B and C are represented by one flow node, at which the flow demand is the measured total flow for these two buildings. Building D is represented as two flow nodes (D-1 and D-2), at which the flow demands are measured by each flow meter.

There are lots of situations where multiple buildings are tied into a branch and that branch is connected to the loop. Whether or not to aggregate them into one flow node is determined by evaluating the purpose of the model. When adding new buildings to a system, the total flow demand of the system will be increased. Consequently, the system pressure drop will be increased. Ensuring adequate differential pressure at the most remote buildings, i.e. buildings that are the farthest from the plant, is essential when adding new buildings. These buildings are usually located at the end of a branch. Therefore, the most remote buildings must be included in the physical model. In addition, even a very large DCS can only cover a few hundred of buildings, a small fraction of those included on a DWS. Therefore, it is preferred that every building on the DCS be included in the model.

6.4 Model Representation

A DCS hydraulic system is basically a pipe network that contains various components of the system, and defines how those components are interconnected. From the modeling point of view, system components can be classified into two basic network

elements: (1) nodes, which represent features at specific locations within the system, and (2) links, which define relationships between nodes. Mathematical models of system components have been well developed and published in various references (Applied Flow Technology, 2004). Pipe network simulation software packages usually have these system components built in so the modeler can easily use them as input-output black boxes. This section is intended to discuss how to use these model components to build the DCS hydraulic system model.

6.4.1 Model Components

The commonly used model components for modeling of a DCS hydraulic system are summarized in **Error! Reference source not found.**. Their type and primary usage in a model are summarized as well. The majority of the model components used for DCS hydraulic system modeling are the same as those used for DWS modeling. Specific considerations for some of the modeling components are discussed in this section.

Reservoir, Assigned Pressure, and Assigned Flow

In the real-world, a reservoir is a large tank or a natural or artificial lake used for collecting and storing water for human consumption or agricultural use. In water distribution system modeling, a *Reservoir* is a boundary node with infinite capacity to supply or accept water so that the hydraulic grade of the reservoir itself remains constant, in other words, a fixed pressure point in the system. A boundary node is a network element used to represent locations with known hydraulic grade elevations. Every model

must have at least one boundary node as a reference point for the rest of the pressure and flow calculations.

Table 2 Commonly Used Model Components for a DCS Hydraulic System

Model Component	Type	Primary Modeling Purpose
Pipe	Pipe	Conveys water from one node to another
Reservoir	Junction	Provides water to the system, behaves as a infinity capacity source of water
Tee/Wye	Junction	A junction that diverts flow from one pipe to multiple pipes or converges flow from multiple pipes to one pipe.
Area Change	Junction	A junction that connects two pipes with different diameters
Bend	Junction	A junction that changes the flow direction in pipes
Pump	Junction	Raises the hydraulic grade to overcome elevation differences and friction losses
Valve	Junction	Reduces the pressure in the system
Control Valve	Junction	Controls flow or pressure in the system based on specified criteria
Assigned Pressure	Junction	Mathematically assigns known pressure at a specified location
Assigned Flow	Junction	Mathematically assigns known flow at a specified location
General Component	Junction	Allows a customized loss model for a general component by specifying the loss factor as a function of flow

Some pipe network simulation software packages provide *Assigned Pressure* and *Assigned Flow* model components to let the user easily assign known boundary conditions to specific locations in the network model. The *Assigned Pressure* component has much in common with the *Reservoir* component. In each case, the user can specify parameters in order to achieve a known boundary condition and the rest of the system distributes the flow in a manner consistent with the defined pressure. However, unlike the *Reservoir* component, which only specifies the static pressure, the *Assigned Pressure* component allows users to select either stagnation pressure or static pressure. This is useful where the measured static pressure is for a location with a velocity. The *Assigned Flow* component allows users to specify a known flow rate entering or leaving the system at a particular location. Because the iteration of the pressure and flow calculation starts from the known pressure, the *Assigned Flow* component is not a boundary node.

The *Reservoir*, *Assigned Pressure*, and *Assigned Flow* Components can be used to define the boundary conditions when modeling a DCS hydraulic system. To specify the boundary conditions, the Plant loop control sequence should be studied. Usually, the plant maintains a set-point schedule of the secondary system differential pressure. With the known plant supply and return pressures, the plant can be represented by a pair of *Reservoir* components or *Assigned Pressure* components. The flow through the reservoirs is automatically balanced by the summation of the flow from individual buildings, i.e. the load system. When the source system consists of multiple plants, the *Assigned Flow* component can be used for certain plants if their flow is a known parameter. At the load system, because the building flow rate is the input parameter, a

pair of *Assigned Flow* components can be used to represent a building with known flow rate.

Junctions

The *Junction* corresponds to a location where two or more pipes meet. The counterpart of a *Junction* in the real-world is fittings, such as tees/wyes, area changes, bends, etc. The scale of a DWS can be very large and cover hundreds of square miles of a metropolitan area, which is much larger than even the largest DCS covered area. Relative to the scattered length of piping, the number of fittings in a DWS is small. Friction losses at fittings are considered as minor losses in DWS modeling and can be ignored (Walski et al. 2001). However, the situation for DCS hydraulic systems is different. Compared with DWSs, the scale of a large DCS hydraulic system is much smaller. Relatively, the number of fittings in a DCS hydraulic system is much higher than in a DWS. Friction losses at fittings need to be counted when modeling a DCS hydraulic system. With modern computer technology, loss models for such fittings are usually built into the simulation software packages. Including fitting losses in the DCS hydraulic system model is no longer a difficult task.

The other major physical characteristic of a *Junction* component is its elevation. This is particularly important in DWS modeling because the discharge pressure at end users is a key question the DWS model needs to answer. In a DCS hydraulic system, especially its distribution system, the supply and return lines are usually laid in parallel. The pressure loss built up by the effect of elevation on the supply side will be canceled out at the return side. Therefore, the elevation of fittings can be neglected. On the other hand,

the building differential pressure, which is driven by the water flowing through buildings, is the most interesting parameter for planning and operation purposes.

General Components

Some pipe network simulation software packages provide a convenient model component called a general component, so that the modeler can build customized model components. The *General Component* can be used to model equipment such as chillers, heat exchangers, etc. Using the *General Component*, the modeler can either specify a *k* factor, or generate a resistance curve for the specific equipment. The resistance curve is usually in the form of:

$$\Delta H = a + b \cdot Q + c \cdot Q^2 + d \cdot Q^3 + ...$$

where:

ΔH = pressure drop across the equipment.

Q = flow rate across the equipment.

The resistance curve can be obtained either from the manufacturer or through field test. For example, in the refrigeration process, the chilled water flows through a bundle of tubes in the evaporator of a chiller and exchanges heat with the refrigerant outside the tubes. Chillers may have single pass, double pass or even multi pass configurations. To build the hydraulic model for a chiller, the manufacturer-provided evaporator hydraulic performance curve is a good reference. If the manufacturer's curve is not available, a field test can be conducted to trend the flow and differential pressure. Then regression analysis can be conducted to obtain the resistance curve.

6.4.2 Network Topology

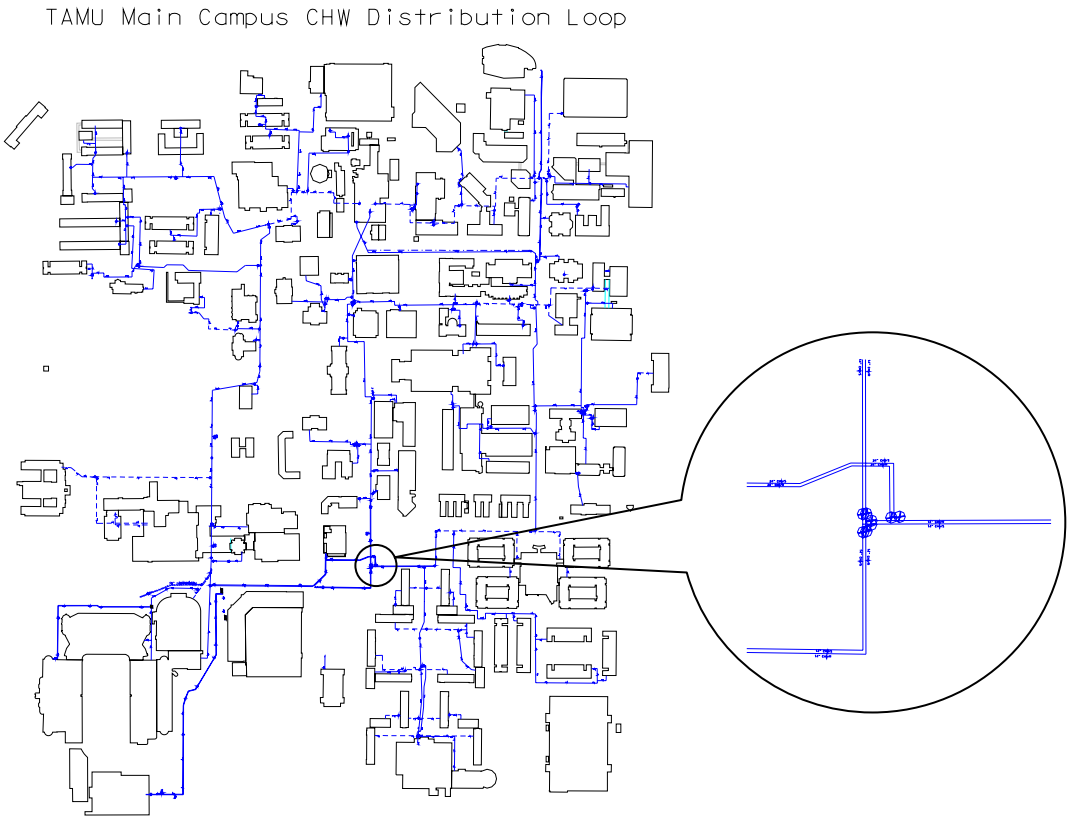

Figure 16 Even a Zoomed View of a System Map May Not Clearly Show the Details of the Piping Interconnection

The most fundamental requirement for the physical model is to have an accurate representation of the network topology, which specifies what the system components are and how they are interconnected. If a model does not faithfully duplicate the actual system layout (for example, the model pipe connects two junctions that are not really connected), then the model will never accurately represent the real-world situation, no

matter how well the quality of the rest of the data. Generally speaking, system maps are good sources of topological information. However, they may lack the detailed level of topological information needed by the modeler. As illustrated in Figure 16, the zoomed intersection of pipes still may not clearly demonstrate the actual piping connection. Such situations may occur frequently when inputting the topological information into the simulation program. The modeler should be very careful of such unclear piping intersections. Otherwise, serious model inaccuracies may result. Field investigation is desirable, if possible, for critical connection points, such as at the connection of independent loops.

6.5 Case Study

This section is intended to demonstrate the physical modeling process through an actual case study, the modeling of the TAMU main campus DCS hydraulic system. The background information about this system has been introduced in chapter III. In the following chapters, other DCS hydraulic system modeling topics such as peak flow demand model process, modeling verification and calibration, and model application will be discussed by using TAMU main campus DCS hydraulic system modeling as examples.

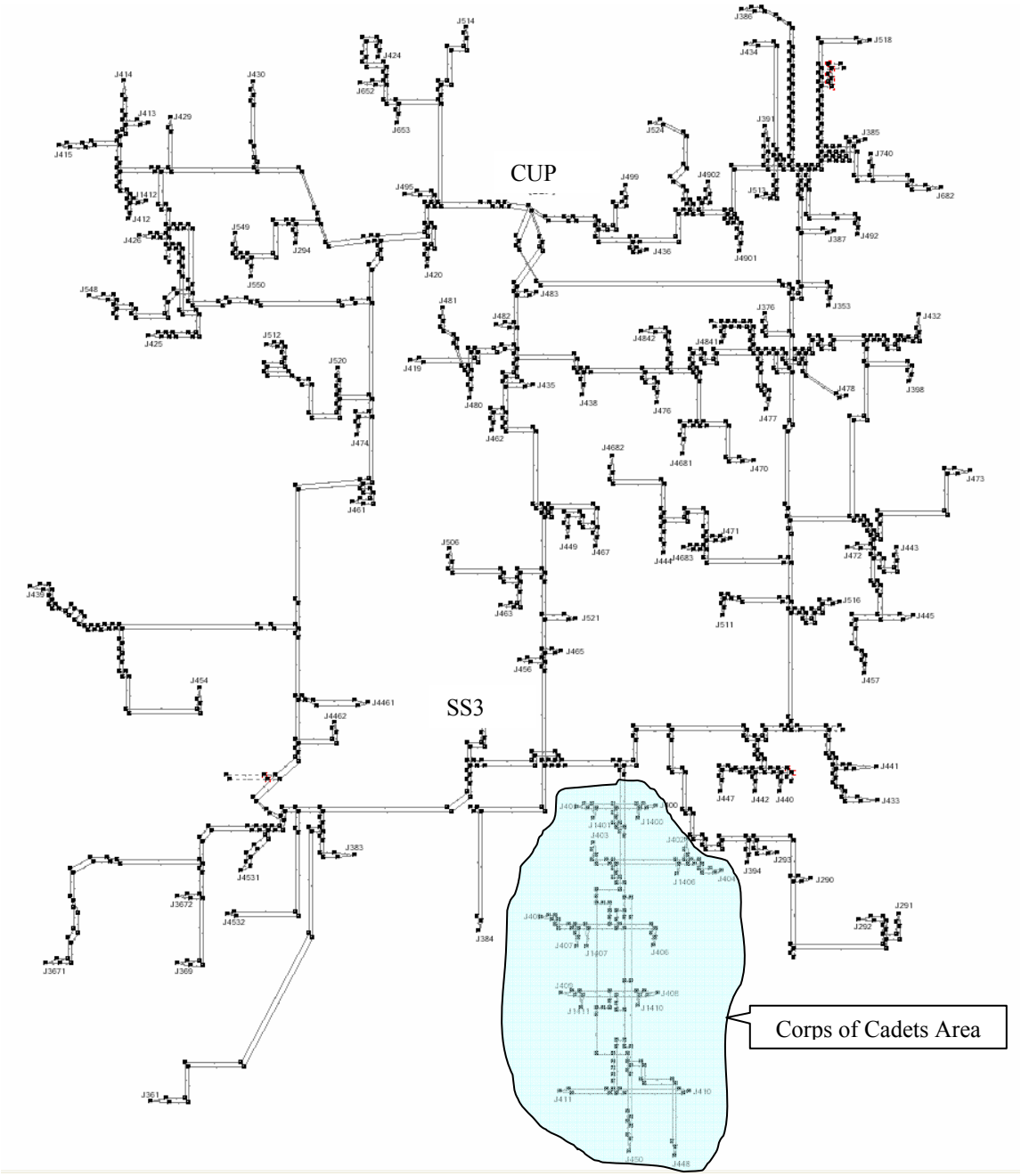

Figure 17 Graphic Layout of TAMU MC DCS Hydraulic System Model

First, system maps and as-built drawings were obtained from the Space Science Laboratory. However, these maps and drawings are not completely accurate fro a variety

of reasons. Because the TAMU main campus began construction early in the last century, there have been decades of expanding, renovation, and reconstruction of buildings and the chilled water system. Some useful information such as building air conditioned area (AC area), design cooling load, design chilled water flow rate, etc is not available for some buildings. The university has also been conducting a large scale energy conservation program for over 10 years. CC® measures have been continuously implemented to optimize the energy performance of buildings. Many building HVAC systems have been retrofitted and their original drawings do not reflect the current system configuration. Moreover, the control programs of many building HVAC systems have been optimized and the actual energy consumption may be lower than the original design values. On the other hand, the energy performance of many old buildings may have deteriorated, and their energy consumption may be higher than normal. To reflect the most updated system structure and to achieve high model accuracy, the author, as part of a team, conducted a field survey of the underground piping infrastructure wherever underground tunnels were available. One-line drawings were made to record the piping connectivity, pipe length, pipe size, location and type of fittings such as valves, area changes, tees/wyes, etc. The field survey covered more than 50% of the total modeled area. By inputting the cross checked information obtained through drawings and the field survey, the physical model was built to represent the current TAMU main campus DCS hydraulic system. Table 3 is a brief summary of the number of selected components included in the physical model.

Table 3 Statistical Summary of the Physical Model of TAMU Main Campus DCS Hydraulic System

Number of modeled pipes	1,747
Total length of modeled pipes (feet)	89,045
Number of modeled junctions	1,479
Tees/wyes	274
Area changes	130
Bends	722
Valves	352
Number of modeled buildings	117

On the Source System side, i.e. the plant side, the Central Utilities Plant (CUP) and the South Satellite Plant (SS3) provide chilled water service to these buildings for space cooling. The CUP supplies chilled water to the campus through four 24" main pipes from a common header in the plant. The plant operation maintains the secondary system differential pressure at its set-point, which follows a schedule according to the weather conditions. Under the peak cooling load condition, the set-point is about 16 psi. The SS3 supplies chilled water to the campus through two 24" main pipes. The chilled water system of this plant is controlled to maintain a fixed chilled water flow rate through individual chillers. Because the decoupler of this plant was shut off, the secondary system of this plant sees a constant chilled water flow rate. In the physical model, Assigned Pressures (see Chapter V) are used to represent CUP and Assigned Flows are used to represent SS3.

On the Load System side, i.e. the building side, all buildings have building pumps and building control valves to control their own primary/secondary systems. Because each building chilled water system is controlled to maintain a certain amount of chilled

water flow through the building, in the physical model, the buildings are represented by flow control devices. Figure 17 is a graphic layout of the physical model.

CHAPTER VII

PEAK FLOW DEMAND MODEL

7.1 Introduction

The energy required for the chilled water to cool the buildings is the driving force behind the thermal dynamics in the DCS. From the hydraulic point of view, the building chilled water flow is the driving force behind the hydraulic dynamics occurring in the DCS hydraulic system.

This chapter explores a practical procedure for developing the demand model for a large DCS hydraulic system for master planning purposes. Using pre-existing data, including metered data, billing records, system operational records, etc., to build the demand model is a well accepted method in water distribution system modeling (Walski et al. 2001). A similar approach is applied to the large DCS hydraulic system.

In the following sections of this chapter, the kind of flow demand model suitable for a master planning study of a large DCS hydraulic system, i.e. demand modeling scope, is defined first. The information to be collected and determination of the peak load conditions are discussed next. Then the detailed approach to peak demand modeling is discussed in the latter part of this chapter.

7.2 Demand Modeling Scope

The objective of the thesis is to develop a method for the modeling of DCS hydraulic systems for master planning purposes. There are two major objectives when conducting a master planning study of a large DCS hydraulic system: (1) determine whether the capacity of the current system would satisfy the demand of planned new buildings; and

(2) determine the impact of the planned new buildings on the existing buildings. The key is to develop the demand model under the maximum flow demand condition. If under the peak flow demand condition, the planned system expansion/demolition could satisfy the pressure requirements of the buildings, it should work for partial demand conditions as well. Therefore, developing a peak flow demand model is essential to meet the master planning needs of a large DCS hydraulic system.

7.3 Information Collection and Verification

To develop the peak flow demand model, a large amount of information and data needs to be collected first. Because the basic approach to develop the peak flow demand model is by using pre-existing data, historical data of the chilled water consumption at buildings and the chilled water production at the plant should to be collected. The DCS plant usually keeps complete historical data of its chilled water production. However, it is rare that a large DCS hydraulic system has enough recorded data to directly define all aspects of chilled water usage of every building. Even in cases where both production data and building data are available, there may be disagreements between the two. Therefore, other kinds of data and information needed to help the modeler to determine the peak flow demand for un-metered buildings should be collected as well. The following parts of this section discuss in detail what kind of data and information should be collected and how to collect them.

7.3.1 Data Records

During years of operation, maintenance, renovation/retrofitting, and CC® efforts, buildings' energy performance will change over time. On the other hand, campus

expansion may result in adding new chillers in the plant. To reflect the current system conditions, the metered data should cover at least the most recent cooling season. When the metered data are not available, the historical data for previous cooling seasons, if available, is also desirable because if the most recent data is not available, it can at least indicate the building's past performance.

With modern computer technology, data records are usually stored in the building metering system or in the plant metering system. Data records also can be obtained from the paper format of operation records or even field measurement records taken during the field investigation.

The data records that should be collected include:

1. *Weather data.* The local dry-bulb and wet-bulb temperature data need to be collected. The weather data are used to determine the peak flow demand condition. Also, it can be used to obtain the peak flow demand for individual buildings. Weather data can be obtained from a local weather station. A building metering system and/or plant metering system may have such information as well, but this may be of questionable accuracy.
2. *Plant chilled water production*. The plant total chilled water flow rate, and supply/return temperatures and pressures need to be collected. The total chilled water flow rate at the plant can be used to balance out the flow of un-metered buildings. The supply and return pressures should be measured on the plant's secondary system side so that they can be used to define the boundary conditions of the DCS hydraulic model. The supply and return temperatures should be measured at the plant's

secondary system as well. The return temperature represents an overall mixed chilled water return temperature from all the buildings. Therefore, the plant differential temperature is a good average differential temperature of the buildings.

3. *Building chilled water consumption*. The building chilled water consumption data needed includes the chilled water flow rate, and supply/return temperatures and pressures if available. All the parameters should be measured at the building's primary system, i.e. at the building entrance.

7.3.2 Building Information

To establish the peak flow demand for un-metered buildings, information that may affect the chilled water consumption should be collected. Such information is mainly related to the building's cooling load, characteristics of the building HVAC system, and the control logic of the building chilled water system. Detailed explanation of the data needed follows.

1. *Gross square footage (GSF) or air-conditioned area if available*. This information enables the modeler to compare the cooling load of different types of buildings on a unit area basis.
2. *Design cooling load*. This parameter is an indication of the maximum cooling load the building would have. However, actual building performance may be very different from the design value. The modeler should be careful when using the design value to determine the peak flow demand.
3. *Design chilled water differential temperature*. Some as-built drawings may show the maximum chilled water differential temperature across the building under the design

condition. This value is usually 12 °F. For newer buildings with energy conservation considered in the design phase, this value may be higher, e.g. 18 °F. However, for a variety of reasons (see chapter II and chapter III), many buildings can not achieve their design building ΔT. This is especially likely for old buildings or buildings converted from three-pipe to two-pipe HVAC control.

4. *Detailed HVAC system information*. Detailed HVAC system information that can help the modeler judge how the chilled water system performs in the building should be collected. Such information includes: three-way or two-way valve controlled cooling coils, pneumatic controlled or Direct Digital Controlled (DDC) valves, constant speed or VFD pumps, control sequences of the pumps and valves, piping structure in the pump room, etc. Usually mechanical drawings provide detailed building chilled water system information. Facility owners keep records of drawings after the building is actually built, or renovated/retrofitted. Such as-built drawings are good sources for building information.

7.3.3 Field Investigation

Many large DCSs do not have full metering coverage for all of their buildings. In many circumstances, the building metering system does not trend all the relevant flow, temperature, and pressure data. As-built drawings may not be available for some buildings and even the available drawings may be outdated. Field investigation is necessary for such situations. The field investigation should:

1. Identify the major function of the building. A university campus building, as an example, may consist of offices, laboratories, and classrooms, while another may include dorm rooms and dining facilities, or one of many other combinations of functions.
2. Trace the chilled water piping in the pump room; identify major devices in the chilled water system, such as control valves, pumps, location of EMCS sensors, system bypass, etc; draw a schematic layout of the building loop structure; determine whether the system is a constant primary system or a variable primary system (see chapter III).
3. Collect pump information; write down the name plate data, such as manufacturer, model number, design flow, head, horsepower, etc; determine whether the pump is constant speed or VFD controlled.
4. Check building HVAC systems; identify the major type of the system (VAV or CAV system). Evaluate the water side control of the building HVAC systems. Determine whether it is DDC or pneumatic controlled. Obtain the control sequences. Identify how the building control valve and pumps are controlled. For example, are they controlled to maintain a building differential pressure or temperature? What is the set-point, or schedule? Rank the operation and maintenance condition of the HVAC system.

Determining the chilled water flow demand is not a straightforward process like collecting data for the physical model of a system. Some data, such as billing and production records, can be collected directly from the utility but are usually not in a form

that can be directly entered into the model. Once this information has been collected, establishing the peak flow demand is a process requiring study of past and present usage trends, and, in some cases, the projection of future usage. The following sections of this chapter will discuss how to use the collected information to develop the peak flow demand model.

7.3.4 Information Verification

Building as-built drawings may not reflect the most recent changes on its chilled water in-building systems because of the on-going CC® process. For example, during the CC® process on TAMU main campus buildings, many buildings have been converted their chilled water in-building systems from constant flow systems to variable flow systems. Constant speed pumps have been converted to VFD pumps. Building by-passes have been removed or valved off, and accordingly, building chilled water controls have been optimized to save the pumping energy. Some times, the function of a building may be changed. For example, one of the student dorms on TAMU main campus has been converted to office building. In this case, the chilled water consumption of this building may be different with its original design. Therefore, before the construction of the demand model, the information collected from maps and drawings should be should be verified and crosschecked with this field investigated results. If they are inconsistent, the field investigated results are more up-to-date and accurate and should be used to construct the demand model.

7.4 Peak Flow Demand Conditions

Identifying the conditions under which the overall system flow peaks is the first step in developing the peak flow demand model. This section defines the peak flow conditions and discusses how to determine the system parameters under the peak flow demand conditions.

The following sub-sections use actual measured data as examples to discuss the peak flow demand. The data were metered by the plant metering system for the time period between 9/6/2005 and 11/23/2005. Usually, it is preferred to have the data from at least a complete cooling season. Since several plant meters were taken out for repair and calibration during 2005, the data before 9/6/2005 could not be collected. However, during summer break, occupancy on campus was lower than normal, so the campus cooling load was not expected to be highest during this break. Also, it was fortunate that the actual peak weather condition occurred near the end of September of 2005. Therefore, the data between 9/6/2005 and 11/23/2005 should cover the actual peak flow demand conditions.

7.4.1 Define the Peak Flow Demand Conditions

Due to the diversity effect, the chilled water flow rate of individual buildings does not peak at the same time and individual buildings may not reach their design peak flow. For example, the actual metered TAMU peak total chilled water flow (2005 data) is around 80% of the summation of the building design values. Therefore, simply adding up design values of individual buildings is likely to overestimate the overall system peak. The peak flow demand conditions should represent a moment when the overall system

flow peaks. The actual metered data of the plant chilled water production are used to determine the peak flow demand conditions as it naturally takes the diversity effect into account.

7.4.2 Factors That Affect the Flow Demand

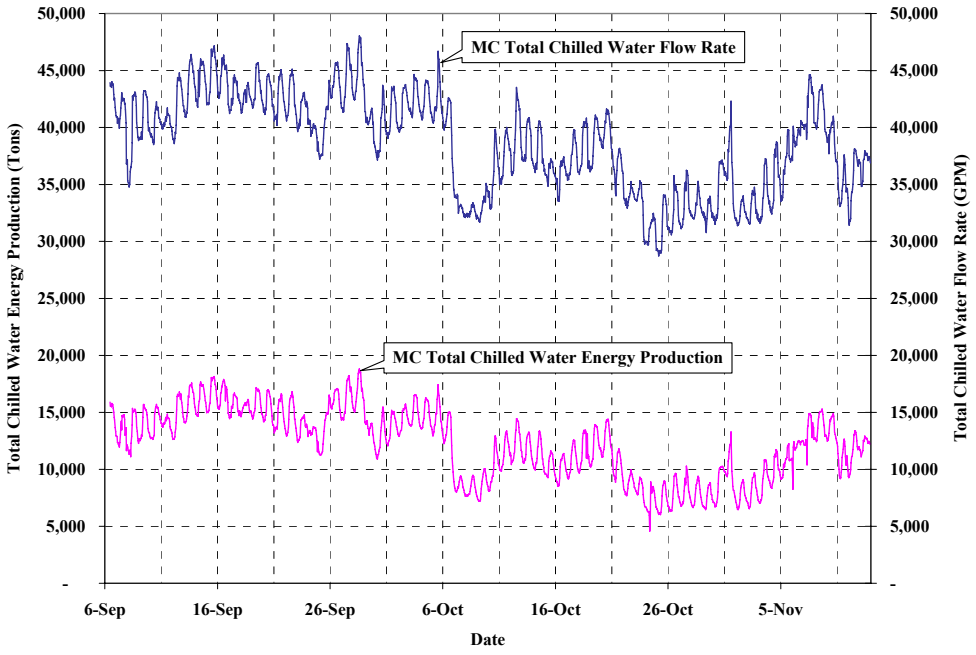

Figure 18 Time Series Plot of TAMU Main Campus Chilled Water Production

As summarized in chapter III, large DCS hydraulic systems are usually variable flow systems. The total chilled water flow rate generally tracks the total cooling load. Therefore, the peak flow demand conditions usually coincide with peak cooling load conditions. For example, Figure 18 is the time series plot of the total chilled water energy production and flow rate of the TAMU main campus DCS. It demonstrates that

the chilled water flow follows the energy use very well. Figure 19 illustrates the relationship between the TAMU main campus chilled water production and the chilled water flow rate. It clearly shows the linear relationship between these two factors, especially at high cooling loads.

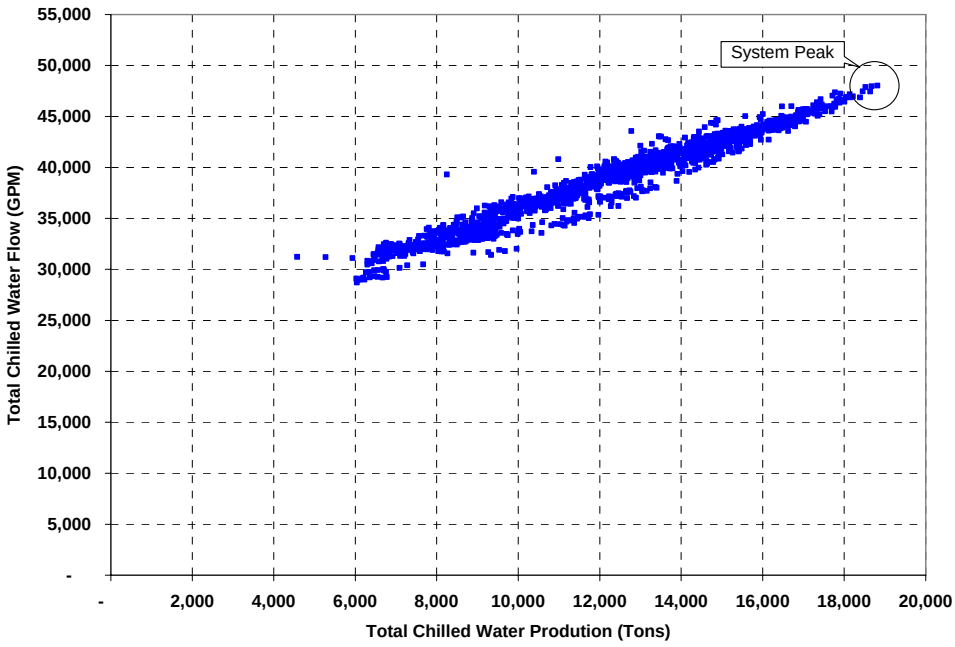

Figure 19 Relationship between TAMU Main Campus Total Chilled Water Production and Flow

As the chilled water flow for a large DCS hydraulic system is proportional to the system cooling load, it can be further related to the weather conditions. Generally speaking, when the ambient temperatures (dry-bulb temperature and wet-bulb temperature) are higher, the system cooling load becomes higher and hence the system chilled water flow becomes higher.

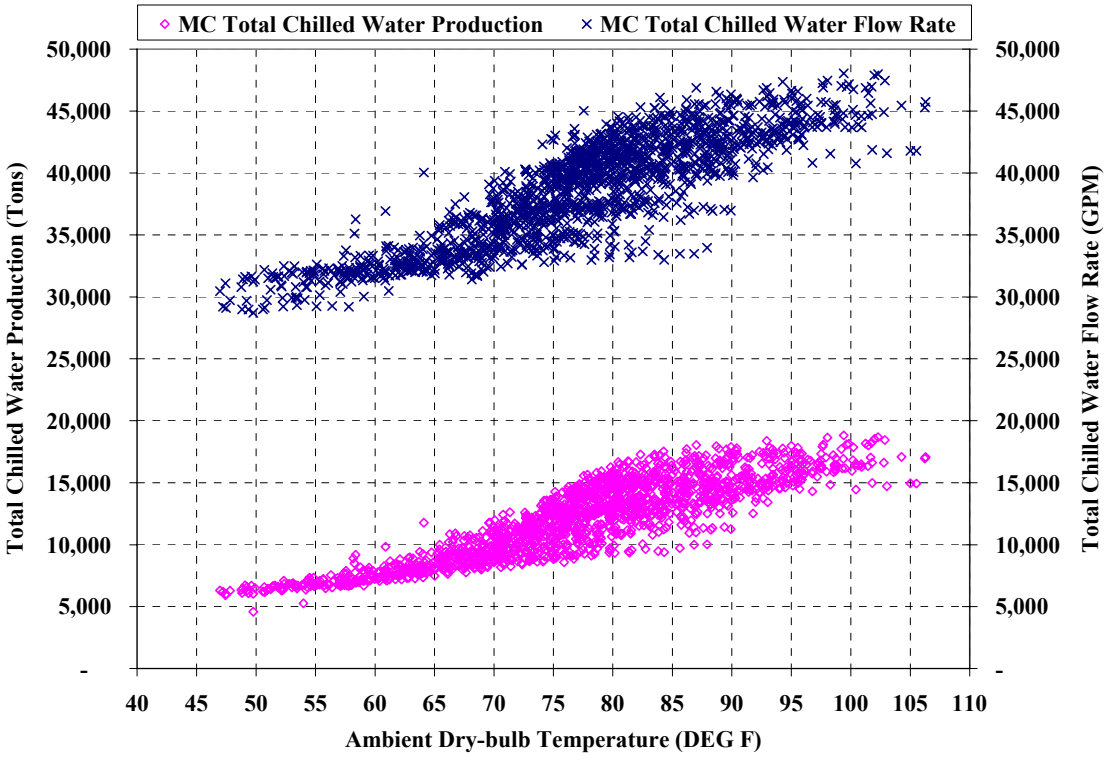

Figure 20 TAMU Main Campus CHW Production and Flow vs. Dry-bulb Temperature

Figure 20 is a scatter plot of the TAMU main campus chilled water production and flow as functions of ambient dry-bulb temperature. It shows when ambient dry-bulb temperature increases, the system load and flow increase as well. However when the ambient dry-bulb temperature reaches maximum e.g. above 103°F, the system load and flow become slightly lower (see the right side of Figure 20). This is because the campus cooling load is not only related to the ambient dry-bulb temperature but also related to the ambient wet-bulb temperature. Figure 21 is a scatter plot of the TAMU main campus chilled water production and flow as functions of ambient wet-bulb temperature. It

clearly shows the system cooling load is proportional to the ambient wet-bulb temperature as well.

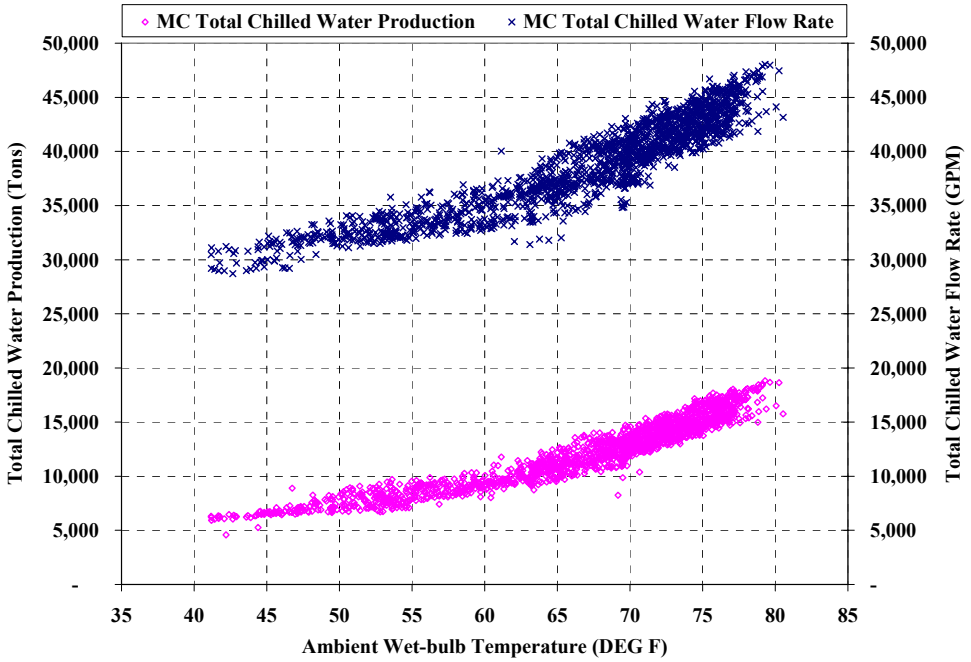

Figure 21 TAMU Main Campus CHW Production and Flow vs. Wet-bulb Temperature

Generally speaking, the system cooling load is proportional to the ambient air enthalpy. Figure 22 is a scatter plot of the TAMU main campus chilled water production and flow over ambient air enthalpy. It clearly shows the system cooling load is proportional to the air enthalpy.

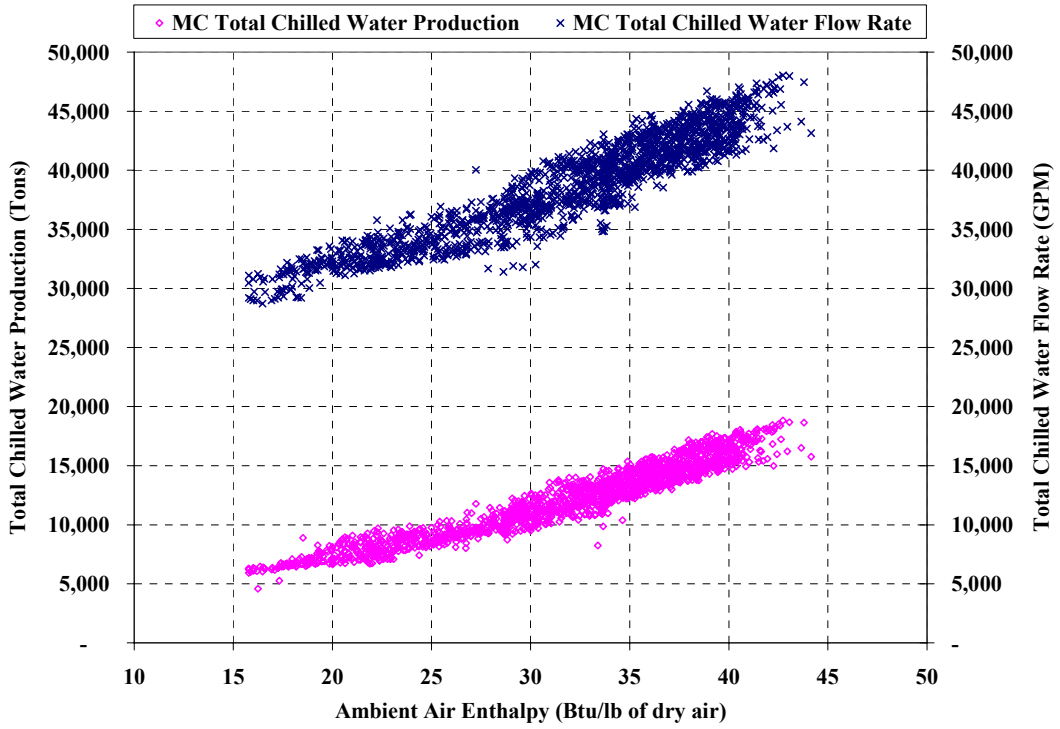

Figure 22 TAMU Main Campus CHW Production and Flow vs. Ambient Air Enthalpy

Based on the psychometric chart, at a certain dry-bulb temperature, the air enthalpy (Btu/lb of dry-air) increases significantly when the wet-bulb temperature increases, means the cooling load increases due to ventilation air. For example, at 80°F dry-bulb temperature, when the wet-bulb temperature varies from 70°F to 80°F, the air enthalpy increases from 34.0 Btu/lb of dry air to 43.7 Btu/lb of dry air. This indicates that at the same dry-bulb temperature, the system load could vary in a wide range (see Figure 20) On the other hand, at a certain wet-bulb temperature, the air enthalpy changes insignificantly when the dry-bulb temperature increases, meaning the cooling load is

almost constant. For example, at 70°F wet-bulb temperature, when the dry-bulb temperature varies from 70°F to 100°F, the air enthalpy only decreases from 34.1 Btu/lb of dry air to 33.8 Btu/lb of dry air. This explains why the band of system load in Figure 20) is thicker than that in Figure 21. From the analysis above, it can be concluded that the air enthalpy is the direct indicator of the peak cooling load condition. If the air enthalpy is not available (it can not be directly measured), the ambient wet-bulb temperature is a better indicator than the dry-bulb temperature.

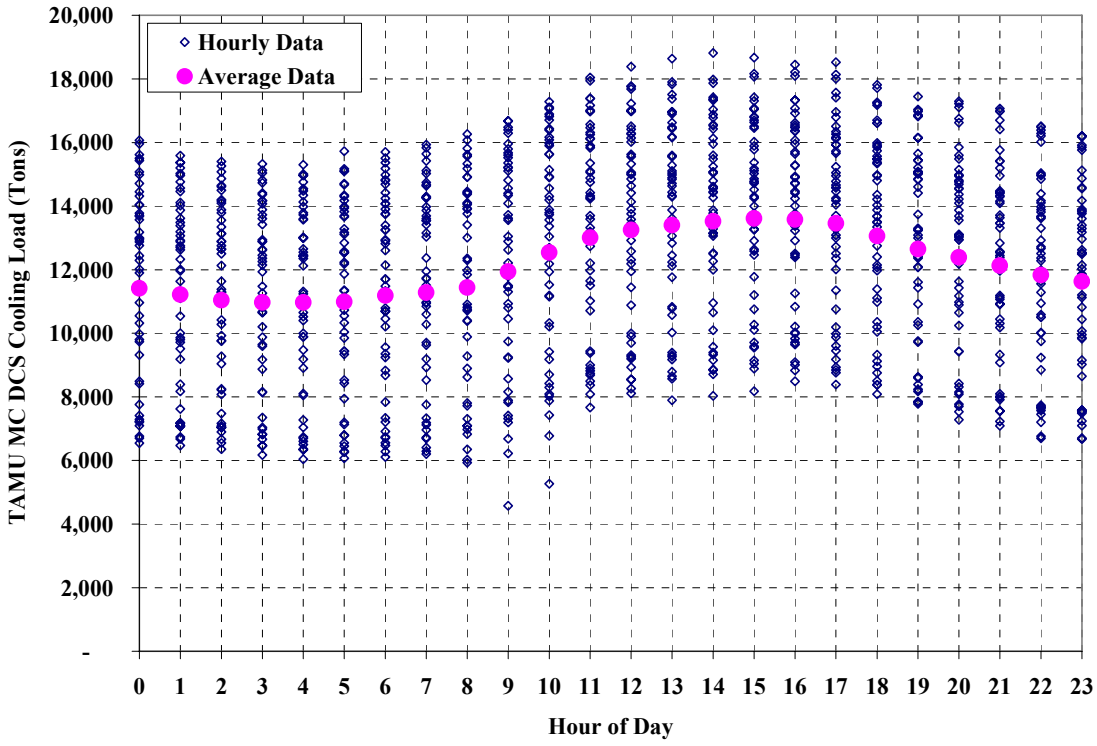

Figure 23 TAMU MC DCS Cooling Load vs. Hour of Day

Besides the weather conditions, occupancy and the corresponding variation in gains from electricity is the other factor that affects the peak cooling load conditions. Especially, for university campuses, during summer break, even if the weather condition reaches peak, the total cooling load on the campus may not reach peak because of lower occupancy and internal heat gain of the buildings. For a normal working schedule of a university campus, the peak cooling load usually appears between 13:00 to 17:00 of a working day. For example, Figure 23 illustrates the TAMU main campus DCS cooling load profile versus the hour of day. The small circles are actual measured hourly data, and the large dots are the average cooling loads for the corresponding hours.

7.4.3 Procedure to Determine the Peak Flow Demand Conditions

This section demonstrates the procedure to determine the peak flow demand condition from actual metered data through a case study of the TAMU main campus DCS.

First, the peak flow demand weather conditions are filtered out by selecting times when the weather conditions equal or exceed the local climate design conditions. According to ASHRAE (2000), the design conditions usually include direct sunlight on the building, 95 to 100°F dry-bulb temperature, and 73 to 78°F wet-bulb temperature. For example, TAMU main campus is located at College Station, Texas. If the 0.4% design criterion is applied, the design dry-bulb temperature and wet-bulb temperature for this location are 98°F and 75°F respectively. The system chilled water energy production and flow corresponding to 98°F dry-bulb temperature and 75°F wet-bulb temperature and above are filtered out and listed in Table 4.

Table 4 Peak Flow Demand Candidates

Time	TDB (°F)	TWB (°F)	Enthalpy (Btu/lb)	Energy (Tons)	Flow (GPM)	Comments
9/15 16:00	99.7	78.1	41.4	18,096	46,937	Wet-bulb temperatures did not reach the highest values on these days hence the cooling load and the flow did not reach the peak.
9/15 17:00	99.8	78.5	41.9	18,137	47,178	
9/17 15:00	98.6	77.2	40.6	16,373	44,130	
9/17 16:00	100.6	77.0	40.3	16,385	43,911	
9/17 17:00	100.9	77.0	40.4	16,276	43,688	
9/18 16:00	100.1	77.1	40.5	15,962	43,681	
9/18 17:00	98.7	77.0	40.4	16,132	43,953	
9/19 16:00	99.4	76.5	39.9	16,924	44,840	
9/22 14:00	98.8	75.7	39.1	16,430	44,612	
9/22 15:00	100.2	76.7	40.0	16,816	45,116	
9/22 16:00	100.9	75.7	39.0	16,487	44,594	
9/25 14:00	100.4	76.1	39.5	14,455	40,769	Week end; although dry bulb temperatures reached peak values for the year, the campus load did not reach the peak.
9/25 15:00	103.0	76.9	40.2	14,722	41,593	
9/25 16:00	105.5	77.6	40.9	14,935	41,794	
9/25 17:00	105.0	77.1	40.4	14,956	41,790	
9/25 18:00	101.8	76.4	39.7	14,980	41,862	
9/25 19:00	98.3	75.5	38.9	14,834	41,560	
9/26 13:00	98.7	75.7	39.1	16,968	45,490	Wet-bulb temperatures did not peak.
9/26 14:00	101.7	75.5	38.9	17,035	45,620	
9/26 15:00	104.3	76.1	39.4	17,082	45,442	
9/26 16:00	106.3	76.2	39.5	17,072	45,735	
9/26 17:00	106.2	76.1	39.3	16,962	45,293	
9/27 14:00	100.2	78.8	42.2	17,868	46,740	Wet-bulb temperature was high but slightly lower than that of 9/28/2005.
9/27 15:00	101.2	78.9	42.3	18,162	46,870	
9/27 16:00	101.8	78.9	42.3	18,214	46,975	
9/27 17:00	101.5	78.7	42.0	18,008	46,452	
9/27 18:00	98.5	76.7	40.0	17,233	45,469	
9/28 13:00	98.0	80.3	43.8	18,638	47,451	Final candidates correspond to the highest day of wet bulb temperatures.
9/28 14:00	99.4	79.3	42.7	18,815	48,033	
9/28 15:00	102.3	79.6	43.1	18,673	47,970	
9/28 16:00	102.9	78.8	42.2	18,452	47,457	
9/28 17:00	102.0	79.1	42.5	18,524	47,875	
9/28 18:00	99.2	77.2	40.5	17,714	47,042	

Note:

- TDB – ambient dry-bulb temperature.
- TWB – ambient wet-bulb temperature.
- ΔP – Differential pressure measured at the plant entrance.
- ΔT – Differential temperature measured at the plant entrance.

Second, the factors that affect the peak flow conditions discussed in the previous section are considered to further determine the peak flow demand conditions among those candidates. As shown in Table 4, from 9/15/2005 to 9/26/2005, the ambient air enthalpies were lower than the rest of the candidate periods. Therefore the data shows lower cooling loads and flow and these data are eliminated from the candidates. Also, it is noted that the cooling load of 9/25/2005 is significantly lower than the rest of the candidates. This is because that day was Sunday with less occupancy on campus. The ambient air enthalpy, system cooling load and flow of 9/27/2005 were lower than those of 9/28/2005. Finally, the time period between 13:00 and 17:00 of 9/28/2005 is when the peak flow demand condition occurs. It is also noted that the peak flow demand condition stably lasted four hours, during which the total chilled water flow varied only 582 GPM (only 1% of the maximum flow of 48,033 GPM). The long time period of these peak flow demand conditions also provided all the buildings on campus enough time to establish a stable peak flow condition. At last, due to the data availability, the final peak flow demand moment is then determined at 9/28/2005 17:00.

After the peak flow demand is determined, system parameters, if metered at this moment, are used to develop the peak flow demand model. The system parameters

should include the boundary pressure conditions, i.e. the plant supply and return pressures, system overall ΔT, system main trunk flows, buildings' chilled water flow, ΔT, and ΔP (if metered).

7.5 Spatial Allocation of Peak Flow Demand

It is ideal if every building on the DCS has an accurate chilled water flow meter, so that the trended data at the peak demand moment can be directly assigned to each building as its peak demand flow. However, it is rare that a large DCS hydraulic system has enough recorded information to directly define all aspects of building chilled water usage. Even in cases where both production data and full building metered data are available, there may be disagreements between the two. The total plant flow may be summarized from multiple plant flow meters, and the total building flow may be summed from hundreds of building flow meters. The accumulated errors of each individual flow meter and other factors (e.g. system time not synchronized in different metering systems) are likely to make the data from plant side and buildings inconsistent.

The total chilled water flow demand can be categorized into *metered demands* and *un-metered demands*. The total of *metered demands* is the metered portion of the total water flow production. The un-metered portion of the total chilled water production plus the system leakage constitute the total of the *un-metered demands*. The key to the demand modeling is how to assign an appropriate flow demand value for each un-metered building.

Following the widely adopted approach used in DWS modeling (Walski et al. 2001), this section is intended to use mass balance to allocate the total of un-metered demand to

those un-metered buildings. The mass balance of the entire system is first discussed. Then, the methods used to determine the peak flow demand for metered buildings and un-metered buildings are discussed in detail. At the end of this section, the reconciliation of the building peak flow demands is discussed.

7.5.1 Mass Balance

Regardless of how the peak flow demand is assigned to individual buildings, the chilled water flow out of the source system must be equal to the total flow through the load system plus the flow leaking out of the system. In equation form, this can be stated as:

$$Q_{source} - \sum Q_i - Q_{makeup} = 0 \qquad 15$$

In Equation 16, Q_{source} is the total chilled water flow out of the source system, such as chiller plants and storage tanks. Q_i is the chilled water flow for building *i* of the load system. Q_{makup} is the make up water flow at the plant expansion tank. For a condenser water system, the typical water makeup is ~1% to compensate for the water evaporation and drift losses. Chilled water systems are closed systems. The water losses are mainly due to leakage. For a well maintained chilled water system the make up rate should be much less than that of the condenser water system. For example, the metered data shows the makeup rate for the TAMU main campus chilled water system is less than 0.1%. Therefore, the makeup flow of a large DCS hydraulic system can be ignored. After categorizing flow demands of individual buildings as *metered buildings* and *un-metered buildings*, Equation 6.5.1 is rewritten as:

$$Q_{source} = \sum Q_{mi} + \sum Q_{uj} \quad (16)$$

Where:

Q_{mi} = flow demand for metered building i.

Q_{uj} = flow demand for un-metered building j.

7.5.2 Metered Building Demands

If the building chilled water consumption is monitored, the metered chilled water flow at the peak demand flow moment can be assigned as its peak demand flow. However, before assigning the metered flow to the building, it must be ensured that: (1) the measured flow corresponds to the locations to which it is assigned; (2) the flow is metered at the building entrance; and (3) the flow meter is properly calibrated. Also, the metered data should be verified and crosschecked before it is assigned to the model.

The measured flow may not represent the flow of the building that is built into the model. For example, during the peak demand modeling process for the TAMU main campus DCS hydraulic system, it was found that a meter designated "HUGHES 426 CHW" does not represent the chilled water flow for the Hughes Building. Instead, it measures the total flow of the Hughes Building and two other downstream buildings. If the metered value is assigned to the Hughes Building, it will overstate its peak flow demand. At the same time, the other two downstream buildings will be assigned flow demands by the modeling process and the overall flow demand of this area will be further overestimated. Another meter designated "MSC 454 CHW" actually accounts for

a very small part of the entire MSC Building. If this value is used as the peak flow demand for the MSC Building, it will be significantly understated.

A meter may measure the chilled water flow for the secondary system of a building. If the building's bypass is open, the metered value does not represent the chilled water flow at the building entrance.

7.5.3 Initial Estimation of Flow Demands for Un-metered Buildings

If the building does not have a meter to measure its chilled water flow, or its metered chilled water flow is not valid, a value should be initially estimated for this building. One of the factors that affect the building's chilled water flow is its cooling energy consumption. However, developing detailed forward models for the cooling energy consumption of hundreds of DCS buildings is too time-consuming to be practical. The other factor that affects the building's chilled water flow is its ΔT, which is related to multiple factors such as the in-building chilled water system configuration, and the condition and performance of the building's HVAC system. A more practical way to estimate the demand of un-metered buildings is to utilize the available data of metered buildings and the collected building information to estimate the flow demands for those un-metered buildings.

Categorizing Demands

Under the same weather condition, buildings serving similar functions tend to require similar cooling energy on a unit area basis, i.e. they tend to have similar cooling load intensity. Buildings on a large university campus can be student dorms, classrooms,

offices, laboratories, libraries, sports facilities, auditoriums, dining halls, and any combinations of the above uses. Different types of buildings will have different levels of cooling requirements. For example, chemistry labs with 100% outside air intake require more cooling energy than a normal office. Buildings with lot of experimental equipment or computers require more cooling energy. If some chilled water consumption data for certain types of buildings is available, it can be used to estimate cooling requirements of other un-metered buildings of this type.

The average cooling load intensity for buildings of type *j* can be expressed as:

$$\bar{I}_j = \frac{\sum_{i=1}^{n_{mj}} q_{mij}}{\sum_{i=1}^{n_{mj}} A_{mij}} \qquad 17$$

where:

$\bar{I}_j$ = average cooling load intensity for buildings of type *j* (Btu/hr-ft^2).

q_{mij} = Metered cooling load of building *i* of type *j* (Btu/hr).

A_{mij} = Air conditioned area of metered building *i* of type *j* (ft^2).

Then the cooling load for an un-metered building of the same type can be estimated as:

$$\hat{q}_{uij} = \bar{I}_j \cdot A_{uij} \qquad 18$$

where:

$\hat{q}_{uij}$ = Estimated cooling load of the un-metered building *i* of type *j* (Btu/hr).

A_{uij} = Air conditioned area of the un-metered building *i* of type *j* (ft^2).

Finally, the chilled water flow for the un-metered building *i* can be estimated as:

$$\hat{Q}_{ui} = \frac{\hat{q}_{ui}}{500 \cdot \Delta\hat{T}_{ui}} \qquad 19$$

where:

$\hat{q}_{ui}$ = Estimated cooling load of un-metered building *i* (Btu/hr).

$\hat{Q}_{ui}$ = Estimated chilled water flow rate for un-metered building *i* (GPM).

$\Delta\hat{T}_{ui}$ = Estimated chilled water differential temperature for un-metered building *i* (°F).

To estimate the $\Delta\hat{T}_{ui}$, the average differential temperature at the plant entrance is a good starting point, as it represents the overall campus chilled water differential temperature. As summarized in chapter III, the in-building chilled water systems can be categorized into variable flow systems (types B and C), and constant flow systems (type A). The intention of varying the chilled water flow through the building is to increase the ΔT under partial load conditions and save pumping energy. For constant flow in-building systems, the chilled water flow is relatively constant and the ΔT fluctuates with the cooling load. The ΔT of a constant flow in-building system tends to be smaller than that of a variable flow in-building system. Therefore, the average building ΔT for metered buildings with a certain type of in-building system should be closer to the actual ΔT than the campus average and will be used to estimate the building ΔT for those un-metered buildings with the same type of in-building system. This can be expressed as:

$$\Delta\hat{T}_{k,ui} = \Delta\overline{T}_{k} = \frac{\sum \Delta T_{k,mi}}{n_{k,m}} \qquad 20$$

where:

$\Delta\hat{T}_{K,ui}$ = Estimated differential temperature for un-metered building *i* with type *K* of in-building system.

$\Delta\overline{T}_K$ = Average differential temperature of type *K* in-building systems.

$\Delta T_{K,mi}$ = Metered differential temperature for metered building *i* with type *K* in-building system.

$n_{K,m}$ = Number of metered buildings with type *K* in-building system.

Justify the Initially Estimated Un-Metered Demands

The historical data reflects how the building performed in the past. If there have been no significant changes in the building's HVAC system condition, operation, and its water side control, the historical data under the peak flow demand weather conditions can be assigned to this building as its initial peak flow demand. However, the performance of building HVAC systems generally deteriorates (Claridge, et al, 2003) over time. Operation and control change over time as well, especially before and after CC® is implemented. The historical data should be as recent as possible and can only be used to verify and cross check the estimated un-metered demands.

Building design information is another resource to justify the estimated un-metered demands. Such information includes: (1) gross area or air conditioned area; (2) design chilled water flow; (3) design cooling load and/or chilled water differential temperature; (4) design flow of chilled water pumps; (5) the size of the chilled water pipe at the building entrance.

For example, if the initially estimated flow demand of a building is significantly higher than the design flow of the building pump, it may be over estimated. In this case, the information used to estimate the peak flow demand of this building, such as the building AC area, the type of the building, and the type of the in-building system, need to be reevaluated. As another example, if the meter shows the building has 460 GPM chilled water flow, whereas the pipe size at the building entrance is only 3 inch, then the metered data may not reliable. Field investigation will be needed to verify the pipe size at the building entrance or if the flow meter measures just this building flow.

7.5.4 Model Reconciliation

With the metered total peak flow demand, the metered demands, and the justified initial estimation of un-metered demands, the overall peak flow model can be reconciled based on mass balance:

$$\hat{Q}_{ui,R} = (Q_{source} - \sum_{i=1}^{n_m} Q_{mi}) \cdot \frac{\hat{Q}_{ui}}{\sum_{i=1}^{n_u} \hat{Q}_{ui}} \qquad 21$$

where:

$\hat{Q}_{ui,R}$ = Reconciled estimate of the peak flow demand for un-metered building *i*.

7.6 Case Study

This case study is the peak flow demand modeling portion of the entire process of modeling the TAMU main campus DCS hydraulic system. It is intended to demonstrate the procedure for developing the building peak flow demands. The data used to develop the peak flow demand model is based on the metered data from 9/6/2005 to 11/23/2005.

After the peak flow demand conditions are determined (see section 6.4), the system parameters under the peak flow demand conditions are listed in Table 5.

Table 5 System Parameters under Peak Flow Demand Conditions

System Parameters	Value	Purpose
Peak flow demand time	9/28/2005 17:00	
Ambient dry-bulb temperature (°F)	102	
Ambient wet-bulb temperature (°F)	79	
Total energy production (Tons)	18,524	
Main campus total flow (GPM)	47,875	Demand balance
CUP east loop	8,522	Verification and calibration
CUP west loop	8,306	Verification and calibration
CUP south loop	11,564	Verification and calibration
CUP central loop	8,508	Verification and calibration
SS3	10,976	Model input
System ΔT (°F)	9.3	Building ΔT estimation
CUP supply pressure (psig)	76.1	Model input
CUP return pressure (psig)	59.3	Model input
SS3 differential pressure (psi)	11.9	Verification and calibration

The chilled water flow data trended from building metering system were processed and validated first. Based on the collected building information, all the buildings on the chilled water system are categorized into four groups: (1) student dorms; (2) general offices, classrooms; (3) laboratory buildings with 100% out side air requirement, such as chemistry labs; (4) mixed use buildings with offices, laboratories, classrooms, etc. Table 6 summarizes the cooling intensities for each type of building based on the metered data under the peak load condition.

Table 6 Estimated Peak Cooling Load Intensity for Different Types of Buildings

Type	Number of Buildings	Number of Metered Buildings	Total AC Area (ft^2)	Metered AC Area (ft^2)	Avg. Peak Cooling Intensity ($Btu/hr\text{-}ft^2$)	Standard Deviation ($Btu/hr\text{-}ft^2$)
1	34	25	1,823,140	1,331,189	21	3.6
2	33	14	2,635,789	1,555,184	16	3.9
3	4	1	538,900	204,972	60	N/A
4	46	21	3,737,232	2,021,370	31	7.9
Overall	117	61	8,735,061	5,112,715	25	9.8

Based on the metered building ΔTs at the peak flow demand condition, and the type of each in-building system, the building ΔT is estimated for those un-metered buildings. Table 7 summarizes the results. About 59% of the buildings have metered building ΔTs. It is clear that the variable flow type in-building systems have higher average ΔT than buildings with constant flow in-building systems. Standard deviations of the ΔTs are provided as well.

Table 7 Estimated Building ΔT for Variable Flow and Constant Flow Types of In-building Systems

BLDG Type	Constant Flow			Variable Flow		
	# Metered / # Total	Average ΔT in Metered BLDGs (°F)	Standard Deviation (°F)	# Metered / # Total	Average ΔT in Metered BLDGs (°F)	Standard Deviation (°F)
1	13/18	7.0	2.3	16/16	9.1	3.3
2	8/19	7.3	1.9	10/15	10.1	3.1
3	0/0	0.0	0.0	1/4	15.1	1.4
4	8/21	7.3	1.9	17/24	11.8	4.5
Overall	**29/58**	**7.2**	**3.2**	**44/59**	**10.5**	**5.7**

The information related to determining the building peak flow demands, the estimated values, and the final results are listed in appendix Table A - 1. Table A - 1 is indexed by the model nodes. Each model node represents one building, part of a building or a combination of several buildings depending on the location of the pump room. For example, some buildings share one pump or one set of building pumps. These buildings are combined into one model node and their demands are aggregated. As another example, some buildings have multiple pump rooms serving different parts of the building. This kind of building is represented by multiple model nodes. A detailed list of model nodes with their corresponding buildings are listed in appendix Table A - 2. The other items in Table A - 1 include: (1) building AC area; (2) type of the building; (3) constant or variable flow type of in-building system; (4) pipe size at the building's entrance; (5) flow, load, and ΔT for metered buildings; (6) historical flow if available under the same weather condition; (7) building design flow, and pump design flow; (8) estimated building cooling load based on building use categorization; (9) estimated building ΔT based on in-building system categorization; (10) calculated building chilled water flow based on the estimated cooling load and ΔT. The initially estimated flow demands for un-metered buildings, flow demand for metered buildings, and the plant metered total flow demand were reconciled. The final results are listed in the last column in Table A – 1.

Table 8 Summary of Peak Flow Demand Model

	Total	Metered	Estimated	Metered %
Number of buildings	117	67	50	57%
Cooling load (Tons)	18,524	10,704	7,820	58%
Building GSF (ft^2)	8,735,061	5,375,424	3,359,637	62%
Flow Demands (GPM)	47,875	27,889	19,986	58%

Table 8 summarizes the metered and un-metered components of the peak flow demand model. It shows about 60% of the building flow demands are determined from the metered data and 40% are estimated. Because the peak flow demand model is based on the available metered data, a high percentage of metering helps improve the model quality.

CHAPTER VIII

MODEL VERIFICATION AND CALIBRATION

8.1 Introduction

Even though the information and data have been collected and entered into a hydraulic simulation software package, we should not take it for granted that the model is an accurate mathematical representation of the real system. The hydraulic simulation software just solves the hydraulic equations by using the supplied data. Therefore, the accuracy of the simulation results heavily relies on the quality of the simulation inputs. The accuracy of the hydraulic model depends on how well it has been calibrated, so a calibration analysis should always be performed before a model is used for decision-making purposes.

Usually, the verification and calibration is a trial and error process. The initial results are compared with the observed values. If the agreement is unacceptable, then a hypothesis explaining the cause of the problem should be developed, modifications made to the model, and the process repeated again. The process is conducted iteratively until a satisfactory match is obtained between modeled and observed values. Calibration of a DCS hydraulic system model may include changing flow demands, fine-tuning the resistance coefficients of model components such as pipes and fittings, altering pump operating characteristics, and adjusting other model parameters that affect simulation results.

A large DCS hydraulic system with hundreds of buildings is usually very complicated. Variations can stem from the cumulative effects of errors, approximations,

and simplifications in the way the system is modeled; site-specific reasons such as outdated system maps, local piping resistance, partially open valves, and more difficult-to-quantify causes like the inherent variability of building flow demands. Therefore, the verification and calibration must be processed systematically.

This chapter begins with a discussion of data required to verify and calibrate the model. Then a systematic procedure for model verification is discussed and the possible reasons for discrepancies between computer-predicted behavior and actual field performance of a large DCS hydraulic system are summarized. Next, the chapter discusses the procedure of calibrating the model. Finally, the chapter concludes with a discussion on the limits of calibration and how to know when the model is sufficiently calibrated. Along with different sections in this chapter, an actual calibration process for the TAMU main campus DCS hydraulic system model is used as an example to demonstrate the concepts and procedures.

8.2 Calibration Data

The collection of data and information for modeling of a large DCS hydraulic system has been discussed in previous chapters. This section discusses the specific requirements of the data for verification and calibration.

8.2.1 Collection of Calibration Data

Two key parameters of a hydraulic system model are flow and pressure. If one of them is input as a known parameter in the model, the other should be verified and calibrated. For example, because the peak flow demand of each building is a known parameter, the simulated differential pressures become the model output and need to be

verified and calibrated. As another example, on the plant side, the known plant ΔP is input as a system boundary condition to the model. Then the main trunk flows that flow out of each of the plant's main loops are simulated results and need to be verified and calibrated. A large DCS may have multiple plants with one serving as a central plant and others serving as satellite plants. Under this circumstance, if the flow of one of the satellite plants is a known parameter, then its plant ΔP should be verified and calibrated.

8.2.2 Location of Calibration Data

It would be rare for a large DCS hydraulic system to have all pressures and flows measured. Too much data could result in possible errors and make calibration even more difficult, unless all data are verified and accurate. Calibration data should be collected at certain locations on the system, to ensure good calibration results. The locations from which calibration data should be collected are discussed as follows.

First of all, the calibration data should be collected at the plant entrance. If error starts from the source, it will spread to the entire system. No matter how well the numbers match up for individual buildings, the simulation results will be questionable if they are incorrect at the plant. The calibration data should be collected from a place close to the system source, such as the plant entrances or buildings that are very close to the plant.

Second, the calibration data should be collected at the main loops and the entrances of major branches. The main loops of a DCS hydraulic system play the role of distributing the water from the source system to branches and individual buildings. If errors start from such places, they will spread to downstream buildings as well.

Therefore, if the data such as pressure and flow at the main loops are available, it is preferred to collect this as well. For example, the Central Utilities Plant (CUP) of the TAMU main campus DCS supplies chilled water to the campus through four major loops (east, west, central, and south). The South Satellite Plant (SS3) supplies the chilled water to the campus through two major loops (east and west). The flows and pressures of these major loops are monitored through the metering system. Therefore, they should be collected and used as part of the calibration data. The other place that the calibration data should be collected on the main loop is the entrances of large branches which cover large numbers of down stream buildings such as the entrance of the branch to the Corps of Cadets Area on the TAMU main campus DCS (see Figure 17 in page 67). However, sensors and meters are seldom installed at such locations where both the building metering system and the plant metering system are hard to reach. Under these circumstances, if possible, field measurement of flow and pressure can be conducted under conditions similar to the peak flow demand conditions.

Finally, the calibration data (i.e. loop ΔP) should be collected at the entrances of buildings. However, rarely do all the buildings have their loop ΔPs monitored. To ensure good calibration results, the calibration data must be collected at some buildings either through the building metering systems or field measurements. If the simulation results at the most remote buildings (such as building #290, 450, 367, 425, etc. on the TAMU main campus DCS) are calibrated well, the predicted ΔPs for the middle buildings of that branch, if unverified, can be assumed acceptable. When the calibration data at the main loops could not be collected, the data for the buildings very close to the main loop (such

as building #461 on the TAMU main campus DCS), if available, should be collected. This provides an indication of the main loop condition at this location. However, using close-to-loop data should be limited, as it does not necessarily represent the actual main loop condition. The local piping between the pressure reading points and the loop tie-in location may cause excessive pressure drop when the flow of the building is large. Under this circumstance, the ΔP at the main loop can be estimated by looking at the local pipe size and the peak flow demand assigned to the building. On the other hand, if the section of local piping is not accurately reflected in the model, this will cause error in the pressure calculation, and the result will give an erroneous value for the main loop ΔP.

8.2.3 Time of Calibration Data

It is ideal if the calibration data are available exactly at the peak flow demand moment and all desired locations. However, in the absence of a computerized metering system at all desired locations, field measurements should be conducted under similar weather conditions. The measured data can be used as the calibration data after it is verified. Building #453 of the TAMU main campus DCS is an example. The building EMCS recorded that the loop ΔP at this building was 23.74 psi and the chilled water flow was 339 GPM at the peak flow demand moment. It is apparent that the 23.74 psi reading for the loop ΔP is not a valid number because the SS3 plant sent out chilled water at the ΔP of 11.9 psi. A field measurement was taken on 9/20/2005 at 16:40 when the ambient temperature was above 100 ºF, which is close to the peak load conditions. The chilled water flow was 378 GPM and the ΔP was three psi. Because the ambient

temperature and the building chilled water flow were close at the two measurement times, the field measured ΔP was used as the calibration data.

8.3 A Systematic Verification Method

As discussed in the previous section, verification and calibration of a large DCS hydraulic system model should be carried out systematically. This section discusses how to compare the model predicted performance and field measured performance from the systems point of view.

8.3.1 Verification of Major System Parameters

The major system parameters include the pressures and/or flows at plant entrances and important locations on the main loops (see section 8.2.2 in page 102). Because the major system parameters represent the source and upstream system conditions, if they are not predicted accurately, errors will spread to all the down stream buildings.

Table 9 Verification of Major System Parameters

Major Loops	Measured	Initial Simulation	Error
CUP east loop supply (GPM)	8,522	8,761	3%
CUP west loop supply (GPM)	8,306	7,418	-11%
CUP south loop supply (GPM)	11,564	11,452	-1%
CUP central loop supply (GPM)	8,508	9,268	9%
SS3 ΔP (psi)	11.9	15.1	27%

Table 9 summarizes the measured and the initial simulated main trunk flows of the TAMU main campus DCS hydraulic system. These main trunk flows are measured for

the CUP east, west, south, and central loops. Comparing the measured and initial simulated flows, it shows the predicted west loop flow is 11% less than the measured flow and the central loop flow is 9% more than measured value. This is an indication that the simulated ΔPs for west loop buildings may be lower than the actual ΔPs whereas the simulated ΔPs for central loop buildings may be higher than the actual ΔPs. It may also be noted that the predicted SS3 ΔP (15.3 psi) is significantly higher than the measured value (11.9 psi). This error will be spread to all the buildings supplied by SS3 and their pressure drops will be over-estimated.

8.3.2 Systematic Representation of Predicted and Measured Building ΔPs

System Map Overlaid with Predicted and Measured Values

To verify the ΔPs of plants and individual buildings, all the numbers should be put together and organized so they can be systematically verified. One commonly used way to organize the measured and predicted values is to put them on a system map at their corresponding locations. For example, Figure 24 is the system map of the TAMU main campus DCS hydraulic system overlaid with the initial simulated building and plant ΔPs (on the right of the symbol "/") and the field measured building and plant ΔPs (on the left of the symbol "/"). Figure 24 shows that the overall simulated building ΔPs are higher than measured values, which indicates the model under estimated the pressure losses in the system. At each step of the calibration process, the simulation results and the measured values can be put on to the system map. From the system map overlaid with simulated and measured values, the results of the current calibration step can be

compared with those of the previous steps. The direction of the next step of calibration can be determined, for example, reduce/increase the overall system resistance factor or reallocate the building demands, etc.

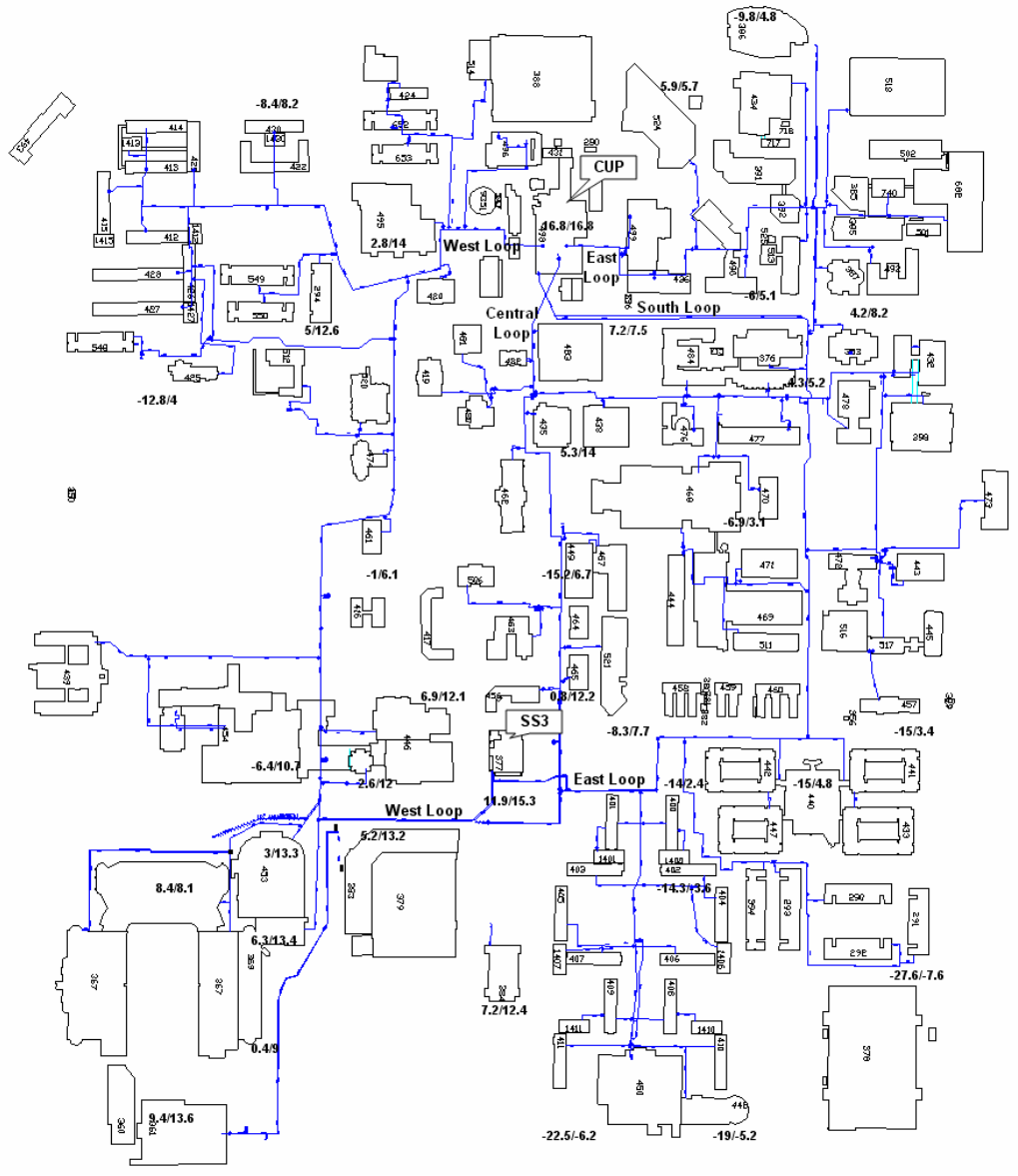

Figure 24 Measured and Predicted ΔPs Overlaid on the Map of TAMU Main Campus DCS Hydraulic System

Differential Pressure Distribution Line

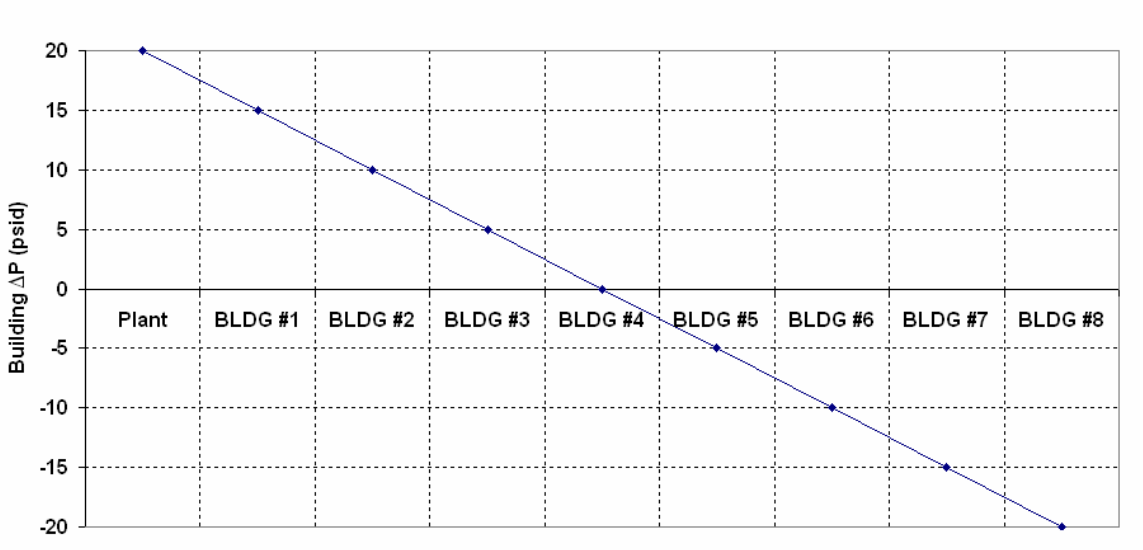

Figure 25 Typical Building ΔP Distribution Line

Generally speaking, because of the friction losses along the piping, the further the building is located downstream of a system, the lower the ΔP it will get from the plant. For a large DCS hydraulic system, the remote buildings may even get negative ΔPs. This provides another way to systematically look at the simulated and predicted buildings ΔPs by drawing a ΔP distribution line over the buildings arranged from the closest to the plant to the most remote buildings. Figure 25 conceptually demonstrates the system ΔP distribution line. With the plant sending out water at ΔP of 20 psi, building #4 in the middle of the loop receives water at ΔP of zero psi and the most remote building (#8) receives water at the ΔP of -20 psi. Generally speaking, if the predicted distribution line ΔP is higher than the measured value, the overall model under estimates the system

resistance. Conversely, if the predicted distribution line ΔP is lower than the measured value, the overall model over estimates the system resistance.

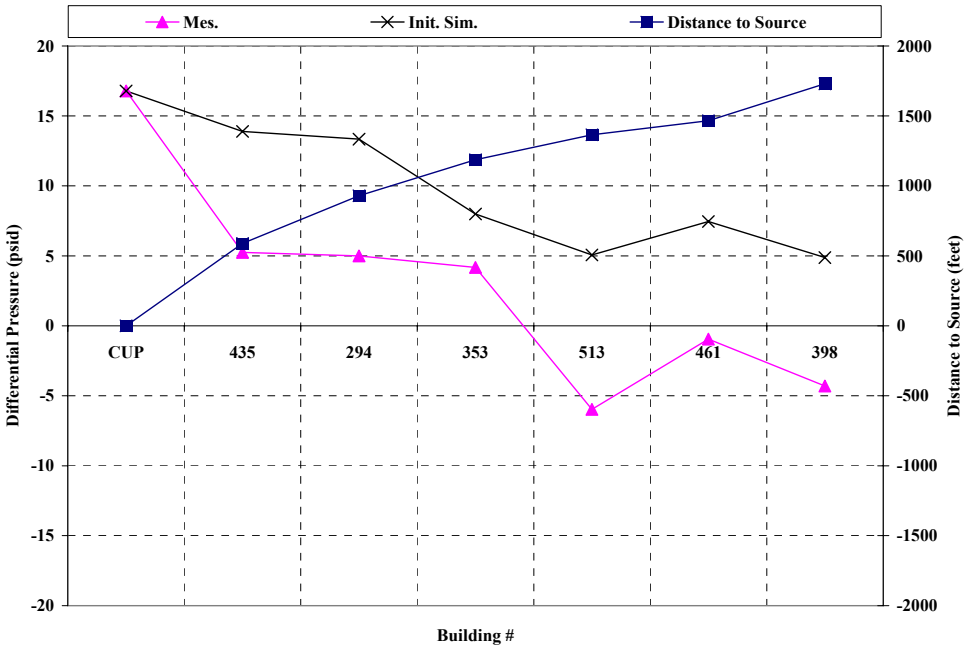

Figure 26 Distribution Line ΔP Values for CUP Supplied Buildings

For example, Figure 26 illustrates the distribution line ΔP values for initially simulated and measured ΔPs for the CUP supplied buildings from the nearest (building #435) to the farthest (building #398) building. The piping distance from each building to the plant entrance is also shown in this figure. The ΔP at the CUP entrance is the model input by using the measured value. Figure 26 shows that the simulated ΔP distribution line generally follows the trend of the measured ΔP line, but its slope is larger, which means the model underestimated the friction losses. Relatively speaking, when pipe flow

or roughness is greater, there will be more pressure loss. Therefore, the possible causes of this error are: (1) The flow demand allocated to this area is not enough; or (2) the system resistance is underestimated.

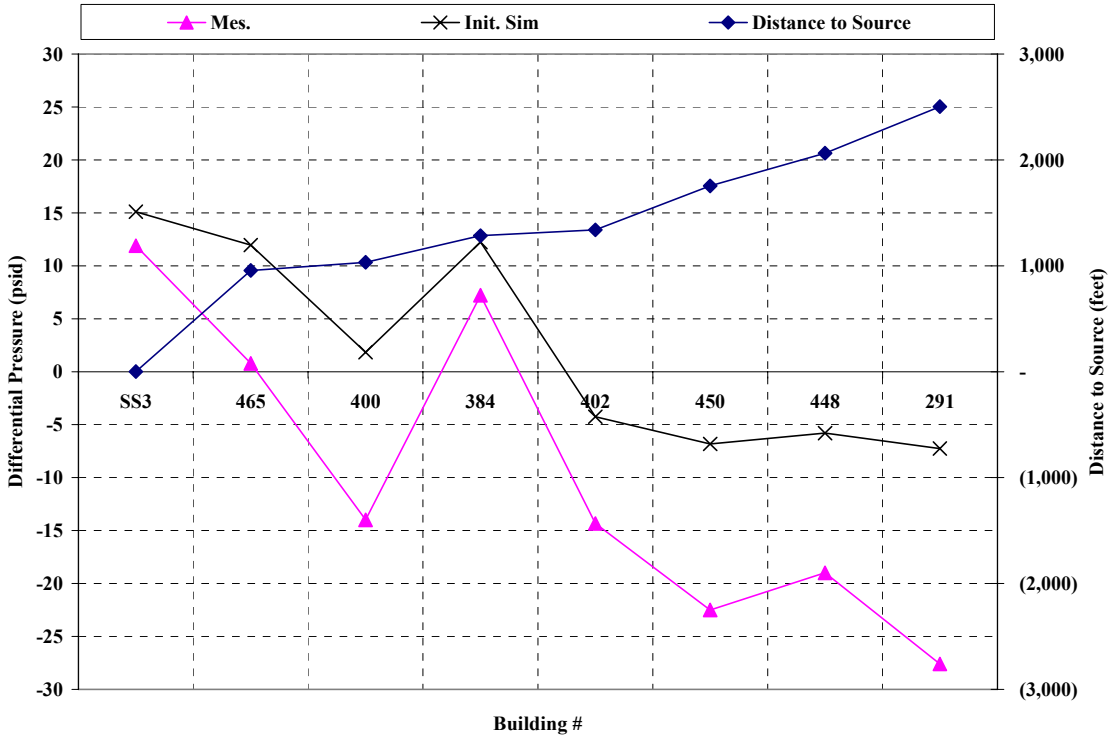

Figure 27 ΔP Distribution Lines for SS3 Supplied Buildings (East Loop)

Figure 27 provides another example for how to use ΔP distribution lines to analyze the predicted and measured performance. The figure shows the ΔP distribution lines for SS3 supplied buildings on its east loop. The simulated ΔP distribution line generally follows the trend of the measured line. The SS3 chilled water flow was input as a known parameter to the model, providing the simulated ΔP values shown. Because the overall

model underestimated the friction losses, the simulated SS3 ΔP is higher than the measured value and consequently, all the ΔPs of down stream buildings are underestimated and the predicted ΔP distribution line is above the measured one.

It is noticed from Figure 26 and Figure 27 that the actual ΔP distribution lines are not exactly straight lines. The zigzag is caused by the error of sensor readings or the combined effect of building flow and the local piping. For building #513 in Figure 26 as an example, the measured ΔP is lower than that of its upstream buildings and even lower than its downstream buildings. Although it is closer to the CUP than the building #461, the more complicated local piping caused more pressure drop than its down stream building #461. Take the building #384 in Figure 27 as another example, its ΔP is higher than that of its downstream buildings and even its upstream buildings. Building #384 is connected to the main loop through 426 feet of four inch pipe and 355 feet of 14 inch pipe. However, this is a small building with metered peak flow demand of 66 GPM. The oversized local piping and the relatively small flow demand caused almost no pressure drop from its tie-in location on the main loop to the building entrance. Its tie-in location on the main loop is only 495 feet away from the SS3 entrance, closer to the source than the its upstream building #465, which is 1,000 feet away from the SS3 entrance.

It is also noticed from Figure 26 that the zigzag of the ΔP distribution line was not predicted very well especially at building #513. The sensor reading may be in question. The flow demand allocated to the building may be too small or the actual pipe size is smaller than that has been input into the model. Also, the system map may not reveal sufficient details of the local piping for this area that caused underestimated pressure loss.

After the initially simulated major system parameters and the building ΔPs are compared with the measured values, the verification findings are:

1. The initially-simulated building ΔPs are significantly higher than the measured values, especially at loop end buildings.
2. The CUP west loop supply flow is under-estimated, while the CUP central loop supply flow is over-estimated.
3. The initially simulated SS3 ΔP is higher than the measured values.

The possible reasons for these errors are:

1. The overall system resistance is under-estimated. When imputing the pipe parameters such as pipe diameters and roughness coefficients to the model, it is usual to use the nominal pipe size and typical roughness coefficient for the initial estimate. However, the underground piping of a large DCS hydraulic system usually has been in place for many years. Chemical processes such as corrosion and deposition occur over time after the pipe has been installed. Consequently, the actual roughness of an old pipe tends to be higher than when it is new, and the difference can be dramatic. For example, according to Lamont (1981), the Hazen-Williams C – factor is 140 for a smooth, new, coated cast iron pipe of 24-inch diameter, while it decreases to 66 when it is 30 years old. According the Hazen-Williams equation, the head loss along a pipe is inversely proportional to the 1.852 power of the C – factor. This means the 30-year old pipe in the example can cause four times more friction losses than when it is brand new. The other possible reason for the modeling

error is an incorrect model - the modeling errors may be due to deficiencies in the maps, which may not be updated, or, more often, may not reveal sufficient details of the local piping.

2. Although the CUP ΔP and the SS3 flow demand (the model inputs) are based on metered values, meters may not yield accurate readings, especially flow meters. Sometimes, the plant flow is calculated by totalizing individual chiller flow meters or individual loop flow meters. Errors may accumulate from the inaccuracy of each individual flow meter. The supply and return pressure meters may not be installed at the same elevation. All these factors may result in errors in the initially-estimated CUP ΔP and SS3 flow demand.
3. The flow demands in the CUP west loop area are under-estimated while the flow demands at CUP central loop area are over-estimated.
4. The flow demands at the loop end buildings are under-estimated.

Consequently, the possible calibration measures are:

1. Change the overall system resistance by adjusting the pipe roughness coefficient or applying an overall system resistance correction factor.
2. Change the CUP ΔP or the SS3 flow.
3. Re-allocate building flow demands.

8.4 Calibration Procedure

After the initial simulation results are compared with the measured values, and the hypothesis explaining the cause(s) of the error is developed, the calibration process is implemented to improve the model prediction accuracy. Ormsbee and Lingireddy (1997)

have developed a seven-step approach that can be used to calibrate a hydraulic network model and it can be applied to DCS hydraulic system model calibration. The seven steps are:

1. Identify the intended use of the model.
2. Determine estimates of model parameters.
3. Collect calibration data.
4. Evaluate model results based on initial estimates of model parameters.
5. Perform a rough-tuning or macro-calibration analysis.
6. Perform a sensitivity analysis.
7. Perform a fine-tuning or micro-calibration analysis.

Step one has been addressed in previous chapters. It is particular important because it not only helps to establish the level of detail needed in the model and the nature of the data collection, but also helps to establish the acceptable level of tolerance for errors between field measurements and simulation results (Walski et al. 2001). Step two has been discussed in the physical modeling and peak flow demand modeling chapters (VI and VII). Steps three and four have been discussed in the second and the third sections of this chapter. This section will focus on and discuss in detail steps five, six and seven.

8.4.1 Sensitivity Analysis

After the possible calibration measures have been identified and the parameters that need changes have been determined, sensitivity analysis should be conducted to learn how performance of the simulation changes with respect to adjustments of these model parameters. The results of the sensitivity analysis can then be used to estimate the

amounts by which these parameters should be adjusted. For example, which factors affect the slope of the ΔP distribution line? If the pipe design factors are globally adjusted by 50 percent, the change in simulated ΔPs may not be significant and the alternative parameters can be adjusted. Sensitivity analysis of the potential parameter adjustments can be conducted to assist the modeler in choosing the calibration direction more wisely. This section discusses how the performance of the calibration changes with respect to the three commonly adjusted parameters, i.e. boundary condition (e.g. CUP ΔP), demand allocation, and system resistance. To evaluate the impact of each of these parameters, one parameter is changed while keeping others fixed.

Boundary Conditions

Table 10 Simulated Results of Major System Parameters by Changing Boundary Condition

Major System Parameters	**CUP** ΔP (psi)		
	16.8	**14.8**	**12.8**
CUP east loop supply (GPM)	8,522	8,522	8,522
CUP west loop supply (GPM)	8,306	8,306	8,306
CUP south loop supply (GPM)	11,564	11,564	11,564
CUP central loop supply (GPM)	8,508	8,508	8,508
SS3 ΔP (psi)	15.1	13.1	11.1

Because changing ΔP at source will spread to all the downstream buildings, the impact of changing the boundary condition is expected to be significant. A sensitivity test of this parameter has been conducted for the TAMU main campus DCS hydraulic

system model. By keeping other parameters fixed at their initial estimates, the CUP ΔP is changed from the initial estimate of 16.8 psi, in two psi steps (12%), to 12.8 psi.

Table 10 lists the simulated results for three values of the CUP ΔP. It clearly shows that the flow demand distribution is not affected by changing the CUP ΔP and the simulated SS3 ΔP drops correspondingly. Each two psi drop of the CUP ΔP results in two psi drop at SS3. Figure 28 further confirms that all building ΔPs drop correspondingly when the CUP ΔP drops. The slope of the ΔP distribution line does not change when the CUP ΔP changes.

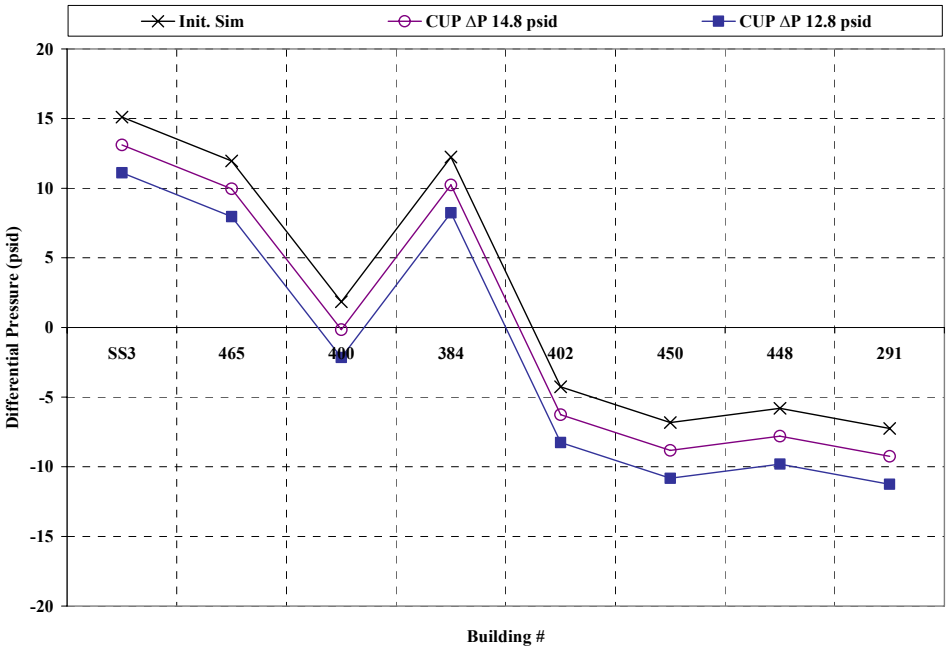

Figure 28 Simulated ΔP Distribution Lines for SS3 Supplied Buildings (East Loop) for Three Values of Boundary Condition

The simulated and measured building ΔPs are listed in Table A - 4. The Root Mean Square Error (RMSE) values weighted by the building AC area are 0.438 psi, 0.378 psi,

and 0.324 psi for the scenarios where the plant ΔP was 16.8 psi, 14.8 psi, and 12.8 psi respectively. From the analysis above, it is clear that adjusting the CUP ΔP improves the match of the simulated SS3 ΔP values with the measured values.

System Resistance

Generally speaking, the pressure drop (ΔP) through a pipe, the resistance factor (k) of this pipe and the flow (Q) through the pipe follow the relationship as:

$$\Delta P \propto kQ^2$$

Therefore, changing the system resistance factor will affect the slope of the ΔP distribution line. A sensitivity test of this parameter has been conducted for the TAMU main campus DCS hydraulic system model. By keeping other parameters fixed at their initial estimates, the global pipe design factor is changed from the initial estimate of one, increasing it to 1.25 and then to 1.5.

Table 11 Simulated Results of Major System Parameters by Changing Pipe Design Factor

Major System Parameters	**Global Pipe Design Factor**					
	1		**1.25**		**1.5**	
	Result	Error %	Result	Error %	Result	Error %
CUP east loop supply (GPM)	8,522	3%	8,782	3%	8,796	3%
CUP west loop supply (GPM)	8,306	-11%	7,438	-10%	7,452	-10%
CUP south loop supply (GPM)	11,564	-1%	11,364	-2%	11,302	-2%
CUP central loop supply (GPM)	8,508	9%	9,315	9%	9,349	10%
SS3 ΔP (psi)	15.1	27%	14.7	24%	14.4	21%

Table 11 lists the simulated results from changing the global pipe design factor. The percent errors compared with the measured values are also provided. The table shows that the main trunk flows change very insignificantly. The simulated SS3 ΔP has a small change due to the cumulative effect of the increased pipe design factor.

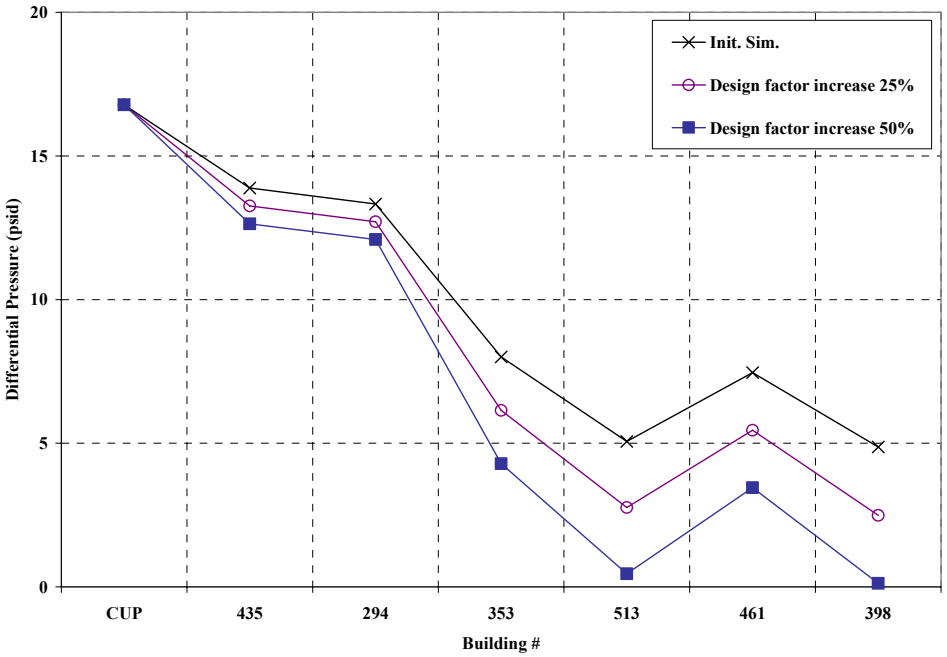

Figure 29 Simulated ΔP Distribution Lines for CUP Supplied Buildings for Three Values of System Resistance

When looking at the simulated ΔP distribution lines for the CUP supplied buildings, shown in Figure 29, it is noted that the slopes of the ΔP distribution lines decrease significantly when the global pipe design factor increases. On the other hand, changing the global pipe design factor will have a larger impact on downstream buildings than on upstream buildings. A linear regression fit of the data on each ΔP distribution line finds

slopes of -2.0, -2.4, and -2.8 for the simulated ΔP distribution lines of the initially simulated, 25% pipe design factor increase and 50% pipe design factor increase respectively. This means each 25% increase of the global pipe design factor will result in 20% increase in the negative slope of the ΔP distribution line. The simulated and measured building ΔPs under these three scenarios are listed in Table A - 5. The RMSE weighted by the building AC area is 0.438 psi, 0.388 psi, and 0.345 psi for the global pipe design factor being set at one, 1.25, and 1.5 respectively.

Flow Demand Distribution

Table 12 Scenarios for Reallocating Flow Demands

Total Building Flow (GPM)	Init. Sim.	Scenario 1	Scenario 2
Supplied by CUP west loop	5,924	6,463	6,459
Supplied by CUP central loop	8,828	8,106	8,024
Supplied by SS3 east loop	4,890	4,932	5,287

Apparently, changing the demand distribution will affect the main trunk flows. Two tests were conducted by modifying the demand distribution among the buildings while keeping other parameters unchanged. Scenario 1 reallocated the flow demands so that the buildings supplied by the CUP west loop had 9% more flow while the buildings supplied by the CUP central loop had 8% less flow. Based on Scenario 1, Scenario 2 further allocated 8% more flow demands to the buildings in the Corps of Cadets area (see Figure 17 in page 67), which is supplied by the SS3 east loop. Table 12 summarizes

the scenarios of flow demand distribution. The detailed building flow demand re-allocation scenarios are documented in appendix Table A - 6.

The modification of flow demands was limited to un-metered buildings unless the metered values are questionable. Table 13 lists the simulated results of major system parameters for the two scenarios. The simulated and measured building ΔPs for the detailed flow demand allocation scenarios are listed in Table A - 6. Table 13 shows that a 9% increase in the total flow of CUP west loop supplied buildings reduced the simulation error of CUP west loop supply flow from -11% to -4%. An 8% decrease in the total flow of CUP central loop supplied buildings reduced the simulation error of CUP central loop supply flow from 9% to 5%. It is also noted that the predicted SS3 ΔP has almost no change because the total flow demand through the SS3 plant did not change.

Table 13 Simulated Results for Major System Parameters by Changing Demand Allocations

Major System Parameters	Init. Sim.		Scenario 1		Scenario 2	
	Result	Error %	Result	Error %	Result	Error %
CUP east loop supply (GPM)	8,522	3%	8,715	2%	8,706	2%
CUP west loop supply (GPM)	8,306	-11%	7,949	-4%	7,959	-4%
CUP south loop supply (GPM)	11,564	-1%	11,319	-2%	11,333	-2%
CUP central loop supply (GPM)	8,508	9%	8,915	5%	8,901	5%
SS3 ΔP (psi)	15.1	27%	15.0	26%	14.9	25%

The RMSE values weighted by the building AC area are 0.438 psi, 0.435 psi, and 0.432 psi for the initial simulation, scenario one, and scenario two respectively. This

means improving the flow demand distribution do not have a significant impact on the overall ΔP distribution. The pressure drop along a pipe is proportional to the square of its flow rate. Changing the flow demands for a building will have significant impact on its ΔP. However, because the overall system demand is fixed, increasing the flow demands for one area of buildings will result in a decrease of the flow demands for other areas. Therefore, adjusting the allocation of flow demands will not affect the slope of the overall system ΔP distribution line.

8.4.2 Model Rough-tuning

Table 14 Verification of Major System Parameters – Rough-tuning Results

Major Loops	Measured	Init. Sim.		Rough-tuning	
		Results	Errors	Results	Errors
CUP east loop supply (GPM)	8,522	8,761	3%	8,750	3%
CUP west loop supply (GPM)	8,306	7,418	-11%	7,983	-4%
CUP south loop supply (GPM)	11,564	11,452	-1%	11,171	-3%
CUP central loop supply (GPM)	8,508	9,268	9%	8,995	6%
SS3 ΔP (psi)	11.9	15.1	27%	12.3	3%

After knowing how and to what extent the adjustment of a parameter would affect the calibration result through the sensitivity analysis, model rough-tuning should be conducted to roughly match the major system parameters instead of trying to match individual building ΔPs. For example, during the rough-tuning process of the TAMU main campus DCS hydraulic system model, the CUP ΔP was reduced from 16.8 psi to 14.8 psi. The pipe design factors were globally adjusted from one to 1.5. Following

option three of the calibration measures, the flow demands were reallocated. The detailed flow demand reallocation and the rough-tuning results are listed in appendix Table A - 3.

Table 14 summarizes the results of the major system parameters after the rough-tuning step. It shows that the major system parameters have been stretched to roughly match the measured values.

Figure 30 compares the ΔP distribution lines for the measured, initially simulated, and rough-tuned results of CUP supplied buildings that are close to the main loop. It shows that the rough-tuning brought the predicted ΔP distribution line much closer to the measured values.

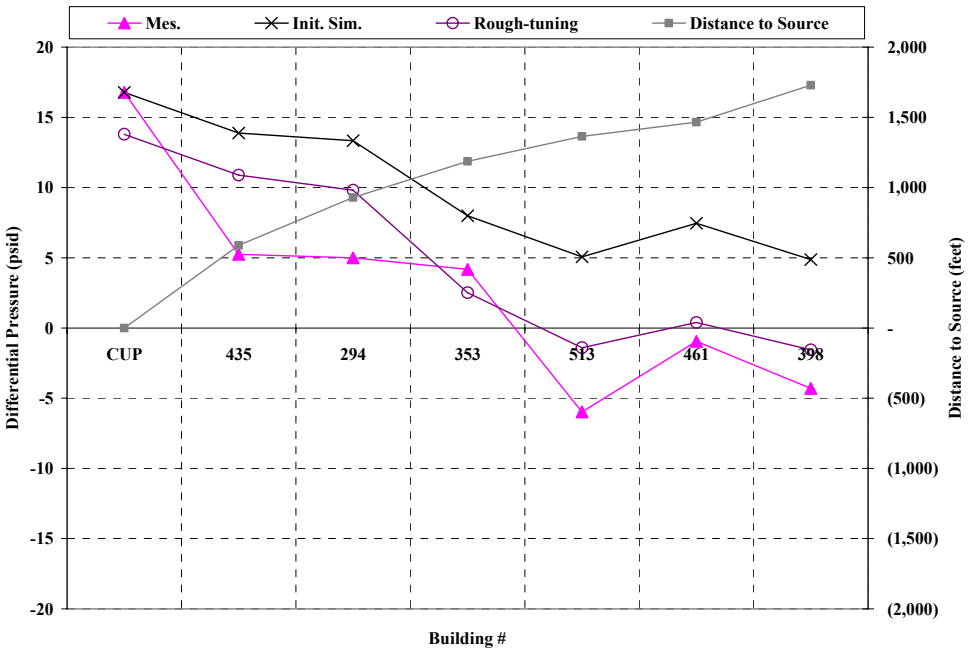

Figure 30 ΔP Distribution Lines for CUP Supplied Buildings – Rough-tuning

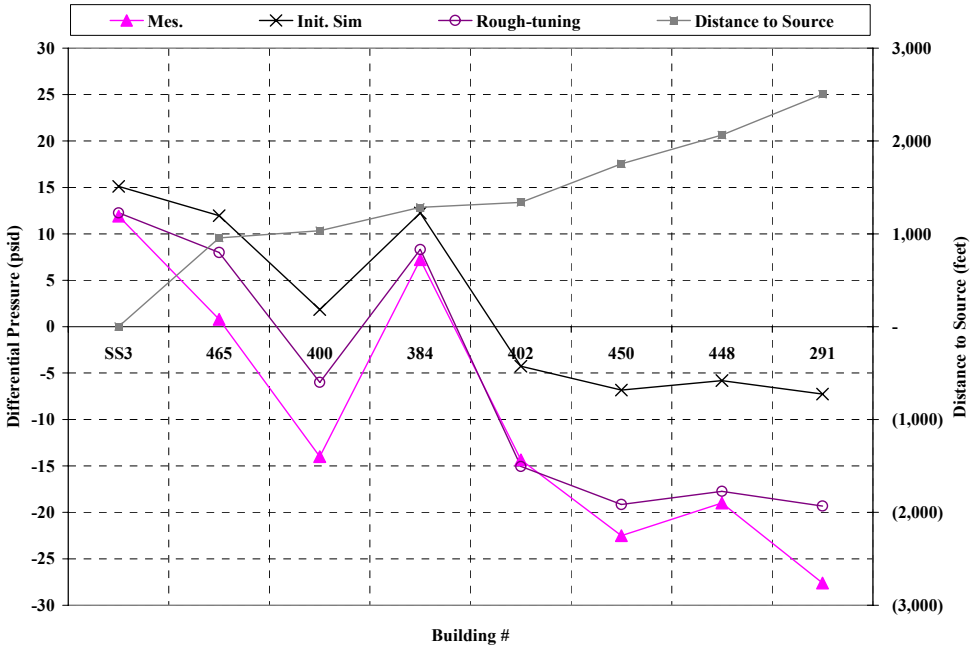

Figure 31 ΔP Distribution Lines for SS3 Supplied Buildings (East Loop) – Rough-tuning

Figure 31 compares the ΔP distribution lines for the measured, initially simulated, and rough-tuned results of the buildings supplied by the SS3 east loop. It shows that the simulated SS3 ΔP dropped significantly and is much closer to the measured value. Consequently, the ΔP values at all the downstream buildings have been brought much closer to the level of the measured values. It is also noticed from Figure 30 and Figure 31 that after the rough-tuning step, the slope of the simulated ΔP distribution line has become more negative. As an overall rough-tuning result, the RMSE weighted by the building AC area is reduced from 0.438 psi (the initial simulation result) to 0.292 psi (the rough-tuning result).

8.4.3 Model Fine-tuning

Fine-tuning of the model involves adjustments of individual model components such as the roughness coefficient of a section of pipe. The collected information and data may need to be further verified and cross checked. Field investigation may be required. For example, after the rough-tuning process, if the flow demand assigned to a building is already significantly higher than its pump design flow, and the predicted building ΔP is still much higher than the measured value, then a field investigation should be conducted. The local piping connection from the building to the main loop should be verified with that of the model input. Frequently, the system map does not reveal sufficient details of local piping connection. Also it should be determined if the valves along the section of pipes are partially opened. Even the metered calibration data should be verified.

For example, after the rough-tuning step, the simulated ΔP of the TAMU main campus DCS building #291 was still 8.3 psi higher than the measured value, means under estimated the pressure loss. It was found later that an engineer had already reported excessive pressure drop for this area due to clogged pipes. However the report did not reveal detailed information. Therefore the local piping resistance of building #291 was increased so that the simulated ΔP could be lower and match the measured value.

For a hydraulic system model that covers hundreds of buildings on a large DCS, The final step of calibration can be time consuming. The iteration process of the calibration can further complicate the fine-tuning stage.

8.5 Acceptance Level of Calibration

Finally, the calibrated model should achieve some level of required performance. However, no performance criterion exists for DCS hydraulic system model calibration. Since the basic hydraulic principles of DCS and DWS are the same, if certain performance criteria exist for DWS model calibration, it provides a good reference for developing the criteria for DCS hydraulic system model calibration. Certain performance criteria have been established in the United Kingdom for DWS model calibration, but such guidelines do not exist in the United States (Walski et al. 2001). Table 15 lists the calibration criteria for flow and pressure, which are applied in the United Kingdom.

Table 15 Calibration Criteria for flow and pressure – DWS Modeling (Walski et al. 2001)

Flow Criteria
(1) Modeled trunk main flows (where the flow is more than 10% of the total demand) should be within ±5% of the measured flows.
(2) Modeled trunk main flows (where the flow is less than 10% of the total demand) should be within ±10% of the measured flows.
Pressure Criteria
(1) 85% of field test measurements should be within ±0.5 m or ±5% of the maximum head loss across the system, whichever is greater
(2) 95% of the field test measurement should be within ±0.75 m or ±7.5% of the maximum head loss across the system, whichever is greater.
(3) 100% of field test measurements should be within ±2 m or ±15% of the maximum head loss across the system, whichever is greater.

In the United States, it is commonly agreed that the level of effort required to calibrate a hydraulic network model, and the desired level of calibrations accuracy will

depend upon the intended use of the model (Ormsbee and Lingireddy, 1997; Cesario, Kroon, Grayman, and Wright, 1996; and Walski, 1995). A generally adopted guideline is that a model can be considered calibrated when the results produced by the model can be used to make decisions confidently, and the cost to improve the model further can not be justified (Walski et. al. 2001).

There are no hard numbers to define whether the calibration accuracy is acceptable or not. A range of values is given for most of the guidelines to reflect the differences among water systems and the needs of model users. A general guideline for master planning purposes of a small DWS system (24 inch pipe or smaller) has been established (Walski et al. 2001). According to this criteria, the model should accurately predict hydraulic grade line (HGL, defined as the summation of elevation head and pressure head) to within 5 – 10 feet (2.2 – 4.3 psia). The high end of the range corresponds to large, more complicated systems, while the lower end of the range is more relevant for smaller, simpler systems.

Because the diameter of the main pipes for a small DWS (24 inches or smaller) is similar to that of a large DCS hydraulic system (e.g. the main pipe diameter of TAMU main campus DCS is 24 inches), the overall water delivering capacity for the two types of systems should be similar. On the other hand, the ΔP distribution line of a DCS hydraulic system presents the same concept of the HGL of a DWS except the elevation effect is cancelled out in the DCS hydraulic system. Therefore, this criterion can also be applied to calibration of a large DCS hydraulic system model for master planning purposes. Since each application of a DCS hydraulic simulation model is unique and has

its specific situations, it is impossible to derive a single set of guidelines to evaluate calibration. Although the above guidelines provide some numerical guidelines for calibration accuracy, they are in no way meant to be definitive even for their own purpose i.e. DWS model calibration (Walski et. al. 2001). For example, due to the budget limitation, a full scale of detailed calibration that covers all the modeled buildings on the TAMU main campus DCS could not be conducted. Instead, a rough-tuning and fine-tuning of several loop-end buildings at the Corps of Cadets area have been conducted. The calibrated model was able to predict the planned changes and was successfully assisted several TAMU master planning decision makings.

CHAPTER IX

MODEL APPLICATION

9.1 Introduction

This chapter is intended to demonstrate how to use the DCS hydraulic model to assist decision making for master planning. During a master planning analysis for a DCS, the underground chilled water distribution system and the current thermal utilities plants are evaluated to see if they could accommodate the planned new buildings. Various options of pipe tie-in location and possible modifications of the current system are usually considered. The hydraulic model for the current system can be modified to represent the planned new buildings, different options for the piping connection, and possible modifications of the current system, so that the planned alternatives can be simulated. Simulation results for different scenarios can be compared and the most desirable alternative can be selected based on comparison of the simulation results. In this chapter, a case study that is a part of the TAMU 30-year master planning analysis is introduced as an example of the DCS hydraulic system model application.

9.2 Case Study – TAMU Master Plan

In a long term master plan, e.g. 30-year master plan, all the planned buildings in different phases may be put into the model to provide an overall evaluation of possible future system expansion. However, a more realistic way is to focus on the buildings that are most likely to be built in the near future. During the TAMU master planning project, one task assigned to the author was to evaluate the existing system capability and future

system expansion possibilities for adding six new buildings in the near future to the main campus DCS.

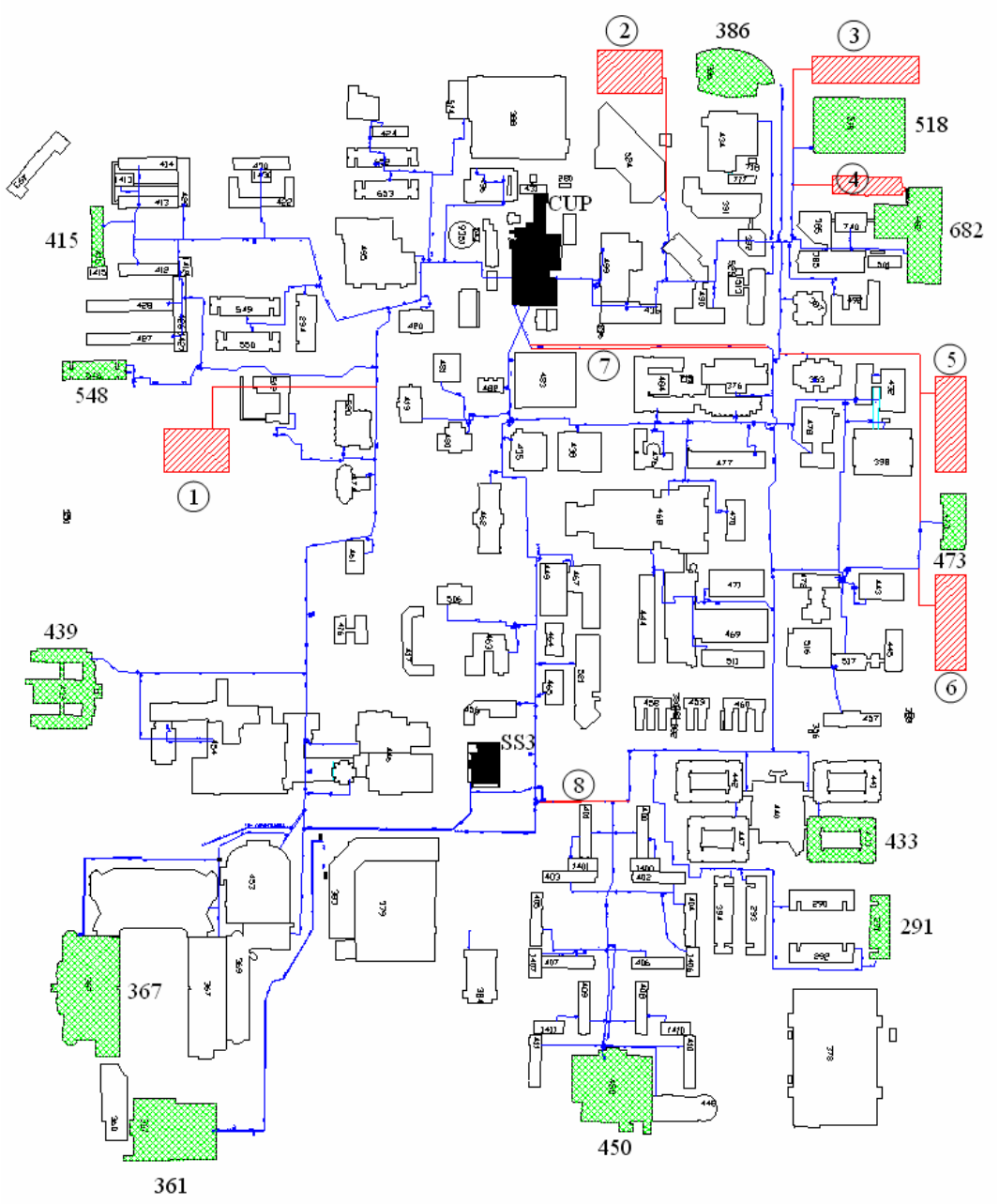

Figure 32 Planned New Buildings and Possible System Piping Expansion

Figure 32 is the system map of the TAMU main campus DCS CHW system. The six planned new buildings are shown as slash hatched blocks in red. Selected loop end buildings are cross hatched and colored in green in Figure 32. The impact of the new buildings on these loop end buildings will be studied. Numbers #1 through #6 are assigned to each of these planned buildings. Building #1 is the Interdisciplinary Life Science Complex that will serve multiple purposes and include offices, biological laboratories, auditoriums, etc. Buildings #2, #3, and #4 are typical engineering buildings including classrooms, offices, and laboratories. Buildings #5 and #6 are two new parking garages. Each garage will be wrapped on two sides with occupied space that is both subservient to and complementary of the Old System Administration Building. In addition to the information about the major functions of these buildings, a few rough design values for these six buildings are available and listed in Table 16.

Table 16 Brief Design Information for the Six Planned New Buildings

# On Map	Building Name	GSF (ft^2)	Design Load (Tons)
1	Interdisciplinary Life Science Complex	N/A	1,750
2	Engineering Precinct 1.B	106,704	N/A
3	Engineering Precinct 2.B	105,770	N/A
4	Engineering Precinct 3.B	65,120	N/A
5	Administration Building West Wing	160,000	N/A
6	Administration Building East Wing	160,000	N/A

9.2.1 Flow Demand Estimation

To estimate the chilled water flow rate for the planned buildings, the following general engineering rules of thumb were applied as assumptions: (1) 350 ft^2/ton for office buildings #5 and #6 (taking into account that half of the building will be used as a parking garage, the cooling load is estimated based on 80,000 ft^2 of conditioned space); (2) 250 ft^2/ton for engineering buildings #2, #3, and #4; and (3) 12°F of building differential temperature. The estimated cooling loads and chilled water flow demands for the planned new buildings are listed in Table 17.

Table 17 Estimated Energy and Flow Demands for Planned New Buildings

#	Building Name	Estimated Load (Tons)	Estimated Flow Demand (GPM)
1	Interdisciplinary Life Science Complex	1,750	3,500
2	Engineering Precinct 1.B	427	854
3	Engineering Precinct 2.B	423	846
4	Engineering Precinct 3.B	260	521
5	Administration Building North Wing	229	457
6	Administration Building South Wing	229	457

9.2.2 Model Modification

To reflect the planned new buildings in the hydraulic model, the hydraulic model for the existing system was modified to reflect the possible piping arrangement for the

planned new buildings. To connect these new buildings to the DCS, hypothetical piping has been sized based on their estimated flow demands and added in the model.

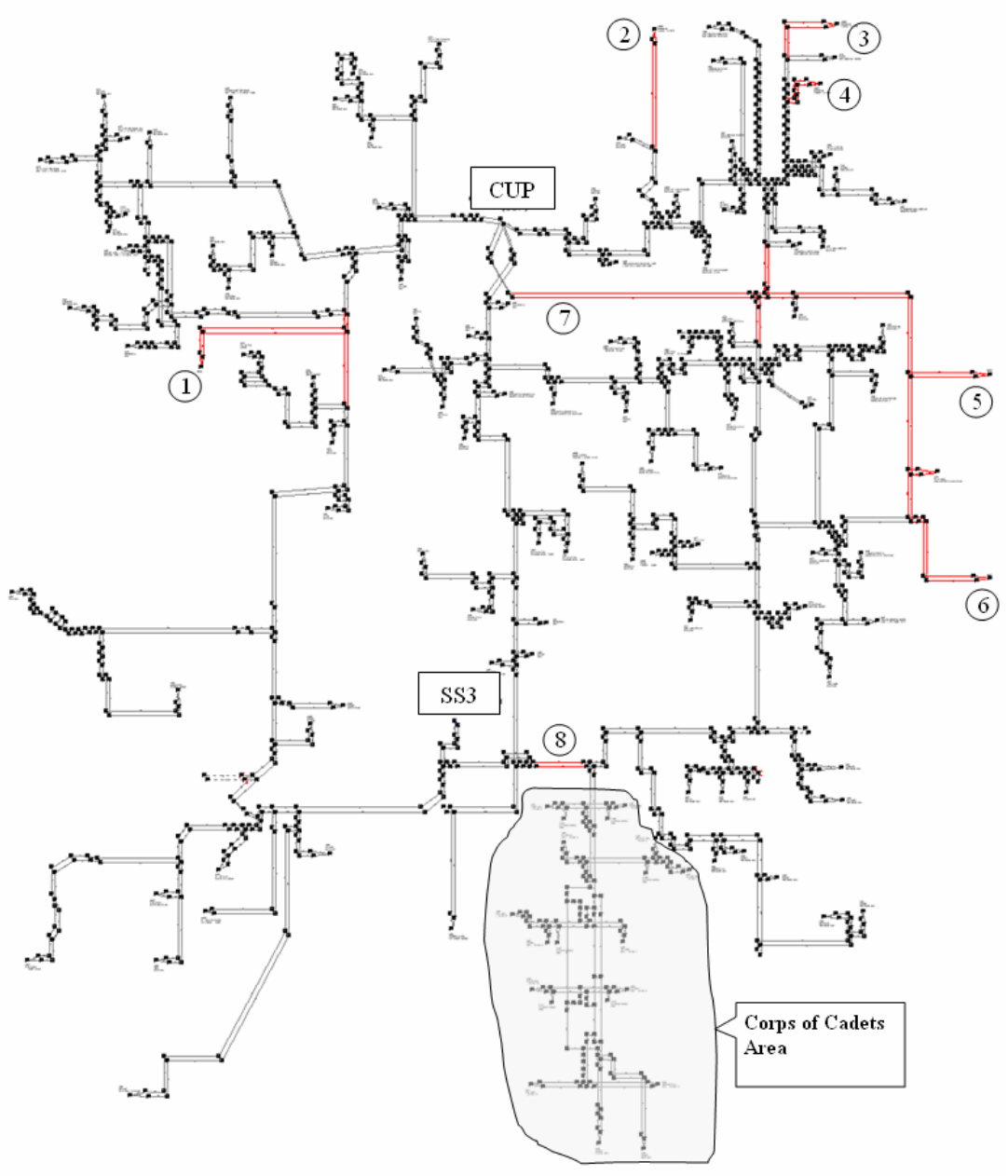

Figure 33 Model Layout of planned TAMU MC DCS Hydraulic System

In Figure 33, the added piping is shown in red. Besides the hypothetical new piping, some existing piping in the system may need to be modified as well. In addition, some piping modifications were going to be made regardless of whether these new buildings were built. For example, the 24" south loop main pipe under Ross Street (marked with number seven in Figure 33) was going to be replaced because it was deteriorating. With the planned new buildings added to the system, the decision maker needed to know whether the pipe needed to be replaced with the same size pipe or if it needed to be enlarged. As another example, a section of the main pipe (14", marked with number eight in Figure 33) on the east loop of SS3 has been identified as undersized for the current load and future load expansion. With the planned new buildings, this section of pipe also required evaluation.

9.2.3 Simulations of Different Scenarios

Adding new buildings to the DCS will require adding cooling capacity, i.e. new chillers at plants, and consequently, adding chilled water flow to the campus. However, the appropriate place(s) to add new chillers (CUP or SS3?) needs to be determined. From the distribution point of view, the second question is whether the current piping infrastructure is capable of delivering the added chilled water to the campus. What are the possible piping modifications to accommodate the expansions becomes the third question. For example, as mentioned in the previous section, by adding the planned buildings, is the 24" main pipe under Ross Street adequate or should it be replaced with a larger pipe? Also, what is the impact of the bottle-neck pipe in the SS3 east loop?

To answer the above questions, a series of scenarios of possible combinations of plant flow allocation and system piping modifications were simulated. The differential pressures for loop-end buildings were compared to determine the impact. Then the optimal way of accommodating the six new buildings to the existing system was selected.

Based on possible piping modification and locations of plant chillers, the following scenarios were considered:

1. Base scenario. This is the simulation of the existing system without any new buildings.
2. Scenario 1. It is assumed that the new chillers will be installed in the CUP, so that the chilled water flow from CUP will be increased. Other system parameters have no change.
3. Scenario 2. This scenario considers replacing the 24" main pipe under Ross Street (number 7 in Figure 32) with a larger 30" pipe, with new chillers installed in the CUP, the same as scenario one.
4. Scenario 3. This scenario considers installing the new chillers in the SS3, which is easily expanded. The main pipe under Ross Street remains at 24-inches
5. Scenario 4. Through the existing system model study, it was determined that a section of the main pipe on the east side of the SS3 (number 8 in Figure 32) is significantly undersized (14"). This scenario considers replacing it with 18" pipe. New chillers are installed in the SS3, so that the SS3 chilled water flow increases from 12,000 GPM to 16,000 GPM.

6. Scenario 5. This scenario considers increasing both the 24-inch main pipe under Ross Street to 30-inch and the 14-inch pipe on SS3 east loop to 18-inches. New chillers are considered to be installed in the SS3.

Table 18 lists the system parameters for these scenarios.

Table 18 System Parameters for Different Scenarios

System Parameters	Scenarios					
	Base	**1**	**2**	**3**	**4**	**5**
CUP differential pressure (psi)	16	16	16	16	16	16
Ross Street pipe (7) size (inch)	24	24	30	24	24	30
SS3 bottle neck pipe (8) size (inch)	14	14	14	14	18	18
CUP total flow (GPM)	35,875	42,510	42,510	38,510	38,510	38,510
SS3 total flow (GPM)	12,000	12,000	12,000	16,000	16,000	16,000
Main campus total flow (GPM)	47,875	54,510	54,510	54,510	54,510	54,510

9.2.4 Results of Simulation Analysis

Table 19 lists the simulation results for the 6 different scenarios. Comparing the simulation results of the base scenario and scenario 1, all the building differential pressures are negatively affected. The result of scenario 2 indicates a significant building DP improvement by replacing the 24" main pipe under Ross Street with a 30" diameter pipe. The result of scenario 3 also demonstrates a good improvement on building ΔP, if new chillers are placed at SS3 and nothing else is changed. Furthermore, the result of scenario 3 shows that the building ΔPs on the south-end of the main campus show significant improvement over the base scenario and scenarios 1 and 2. The result becomes even better when applying scenario 4, which further increases the 14" pipe to

18". The building ΔPs in the Corps of Cadets area (see shaded area of Figure 33) significantly improved. Finally, the overall campus building ΔPs are further improved when applying scenario 5.

Table 19 Simulated Building Differential Pressures for Different Scenarios

BLDG #	BLDG Name	Scenarios					
		Base	**1**	**2**	**3**	**4**	**5**
291	Rudder Residence Hall	-25.0	-28.2	-22.4	-24.0	-20.1	-16.3
433	Mosher Residence Hall	-4.2	-7.5	-1.4	-3.8	-1.4	3.6
450	Duncan Dining Hall	-23.7	-26.9	-21.5	-21.6	-17.2	-13.2
361	Bright Football Complex	8.7	4.3	7.0	16.9	11.3	14.0
367	Kyle Field – West Stand	6.3	1.8	4.6	14.3	8.8	11.5
439	Cain hall	-1.6	-7.4	-6.0	-2.3	-4.1	-3.2
548	Clements Residence Hall	7.6	2.4	3.1	5.3	4.1	4.7
415	Davis-Gary Residence Hall	-6.7	-11.0	-10.4	-8.6	-9.6	-9.1
386	Chemistry Engineering Building	-2.3	-5.9	0.1	-4.3	-3.3	1.3
518	Zachary Engineering Center	3.1	-2.7	3.3	-1.1	0.0	4.4
682	Wisenbaker Engineering Center	-2.5	-6.4	-0.4	-4.8	-3.7	0.8
473	Administration Building	-4.4	-7.6	-0.6	-4.8	-3.1	2.3
6	Administration Building – South	X	-9.0	-2.0	-6.2	-4.5	0.9
5	Administration Building – North	X	-7.6	-0.6	-5.0	-3.3	2.1
1	Life Science Building	X	-3.5	-2.6	0.1	-1.4	-0.7
4	Engineering Precinct In-Fill 3B	X	-7.3	-1.3	-5.7	-4.6	-0.1
3	Engineering Precinct In-Fill 2B	X	-10.3	-4.4	-8.7	-7.7	-3.2
2	Engineering Precinct In-Fill 1B	X	-2.5	0.9	-1.6	-1.0	1.6

Table 20 summarizes the simulation results from the pumping point of view. Compared with scenario 1, which requires 208 horsepower of pumping power for the selected buildings, scenario 5 will require the lowest pumping power among the scenarios. From the comparison of the different scenarios, it can be concluded that installing new chillers at the SS3 is a better choice. In addition, increasing pipe sizes will also help the pressure distribution. Therefore, the cost becomes the key issue for the decision-making process.

Table 20 Simulation Results from the Pumping Point of View

#	BLDG Name	Base	Scn. 1	Pumping power decrease			
		(psi)	(psi)	Scn. 2	Scn. 3	Scn. 4	Scn. 5
291	Rudder Residence Hall	-25	-28.2	13%	10%	19%	28%
433	Mosher Residence Hall	-4.2	-7.5	27%	16%	27%	49%
450	Duncan Dining Hall	-23.7	-26.9	13%	13%	23%	33%
361	Bright Football Complex	8.7	4.3	25%	100%	65%	91%
367	Kyle Field – West Stand	6.3	1.8	21%	95%	53%	73%
439	Cain Hall	-1.6	-7.4	6%	23%	15%	19%
548	Clements Residence Hall	7.6	2.4	6%	23%	13%	18%
415	Davis-Gary Residence Hall	-6.7	-11	2%	9%	5%	7%
386	Chemistry Engineering Building	-2.3	-5.9	29%	8%	12%	34%
518	Zachary Engineering Center	3.1	-2.7	34%	9%	15%	40%
682	Wisenbaker Engineering Center	-2.5	-6.4	28%	7%	13%	34%
473	Administration Building	-4.4	-7.6	31%	12%	20%	44%
1	Life Science Building	X	-3.5	5%	19%	11%	15%
2	Engineering Precinct In-Fill 1B	X	-2.5	19%	5%	9%	23%
3	Engineering Precinct In-Fill 2B	X	-10.3	23%	6%	10%	28%
4	Engineering Precinct In-Fill 3B	X	-7.3	27%	7%	12%	32%
5	Administration Building – North	X	-7.6	31%	12%	19%	43%
6	Administration Building – South	X	-9	29%	12%	19%	41%
Overall			**208 HP**	**18%**	**17%**	**16%**	**30%**

9.3 Summary

With engineering assumptions, planned new buildings can be added into the model of the existing system. Scenarios can be designed to represent possible system changes. The modeler can explore different possibilities and compare the simulation results to identify an optimal way of satisfying the requirements of the new buildings. The case

study demonstrates that the DCS hydraulic model can be used as a powerful analysis tool to assist the decision making for master planning.

CHAPTER X

SUMMARY AND CONCUSIONS

A practical procedure has been developed for modeling large DCS hydraulic systems for master planning purposes. Although mature modeling methodology has been developed for DWSs, and DCS hydraulic systems are similar to DWSs, there are no previously published studies of complete DCS hydraulic modeling. Various publications relating to DWS modeling technology, characteristics of large DCS, DCS building cooling energy consumption modeling, and characteristics of building chilled water systems, have been reviewed. The characteristics of a large DCS hydraulic system have been thoroughly studied. It was found that although the DWS modeling methodology can be generally applied to DCS hydraulic systems, significant differences exist which require unique solutions in order to develop a suitable hydraulic system model for a large DCS. The major differences lie in the process of physical model construction and the demand model development.

Taken the DWS modeling methodology as a reference, and based on the characteristics of large DCS hydraulic systems, a generalized modeling process for large DCS hydraulic systems has been developed. The modeling method is summarized from actual modeling experience with one of the largest DCSs in the USA. Information and data to be collected have been summarized. Specific considerations relating to the physical model construction have been discussed. The level of Skeletonization suitable for large DCS hydraulic system modeling has been discussed. An example was given to

see the impact of planned new buildings on the existing system, which indicated that every major building should be included in the model.

A method to model the peak flow demand has been developed. This method uses actual metered data and a variety of information and data to categorize the building energies and differential temperatures and then determine the building peak flow demands based on mass conservation. Although this method is developed to determine building peak flow demands, it could also be used to determine building flow demands under partial load conditions if more data were collected. The effectiveness of this method depends on the data availability and reliability. A systematic procedure for model calibration has been introduced through a case study.

The major difference between the DCS hydraulic modeling procedure and the DWS modeling procedure lies in their demand modeling processes. Instead of dealing with one parameter i.e. flow in DWS demand modeling, the DCS demand modeling involves two parameters i.e. energy and temperature.

The methodology developed in this thesis can be applied for broader purposes, such as operation optimization and system continuous commissioning®. This creates the opportunity for future study to expand on the current research. To expand this methodology to broader applications, the key is to develop the flow demand models under various load conditions.

REFERENCES

Applied Flow Technology. 2004. *AFT Fathom™ User's Guide*. Woodland Park, CA: Applied Flow Technology Corporation.

ASHRAE. 1999. *Handbook of Applications*. Atlanta: American Society of Heating, Refrigerating and Air-Conditioning Engineers.

ASHRAE. 2000. *Handbook of Systems and Equipment*. Atlanta: American Society of Heating, Refrigerating and Air-Conditioning Engineers.

ASHRAE. 2001. *Handbook of Fundamentals*. Atlanta: American Society of Heating, Refrigerating and Air-Conditioning Engineers.

Cesario, A. L., Kroon, J. R., Grayman, W., and Wright, G. 1996. New Perspectives on Calibration of Water Distribution System Models. *Proceedings of the AWWA Annual Conference*. Toronto, Canada: American Water Works Association.

Chen, Q., Xu, C., Deng, S., Claridge, D.E., and Turner, W.D. 2002. Chilled Water System Hydraulic Study - The University of Texas at San Antonio. Energy System Lab Technical Report (ESL-TR-02/01-01).

Chow, T. T., A. L. S. Chan, and Song, C.L. 2004. Building-mix optimization in district cooling system implementation. *Applied Energy* 77(1): 1-13.

Deng, S., Turner, W.D., Claridge, D.E., Liu, M., Bruner, H.L., and Wei, G. 2002. Retro-commissioning of central chilled/hot water systems. *ASHRAE Transactions* 108(2): 75-81.

Dotzauer, E. 2002. Simple model for prediction of loads in district-heating systems. *Applied Energy* 73(3-4): 277-284.

Eggener, C.L., and Polkowski, L.B. 1976. Network models and impact of modeling assumptions. *Journal of the American Water Works Association* 68(4): 189-196.

Fels, M. and M. Goldberg, 1986. Refraction of PRISM results in components of saved energy. Energy and Buildings 9:169.

Fiorino, D.P. 1999. Achieving high chilled-water delta Ts. *ASHRAE Journal* 41(11): 24-30.

IDEA 2002. Cooling, heating, and power in the nation's college & universities – census, survey, and lessons learned. *Report*. Westborough, MA: International District Energy Association.

Katipamula, S., Reddy, T.A., and Claridge, D.E. 1994. Development and application of regression models to predict cooling energy consumption in large commercial buildings. *Proceedings of the 1994 ASME/JSME/JSES International Solar Energy Conference*, San Francisco, March 27-30, PP. 307.

Kissock, J.K., Reddy, T.A., Haberl, J.S., and Claridge, D.E. 1993. E-model: A new tool for analyzing building energy use data. *Proceedings Intl. Indust. Energy Tech. Conf.*, Texas A&M University, College Station.

Lamont, P. A. 1981. Common Pipe Flow Formulas Compared with the Theory of Roughness. *Journal of the American Water Works Association*: 73(5), 274.

Larock, B.E., Jeppson, R.W., and Watters, G.Z. 2001. *Hydraulics of Pipeline Systems,*

Ormsbee, L. E., and Lingireddy, S. 1997. *Calibration of Hydraulic Network Models. Water Distribution Systems Handbook.* Mays, L. W., ed., New York: McGraw-Hill.

Pálsson, H., Larsen H.V., Bøhm, B., Ravn, H.F., and Zhou, J. 1999. *Equivalent Models of District Heating Systems – For On-line Minimization of Operational Costs of the Complete District Heating System*. Denmark: Department of Energy Engineering. Technical University of Denmark.

Phetteplace, G. 1995. Optimal Design of Piping Systems for District Heating. Cold Region Research and Engineering Laboratory Report 95-17.

Reddy, T.A., Saman, N.F., Claridge, D.E., Haberl, J.S., Turner, W.D., and Chalifoux, A. 1997. Baselining methodology for facility level monthly energy use—Part 1: Theoretical aspects. *ASHRAE Transactions* 103(2): 336-47.

Ruch, D. and Claridge, D.E. 1991. A Four Parameter Change Point Model for Prediction Energy Consumption in Commercial Buildings. *Proceedings of the ASME-JSES-SSME International Solar Energy Conference.* pp. 433-439.

Sauer, J.M. 1989. Diagnosing low temperature differential. *ASHRAE Journal* 31(6): 32-35

Thamilseran, S. and Haberl, J. 1995. A bin method for calculation energy conservation retrofit savings in commercial buildings. *Proceedings 1995 ASME/JSME/JSES Intl. Solar Energy Conference.* pp. 111-124.

Walski, T.M. 1984. Analysis of Water Distribution Systems. New York: Van Nostrand Reinhold Co.

Walski, T.M. 1995. Standards for Model Calibration. *Proceedings of the AWWA Computer Conference*. Norfolk, VA: American Water Works Association,

Walski, T.M., Chase, D.V., and Savic, D.A. 2001. *Water Distribution Modeling*, 1st ed. Waterbury, CT: Haestad Methods, Inc.

Yik, F. W. H., Burnett, J. and Prescott, I. 2001a. Predicting air-conditioning energy consumption of a group of buildings using different heat rejection methods. *Energy and Buildings* 33(2): 151-166.

Yik, F.W.H., Burnett, J. and Prescott, I. 2001b. A study on the energy performance of three schemes for widening application of water-cooled air-conditioning systems in Hong Kong. *Energy and Buildings* 33(2): 167-182.

APPENDIX

Table A - 1 Building Peak Flow Demands for TAMU Main Campus DCS

Node #	AC Area (ft^2)	Pipe Diameter (inches)	BLDG Type	Type of In-BLDG System	Metered Data			Historical Peak (GPM)	BLDG Design Flow (GPM)	Pump Design Flow (GPM)	Initial Estimation			Final Flow (GPM)
					Flow (GPM)	ΔT (°F)	Load (Tons)				Load (Tons)	ΔT (°F)	Flow (GPM)	
290	67,283	8	1	Variable	343	8.3	118	450	200	610	116.2	8.3	336	343
291	67,283	8	1	Variable	N/A	8.9	N/A	380	240	610	116.2	8.9	313	314
292	67,283	8	1	Variable	271	9.6	109	376	194	610	116.2	9.6	292	271
293	82,767	8	1	Variable	406	9.7	164	560	274	610	143.0	9.7	354	406
294	59,541	6	1	Variable	234	9.6	94	300	200	505	102.8	9.6	257	234
353	148,837	8	4	Variable	561	15.1	354	1,300	900	N/A	384.3	15.1	612	561
361	124,971	10	4	Variable	N/A	N/A	232	N/A	897	N/A	322.7	10.2	759	475
369	153,886	8	2	Variable	542	7.6	170	570	700	510	211.1	7.6	670	542
376	115,797	14	3	Variable	N/A	N/A	N/A	1,700	2,425	1,710	579.1	10.2	1363	1365
383	110,272	8	2	Variable	N/A	12.0	N/A	500	N/A	1,220	151.3	12.0	303	303
384	19,363	4	2	Variable	66	13.6	37	N/A	N/A	N/A	26.6	13.6	47	66
385	157,844	8	4	Variable	904	9.4	359	1,300	1,469	514	407.5	9.4	1044	904
386	204,972	12	3	Variable	1,635	15.1	1,025	N/A	N/A	N/A	1025.2	15.1	1630	1635
387	109,228	8	4	Variable	N/A	N/A	N/A	1,100	750	N/A	282.0	10.2	664	665
391	115,288	8	4	Variable	842	9.9	347	N/A	1,476	560	297.7	9.9	722	842
394	81,730	8	1	Variable	349	10.3	151	400	271	600	141.2	10.3	330	349
398	102,105	8	2	Constant	528	8.7	189	500	N/A	1,220	140.1	8.7	388	528
400	31,952	6	1	Variable	241	4.9	50	N/A	N/A	340	55.2	4.9	270	241
401	31,952	6	1	Constant	182	6.2	48	N/A	N/A	340	55.2	6.2	214	182
402	32,139	4	1	Variable	119	11.1	55	N/A	N/A	340	55.5	11.1	120	119
403	31,952	4	1	Constant	170	N/A	N/A	N/A	N/A	340	55.2	7.6	174	170
404	33,904	4	1	Variable	198	5.1	42	N/A	N/A	336	58.6	5.1	277	198
405	31,052	4	1	Constant	175	8.6	64	N/A	N/A	190	53.6	8.6	150	175
406	31,952	4	1	Variable	N/A	6.9	N/A	N/A	N/A	336	55.2	6.9	193	193

407	31,952	4	1	Constant	171	7.7	56	N/A	N/A	190	55.2	7.7	172	171
408	31,952	6	1	Variable	167	5.2	37	N/A	N/A	336	55.2	5.2	257	167
409	31,952	6	1	Constant	152	7.4	48	N/A	N/A	190	55.2	7.4	179	152
410	31,952	4	1	Variable	133	8.2	46	180	N/A	336	55.2	8.2	161	133
411	31,952	4	1	Constant	126	9.6	51	N/A	N/A	190	55.2	9.6	138	126
412	40,828	5	1	Constant	301	5.5	69	N/A	N/A	336	70.5	5.5	308	301
413	40,828	5	1	Constant	278	5.7	66	N/A	N/A	336	70.5	5.7	298	278
414	40,828	5	1	Constant	N/A	N/A	N/A	N/A	N/A	336	70.5	7.6	223	223
415	40,828	5	1	Constant	277	5.1	58	N/A	N/A	336	70.5	5.1	335	277
419	45,134	5	2	Constant	175	5.6	41	N/A	N/A	N/A	61.9	5.6	267	175
420	45,134	5	1	Constant	N/A	N/A	N/A	N/A	N/A	212	78.0	7.6	246	247
424	18,500	4	1	Constant	N/A	N/A	N/A	N/A	N/A	160	32.0	7.6	101	101
425	22,185	4	4	Variable	155	10.8	69	N/A	N/A	158	57.3	10.8	127	155
426	118,841	6	1	Variable	574	12.2	288	N/A	N/A	510	205.3	12.2	403	574
429	31,184	3	1	Constant	N/A	8.8	N/A	N/A	N/A	65	53.9	8.8	147	147
430	40,957	6	1	Variable	125	16.2	86	140	N/A	100	70.7	16.2	105	125
432	69,914	10	2	Variable	N/A	N/A	N/A	470	N/A	505	95.9	10.2	226	226
433	155,430	6	1	Variable	N/A	8.6	N/A	500	N/A	555	268.5	8.6	747	748
434	80,464	8	4	Constant	N/A	N/A	N/A	930	N/A	N/A	207.7	7.6	656	657
435	130,844	6	2	Variable	300	16.2	201	500	670	N/A	179.5	16.2	265	300
436	80,218	8	4	Constant	691	8.3	239	770	N/A	622	207.1	8.3	599	691
438	61,860	6	2	Constant	500	4.3	91	560	350	455	84.9	4.3	470	500
439	92,812	8	2	Variable	N/A	N/A	N/A	450	N/A	675	127.3	10.2	300	300
440	57,500	8	4	Variable	N/A	8.5	N/A	700	N/A	855	148.5	8.5	417	418
441	112,133	6	2	Variable	341	7.8	111	500	N/A	550	153.9	7.8	471	341
442	112,133	8	2	Variable	385	6.1	99	500	N/A	550	153.9	6.1	603	385
443	180,316	10	4	Variable	N/A	N/A	N/A	1,000	N/A	700	465.5	10.2	1095	1098
444	84,831	8	4	Constant	756	9.8	308	750	N/A	780	219.0	9.8	537	756
445	89,735	8	2	Variable	N/A	N/A	N/A	350	N/A	1,300	123.1	10.2	290	290
447	113,388	10	1	Variable	431	8.3	150	680	N/A	550	195.9	8.3	564	431
448	54,960	6	2	Constant	140	10.0	63	210	N/A	245	75.4	10.0	181	140
449	96,038	8	4	Constant	625	8.9	229	670	N/A	815	248.0	8.9	671	625
450	55,053	6	4	Variable	471	9.6	189	570	N/A	750	142.1	9.6	356	471
454	301,400	12	2	Variable	926	8.9	454	2,000	N/A	1,080	413.5	8.9	1113	926
456	42,532	6	2	Constant	N/A	N/A	N/A	N/A	N/A	226	58.4	7.6	184	185

457	16,364	4	2	Constant	N/A	N/A	N/A	N/A	N/A	60	22.5	7.6	71	71
461	24,466	3	4	Constant	N/A	10.0	N/A	180	N/A	N/A	63.2	10.0	152	152
462	88,102	10	2	Constant	N/A	N/A	N/A	800	N/A	980	120.9	7.6	382	600
463	58,820	6	4	Constant	214	23.4	200	N/A	N/A	435	151.9	23.4	156	214
465	29,699	4	2	Constant	97	8.4	34	190	N/A	190	40.7	8.4	117	97
467	61,586	8	4	Variable	461	8.3	158	580	N/A	616	159.0	8.3	461	461
470	39,887	4	2	Constant	N/A	N/A	N/A	N/A	N/A	371	54.7	7.6	173	173
471	40,062	5	2	Constant	216	6.3	56	N/A	N/A	108	55.0	6.3	210	216
472	44,856	4	2	Constant	N/A	N/A	N/A	N/A	N/A	325	61.5	7.6	194	195
473	69,898	8	2	Variable	N/A	N/A	N/A	340	N/A	N/A	95.9	10.2	226	249
474	33,814	3	2	Constant	N/A	N/A	N/A	N/A	N/A	349	46.4	7.6	147	147
476	36,850	4	4	Constant	N/A	N/A	N/A	N/A	N/A	371	95.1	7.6	300	301
477	51,592	6	4	Constant	494	4.9	103	N/A	N/A	590	133.2	4.9	651	494
478	62,228	6	2	Constant	N/A	N/A	N/A	130	N/A	350	85.4	7.6	270	88
480	39,686	6	2	Constant	N/A	N/A	N/A	N/A	N/A	254	54.5	7.6	172	172
481	13,700	3	2	Constant	N/A	N/A	N/A	N/A	100	100	18.8	7.6	59	59
482	19,074	3	2	Constant	N/A	N/A	N/A	N/A	N/A	N/A	26.2	7.6	83	83
483	81,404	3	2	Constant	429	5.5	98	300	N/A	445	111.7	5.5	484	429
492	56,537	6	4	Constant	N/A	N/A	N/A	330	N/A	340	146.0	7.6	461	270
495	71,092	8	4	Variable	N/A	N/A	N/A	960	N/A	660	183.5	10.2	432	433
499	26,865	12	4	Constant	N/A	1.3	N/A	N/A	142	185	69.4	1.3	1332	219
506	32,306	4	4	Constant	184	10.3	77	N/A	N/A	N/A	83.4	10.3	195	184
511	40,476	6	4	Constant	N/A	N/A	N/A	N/A	N/A	534	104.5	7.6	330	331
512	8,999	3	2	Constant	N/A	9.8	N/A	N/A	N/A	90	12.3	9.8	30	30
513	42,336	6	4	Constant	458	5.4	103	N/A	N/A	500	109.3	5.4	482	458
514	22,134	6	2	Constant	N/A	N/A	N/A	N/A	N/A	160	30.4	7.6	96	96
516	30,014	4	4	Variable	N/A	10.3	N/A	N/A	504	N/A	77.5	10.3	181	181
518	258,600	14	4	Variable	N/A	9.0	N/A	1,130	N/A	2,000	667.7	9.0	1780	1784
520	50,015	6	4	Constant	460	4.7	90	380	430	120	129.1	4.7	658	460
521	104,949	8	4	Constant	1,264	6.3	328	1,100	830	830	271.0	6.3	1039	1264
524	257,953	8	4	Variable	935	20.6	805	1,200	1,496	749	666.0	20.6	778	935
548	62,156	10	1	Constant	428	6.3	113	600	235	600	107.4	6.3	407	428
549	69,688	6	1	Constant	N/A	N/A	N/A	690	263	648	120.4	7.6	380	381
550	62,156	6	1	Variable	280	11.4	133	420	295	600	107.4	11.4	226	280
652	69,688	6	1	Constant	380	6.0	97	530	263	648	120.4	6.0	478	380

653	62,156	6	1	Constant	460	5.5	107	560	295	600	107.4	5.5	466	460
682	177,704	8	2	Variable	761	9.0	285	1,100	1,021	595	243.8	9.0	650	761
740	20,904	6	4	Constant	N/A	N/A	N/A	N/A	N/A	223	54.0	7.6	170	171
1400	3,456	2	4	Constant	N/A	N/A	N/A	N/A	N/A	N/A	8.9	7.6	28	28
1401	5,031	2	4	Constant	N/A	N/A	N/A	N/A	N/A	N/A	13.0	7.6	41	41
1406	5,143	2	4	Constant	N/A	N/A	N/A	N/A	N/A	N/A	13.3	7.6	42	42
1407	5,012	2	4	Constant	N/A	N/A	N/A	N/A	N/A	N/A	12.9	7.6	41	41
1410	5,047	2	4	Constant	N/A	N/A	N/A	N/A	N/A	N/A	13.0	7.6	41	41
1411	3,456	2	4	Constant	N/A	N/A	N/A	N/A	N/A	N/A	8.9	7.6	28	28
1412	1,970	2	4	Constant	N/A	N/A	N/A	N/A	N/A	N/A	5.1	7.6	16	16
3671	100,000	10	4	Variable	N/A	N/A	N/A	530	610	610	258.2	10.2	607	609
3672	200,000	10	4	Variable	953	N/A	351	1,000	852	N/A	516.4	10.2	1215	953
4461	76,470	8	4	Variable	589	N/A	251	800	N/A	N/A	197.4	10.2	465	589
4462	225,770	8	2	Variable	N/A	N/A	N/A	N/A	N/A	N/A	309.8	10.2	729	730
4531	151,860	8	2	Variable	339	16.3	232	1,200	N/A	1,595	208.4	16.3	308	339
4532	25,978	8	4	Variable	226	10.9	103	430	183	N/A	67.1	10.9	147	226
4681	244,000	8	4	Variable	N/A	N/A	N/A	800	1,160	N/A	630.0	10.2	1482	1485
4682	200,100	8	4	Variable	N/A	N/A	N/A	920	N/A	1,290	516.6	10.2	1216	1218
4683	174,100	12	4	Variable	704	N/A	324	N/A	N/A	N/A	449.5	10.2	1058	704
4841	73,000	10	3	Variable	N/A	N/A	N/A	800	N/A	N/A	365.1	10.2	859	861
4842	145,131	10	3	Variable	N/A	N/A	N/A	2,100	N/A	N/A	725.9	10.2	1708	1711
4901	61,200	6	2	Variable	N/A	N/A	N/A	600	480	N/A	84.0	10.2	198	198
4902	59,600	6	4	Variable	N/A	N/A	N/A	430	387	388	153.9	10.2	362	388

Table A - 2 Basic Information about Model Nodes and Corresponding Buildings

Node #	BLDG #	Building Name	AC Area (ft^2)
290	290	WELLS RESIDENCE HALL	67,283
291	291	RUDDER RESIDENCE HALL	67,283
292	292	EPPRIGHT RESIDENCE HALL	67,283
293	293	APPELT RESIDENCE HALL	82,767
294	294	LECHNER RESIDENCE HALL	59,541
353	353	BRIGHT BUILDING	148,837
361	361	BRIGHT FOOTBALL COMPLEX	124,971
369	369	READ BUILDING	153,886
376	376	CHEMISTRY BUILDING ADDITION	121,911
383	379	KOLDUS BUILDING	113,272
384	384	SANDERS CORPS OF CADETS CENTER	19,363
385	385	CE/TTI OFFICE & LAB BUILDING	157,844
386	386	JACK BROWN CHEMISTRY ENGINEERING BUILDING	204,972
387	387	RICHARDSON PETROLEUM ENGINEERING BUILDING	113,700
391	391	ENGINEERING/PHYSICS BUILDING	115,288
394	394	UNDERWOOD RESDIENCE HALL	81,730
398	398	LANGFORD ARCHITECTURE CENTER BUILDING A	102,105
400	400	SPENCE HALL - DORM 1	31,952
401	401	KIEST HALL - DORM 2	31,952
402	402	BRIGGS HALL - DORM 3	32,139
403	403	FOUNTAIN HALL - DORM 4	31,952
404	404	GAINER HALL - DORM 5	33,904
405	405	LACY HALL - DORM 6	31,052
406	406	LEONARD HALL - DORM 7	31,952
407	407	HARRELL HALL - DORM 8	31,952
408	408	WHITELY HALL - DORM 9	31,952
409	409	WHITE HALL - DORM 10	31,952
410	410	HARRINGTON HALL - DORM 11	31,952
411	411	UTAY HALL - DORM 12	31,952
412	412	MOSES RESIDENCE HALL	40,828
413	413	MOORE RESIDENCE HALL (413) + LOUNGE (1413)	40,828
414	414	CROCKER RESIDENCE HALL	40,828
415	415	DAVIS-GARY RESIDENCE HALL (415) + LOUNGE (1415)	40,828
419	419	LEGETT RESIDENCE HALL	45,134
420	420	MILNER HALL	48,268
424	424	HOTARD RESIDENCE HALL	18,500
425	425	HENDERSON HALL	22,185
426	426	HUGHES (426) + FOWLER (427) + KEATHLEY (428) + LOUNGE (1427)	118,841
429	429	MCINNIS RESIDENCE HALL	31,184

430	430	SCHUHMACHER RESIDENCE HALL (430) + LOUNGE (1430)	40,957
432	432	ARCHITECTURE BUILDING C	69,914
433	433	MOSHER RESIDENCE HALL	155,430
434	434	LUEDECKE BUILDING (CYCLOTRON)	80,464
435	435	HARRINGTON EDUCATION CENTER OFFICE TOWER	130,844
436	436	REED-MCDONALD BUILDING (436) + BUS STOP SNACK BAR (396)	78,035
438	438	HARRINGTON EDUCATION CENTER CLASSROOM BUILDING	61,860
439	439	CAIN HALL	92,812
440	440	COMMONS	84,500
441	441	KRUEGER RESIDENCE HALL	112,133
442	442	DUNN RESIDENCE HALL	112,133
443	443	OCEANOGRAPHY & METEOROLOGY BUILDING	180,316
444	444	PETERSON BUILDING	84,831
445	445	TEAGUE RESEARCH CENTER (445) + DPC ANNEX (517)	89,735
447	447	ASTON RESIDENCE HALL	113,388
448	448	ADAMS BAND HALL	55,248
449	449	BIOLOGICAL SCIENCES BLDG. WEST	96,038
450	450	DUNCAN DINING HALL	128,482
454	454	MEMORIAL STUDENT CENTER	368,935
456	456	MILITARY SCIENCES BUILDING	43,808
457	457	TAES ANNEX BUILDING	16,364
461	461	COKE BUILDING	24,466
462	462	ACADEMIC BUILDING	82,555
463	463	PSYCHOLOGY BUILDING	38,469
465	465	BUTLER HALL	29,699
467	467	BIOLOGICAL SCIENCES BLDG. EAST	62,273
470	470	GLASSCOCK HISTORY BUILDING	39,887
471	471	PAVILION	40,062
472	472	ANIMAL INDUSTRIES BUILDING	44,856
473	473	WILLIAMS ADMINISTRATION BUILDING	69,898
474	474	YMCA BUILDING	33,814
476	476	FRANCIS HALL	36,850
477	477	ANTHROPOLOGY BUILDING	51,592
478	478	SCOATES HALL	62,228
480	480	BOLTON HALL	39,686
481	481	HEATON HALL	13,700
482	482	FERMIER HALL	19,074
483	483	THOMPSON HALL	81,404
492	492	CIVIL ENGINEERING BUILDING	56,537
495	495	SBISA DINING HALL	94,233
499	499	GRAPHIC SERVICES	29,782
506	506	NAGLE HALL	32,306
511	511	HEEP LABORATORY BUILDING	40,476
512	512	ALL FAITHS CHAPEL	8,999
513	513	DOHERTY BUILDING	42,336

514	514	FACILITIES PLANNING & CONSTRUCTION	22,134
516	516	COMPUTING SERVICES CENTER	30,014
518	518	ZACHRY ENGINEERING CENTER	324,000
520	520	BEUTEL HEALTH CENTER	61,945
521	521	HELDENFELS HALL	104,949
524	524	BLOCKER BUILDING	257,953
548	548	CLEMENTS RESIDENCE HALL	62,156
549	549	HAAS RESIDENCE HALL	62,156
550	550	MCFADDEN RESIDENCE HALL	69,668
652	652	NEELEY RESIDENCE HALL	62,156
653	653	HOBBY RESIDENCE HALL	69,668
682	682	WISENBAKER ENGINEERING RESEARCH CENTER	177,704
740	740	MCNEW LABORATORY	20,904
1400	1400	LOUNGE-DUNCAN AREA	3,456
1401	1401	LOUNGE-DUNCAN AREA	5,031
1406	1406	LOUNGE-DUNCAN AREA	5,143
1407	1407	LOUNGE-DUNCAN AREA	5,012
1410	1410	LOUNGE-DUNCAN AREA	5,047
1411	1411	LOUNGE-DUNCAN AREA	3,456
1412	1412	CIVILIAN LOUNGES	1,970
3671	367	KYLE FIELD - WEST STAND	260,575
3672	367	KYLE FIELD - NORTH END ZONE	391,516
4461	446	RUDDER AUDITORIUM	76,470
4462	446	RUDDER TOWER	225,770
4531	453	G. ROLLIE WHITE COLISEUM	151,860
4532	453	G. ROLLIE WHITE COLISEUM - ANNEX	25,978
4681	468	EVANS LIBRARY - EVANS 79 ADDITION	244,000
4682	468	EVANS LIBRARY - CUSHING + EVANS (OLD)	200,100
4683	468	EVANS LIBRARY - ANNEX	174,100
4841	484	CHEMISTRY BUILDING - 72 WING	73,000
4842	484	CHEMISTRY BUILDING - 28/32/59 WING	145,131
4901	490	HALBOUTY GEOSCIENCES BUILDING (OLD)	61,200
4902	490	HALBOUTY GEOSCIENCES BUILDING (NEW)	59,600

Table A - 3 Simulation Results after Model Rough-tuning

NODE #	Measured		Init. Sim.		Rough-tuning	
	Demands (GPM)	ΔP (Psi)	Demands (GPM)	ΔP (Psi)	Demands (GPM)	ΔP (Psi)
290	343	N/A	343	-6.28	343	-17.76
291	218	-27.61	314	-7.26	329	-19.32
292	271	N/A	271	-7.20	271	-19.23
293	406	N/A	406	-4.94	406	-15.89
294	234	5.00	234	13.33	234	9.82

353	561	4.18	561	8.00	561	2.52
361	N/A	9.43	475	13.19	497	9.50
369	542	0.40	542	8.55	542	2.73
376	N/A	N/A	1365	7.29	1429	1.68
383	N/A	5.20	303	13.39	317	9.84
384	66	7.22	66	12.24	66	8.31
385	904	N/A	904	5.04	904	-1.32
386	1,635	-9.76	1635	4.51	1635	-2.23
387	N/A	N/A	665	8.03	696	2.52
391	842	N/A	842	7.76	842	2.50
394	349	N/A	349	-4.73	349	-15.48
398	528	-4.30	528	4.87	528	-1.55
400	241	-14.00	241	1.84	241	-5.99
401	182	N/A	182	2.05	182	-5.69
402	119	-14.34	119	-4.26	119	-15.05
403	170	N/A	170	-4.18	170	-14.92
404	198	N/A	198	-5.47	198	-16.77
405	175	N/A	175	-8.98	175	-21.95
406	95	N/A	193	-8.45	202	-21.63
407	171	N/A	171	-6.56	171	-18.25
408	167	N/A	167	-5.68	167	-17.36
409	152	N/A	152	-5.61	152	-17.25
410	133	N/A	133	-7.97	133	-20.92
411	126	N/A	126	-7.68	126	-20.51
412	301	N/A	301	7.34	301	1.07
413	278	N/A	278	3.38	278	-4.67
414	N/A	N/A	223	2.91	233	-5.78
415	277	N/A	277	3.08	277	-4.99
419	175	N/A	175	13.01	175	9.62
420	N/A	N/A	247	14.11	258	10.64
424	N/A	N/A	101	5.37	106	-2.17
425	150	-12.84	155	4.18	155	-3.51
426	574	N/A	574	11.05	574	6.83
429	79	N/A	147	5.40	154	-3.06
430	125	-8.40	125	8.45	125	2.50
432	N/A	N/A	226	6.10	237	-0.05
433	273	N/A	748	-0.14	783	-8.64
434	N/A	N/A	657	4.35	688	-2.97
435	300	5.25	300	13.88	300	10.89
436	691	N/A	691	14.13	691	11.23
438	500	N/A	500	11.12	500	7.71
439	N/A	N/A	300	11.66	314	7.37
440	2,700	-15.00	418	4.91	437	-1.61
441	341	-15.00	341	1.10	341	-6.90
442	385	N/A	385	4.87	385	-1.62
443	N/A	-6.90	1098	1.86	1148	-5.98

444	756	N/A	756	2.43	756	-3.82
445	N/A	N/A	290	2.54	304	-5.05
447	431	N/A	431	5.03	431	-1.46
448	140	-19.00	140	-5.81	140	-17.73
449	625	-15.22	625	6.54	625	0.83
450	471	-22.51	471	-6.83	471	-19.15
454	926	-6.44	926	10.89	926	6.34
456	N/A	N/A	185	12.07	193	8.15
457	N/A	N/A	71	2.31	74	-5.41
461	488	-0.95	152	7.46	159	0.39
462	N/A	N/A	600	13.80	600	10.82
463	214	N/A	214	10.51	214	6.01
465	97	0.78	97	11.96	97	7.99
467	461	N/A	461	7.31	461	1.78
470	N/A	N/A	173	1.18	181	-4.55
471	216	N/A	216	3.55	216	-2.85
472	N/A	N/A	195	2.41	204	-5.15
473	N/A	N/A	249	2.50	249	-4.92
474	N/A	N/A	147	10.56	154	5.26
476	N/A	N/A	301	1.83	315	-6.63
477	494	N/A	494	5.05	494	-1.42
478	N/A	N/A	88	7.32	88	1.75
480	N/A	N/A	172	14.21	180	11.31
481	N/A	N/A	59	12.37	62	8.36
482	N/A	N/A	83	14.36	87	11.39
483	429	N/A	429	4.44	429	-3.10
492	N/A	N/A	270	6.97	270	1.03
495	N/A	2.81	433	15.37	900	10.90
499	72	N/A	219	15.27	230	12.74
506	184	N/A	184	4.73	184	-2.27
511	N/A	N/A	331	3.86	346	-3.49
512	58	N/A	30	13.38	32	9.85
513	458	-5.97	458	5.06	458	-1.41
514	N/A	N/A	96	9.60	101	4.10
516	97	N/A	181	3.24	189	-4.35
518	859	N/A	1784	6.69	1866	0.57
520	460	N/A	460	13.30	460	9.85
521	1,264	-8.34	1264	7.47	1264	1.73
524	935	5.91	935	5.69	935	-0.36
548	428	N/A	428	12.25	428	8.25
549	N/A	N/A	381	10.73	398	5.78
550	280	N/A	280	10.80	280	6.02
652	380	N/A	380	6.27	380	-0.47
653	460	N/A	460	6.24	460	-0.38
682	761	N/A	761	4.33	761	-2.56
740	N/A	N/A	171	6.38	179	0.39

1400	N/A	N/A	28	-3.41	30	-14.42
1401	N/A	N/A	41	-8.61	43	-22.78
1406	N/A	N/A	42	-31.70	44	-59.69
1407	N/A	N/A	41	-22.40	43	-44.10
1410	N/A	N/A	41	-16.40	43	-34.56
1411	N/A	N/A	28	-10.88	30	-25.71
1412	N/A	N/A	16	6.67	17	-0.02
3671	211	N/A	609	8.69	637	2.85
3672	953	8.40	953	7.60	953	1.81
4461	589	6.86	589	12.03	589	7.94
4462	341	2.60	730	11.70	764	7.36
4531	339	3.00	339	13.16	339	9.58
4532	226	6.25	226	13.25	226	9.63
4681	N/A	N/A	1485	-0.64	906	-0.56
4682	N/A	N/A	1218	-2.34	850	-7.09
4683	704	N/A	704	3.94	704	-2.32
4841	N/A	N/A	861	6.89	901	1.35
4842	N/A	N/A	1711	6.65	1492	2.80
4901	N/A	N/A	198	10.17	207	5.58
4902	N/A	N/A	388	10.62	388	6.38

Table A - 4 Simulation Results of Sensitivity Study by Adjusting Boundary Condition

NODE #	Measured		Init. Sim. (CUP ΔP = 16.8 psi)		CUP ΔP = 14.8 psi		CUP ΔP = 12.8 psi	
	Demands (GPM)	ΔP (Psi)	Demands (GPM)	ΔP (Psi)	Demands (GPM)	ΔP (Psi)	Demands (GPM)	ΔP (Psi)
290	343	N/A	343	-6.28	343	-8.28	343	-10.28
291	218	-27.61	314	-7.26	329	-9.26	331	-11.26
292	271	N/A	271	-7.20	271	-9.20	271	-11.20
293	406	N/A	406	-4.94	406	-6.94	406	-8.94
294	234	5.00	234	13.33	234	11.33	234	9.33
353	561	4.18	561	8.00	561	6.00	561	4.00
361	N/A	9.43	475	13.19	497	11.19	485	9.19
369	542	0.40	542	8.55	542	6.55	542	4.55
376	N/A	N/A	1365	7.29	1429	5.29	1392	3.29
383	N/A	5.20	303	13.39	317	11.39	309	9.39
384	66	7.22	66	12.24	66	10.24	66	8.24
385	904	N/A	904	5.04	904	3.04	904	1.04
386	1,635	-9.76	1635	4.51	1635	2.51	1635	0.51
387	N/A	N/A	665	8.03	696	6.03	678	4.03
391	842	N/A	842	7.76	842	5.76	842	3.76
394	349	N/A	349	-4.73	349	-6.73	349	-8.73

398	528	-4.30	528	4.87	528	2.87	528	0.87
400	241	-14.00	241	1.84	241	-0.16	200	-2.16
401	182	N/A	182	2.05	182	0.05	200	-1.95
402	119	-14.34	119	-4.26	119	-6.26	200	-8.26
403	170	N/A	170	-4.18	170	-6.18	200	-8.18
404	198	N/A	198	-5.47	198	-7.47	200	-9.47
405	175	N/A	175	-8.98	175	-10.98	200	-12.98
406	95	N/A	193	-8.45	202	-10.45	200	-12.45
407	171	N/A	171	-6.56	171	-8.56	200	-10.56
408	167	N/A	167	-5.68	167	-7.68	200	-9.68
409	152	N/A	152	-5.61	152	-7.61	200	-9.61
410	133	N/A	133	-7.97	133	-9.97	200	-11.97
411	126	N/A	126	-7.68	126	-9.68	200	-11.68
412	301	N/A	301	7.34	301	5.34	301	3.34
413	278	N/A	278	3.38	278	1.38	278	-0.62
414	N/A	N/A	223	2.91	233	0.91	235	-1.09
415	277	N/A	277	3.08	277	1.08	277	-0.92
419	175	N/A	175	13.01	175	11.01	175	9.01
420	N/A	N/A	247	14.11	258	12.11	260	10.11
424	N/A	N/A	101	5.37	106	3.37	107	1.37
425	150	-12.84	155	4.18	155	2.18	155	0.18
426	574	N/A	574	11.05	574	9.05	574	7.05
429	79	N/A	147	5.40	154	3.40	155	1.40
430	125	-8.40	125	8.45	125	6.45	125	4.45
432	N/A	N/A	226	6.10	237	4.10	231	2.10
433	273	N/A	748	-0.14	783	-2.14	788	-4.14
434	N/A	N/A	657	4.35	688	2.35	670	0.35
435	300	5.25	300	13.88	300	11.88	300	9.88
436	691	N/A	691	14.13	691	12.13	691	10.13
438	500	N/A	500	11.12	500	9.12	500	7.12
439	N/A	N/A	300	11.66	314	9.66	306	7.66
440	2,700	-15.00	418	4.91	437	2.91	426	0.91
441	341	-15.00	341	1.10	341	-0.90	341	-2.90
442	385	N/A	385	4.87	385	2.87	385	0.87
443	N/A	-6.90	1098	1.86	1148	-0.14	1119	-2.14
444	756	N/A	756	2.43	756	0.43	756	-1.57
445	N/A	N/A	290	2.54	304	0.54	296	-1.46
447	431	N/A	431	5.03	431	3.03	431	1.03
448	140	-19.00	140	-5.81	140	-7.81	140	-9.81
449	625	-15.22	625	6.54	625	4.54	625	2.54
450	471	-22.51	471	-6.83	471	-8.83	471	-10.83
454	926	-6.44	926	10.89	926	8.89	926	6.89
456	N/A	N/A	185	12.07	193	10.07	188	8.07
457	N/A	N/A	71	2.31	74	0.31	72	-1.69
461	488	-0.95	152	7.46	159	5.46	155	3.46
462	N/A	N/A	600	13.80	600	11.80	600	9.80

463	214	N/A	214	10.51	214	8.51	214	6.51
465	97	0.78	97	11.96	97	9.96	97	7.96
467	461	N/A	461	7.31	461	5.31	461	3.31
470	N/A	N/A	173	1.18	181	-0.82	177	-2.82
471	216	N/A	216	3.55	216	1.55	216	-0.45
472	N/A	N/A	195	2.41	204	0.41	199	-1.59
473	N/A	N/A	249	2.50	249	0.50	249	-1.50
474	N/A	N/A	147	10.56	154	8.56	150	6.56
476	N/A	N/A	301	1.83	315	-0.17	307	-2.17
477	494	N/A	494	5.05	494	3.05	494	1.05
478	N/A	N/A	88	7.32	88	5.32	88	3.32
480	N/A	N/A	172	14.21	180	12.21	176	10.21
481	N/A	N/A	59	12.37	62	10.37	61	8.37
482	N/A	N/A	83	14.36	87	12.36	84	10.36
483	429	N/A	429	4.44	429	2.44	429	0.44
492	N/A	N/A	270	6.97	270	4.97	270	2.97
495	N/A	2.81	433	15.37	900	13.37	900	11.37
499	72	N/A	219	15.27	230	13.27	224	11.27
506	184	N/A	184	4.73	184	2.73	184	0.73
511	N/A	N/A	331	3.86	346	1.86	337	-0.14
512	58	N/A	30	13.38	32	11.38	31	9.38
513	458	-5.97	458	5.06	458	3.06	458	1.06
514	N/A	N/A	96	9.60	101	7.60	98	5.60
516	97	N/A	181	3.24	189	1.24	185	-0.76
518	859	N/A	1784	6.69	1866	4.69	1819	2.69
520	460	N/A	460	13.30	460	11.30	460	9.30
521	1,264	-8.34	1264	7.47	1264	5.47	1264	3.47
524	935	5.91	935	5.69	935	3.69	935	1.69
548	428	N/A	428	12.25	428	10.25	428	8.25
549	N/A	N/A	381	10.73	398	8.73	401	6.73
550	280	N/A	280	10.80	280	8.80	280	6.80
652	380	N/A	380	6.27	380	4.27	380	2.27
653	460	N/A	460	6.24	460	4.24	460	2.24
682	761	N/A	761	4.33	761	2.33	761	0.33
740	N/A	N/A	171	6.38	179	4.38	174	2.38
1400	N/A	N/A	28	-3.41	30	-5.41	29	-7.41
1401	N/A	N/A	41	-8.61	43	-10.61	42	-12.61
1406	N/A	N/A	42	-31.70	44	-33.70	43	-35.70
1407	N/A	N/A	41	-22.40	43	-24.40	42	-26.40
1410	N/A	N/A	41	-16.40	43	-18.40	42	-20.40
1411	N/A	N/A	28	-10.88	30	-12.88	29	-14.88
1412	N/A	N/A	16	6.67	17	4.67	16	2.67
3671	211	N/A	609	8.69	637	6.69	621	4.69
3672	953	8.40	953	7.60	953	5.60	953	3.60
4461	589	6.86	589	12.03	589	10.03	589	8.03
4462	341	2.60	730	11.70	764	9.70	745	7.70

4531	339	3.00	339	13.16	339	11.16	339	9.16
4532	226	6.25	226	13.25	226	11.25	226	9.25
4681	N/A	N/A	1485	-0.64	906	-2.64	906	-4.64
4682	N/A	N/A	1218	-2.34	850	-4.34	850	-6.34
4683	704	N/A	704	3.94	704	1.94	704	-0.06
4841	N/A	N/A	861	6.89	901	4.89	878	2.89
4842	N/A	N/A	1711	6.65	1492	4.65	1454	2.65
4901	N/A	N/A	198	10.17	207	8.17	202	6.17
4902	N/A	N/A	388	10.62	388	8.62	388	6.62

Table A - 5 Simulation Results of Sensitivity Study by Adjusting Global Pipe Design Factor (DF)

NODE #	Measured		Init. Sim. (DF = 1)		DF = 1.25		DF = 1.5	
	Demands (GPM)	ΔP (Psi)	Demands (GPM)	ΔP (Psi)	Demands (GPM)	ΔP (Psi)	Demands (GPM)	ΔP (Psi)
290	343	N/A	343	-6.28	343	-11.06	343	-15.82
291	218	-27.61	314	-7.26	314	-12.28	314	-17.28
292	271	N/A	271	-7.20	271	-12.21	271	-17.22
293	406	N/A	406	-4.94	406	-9.46	406	-14.00
294	234	5.00	234	13.33	234	12.71	234	12.09
353	561	4.18	561	8.00	561	6.14	561	4.29
361	N/A	9.43	475	13.19	475	12.47	475	11.75
369	542	0.40	542	8.55	542	6.79	542	5.03
376	N/A	N/A	1365	7.29	1365	5.36	1365	3.44
383	N/A	5.20	303	13.39	303	12.73	303	12.07
384	66	7.22	66	12.24	66	11.31	66	10.39
385	904	N/A	904	5.04	904	2.78	904	0.54
386	1,635	-9.76	1635	4.51	1635	2.06	1635	-0.39
387	N/A	N/A	665	8.03	665	6.21	665	4.39
391	842	N/A	842	7.76	842	6.06	842	4.34
394	349	N/A	349	-4.73	349	-9.16	349	-13.60
398	528	-4.30	528	4.87	528	2.49	528	0.12
400	241	-14.00	241	1.84	241	-1.19	241	-4.21
401	182	N/A	182	2.05	182	-0.93	182	-3.90
402	119	-14.34	119	-4.26	119	-8.72	119	-13.18
403	170	N/A	170	-4.18	170	-8.62	170	-13.08
404	198	N/A	198	-5.47	198	-10.17	198	-14.89
405	175	N/A	175	-8.98	175	-14.47	175	-19.98
406	95	N/A	193	-8.45	193	-13.84	193	-19.23
407	171	N/A	171	-6.56	171	-11.42	171	-16.28
408	167	N/A	167	-5.68	167	-10.57	167	-15.44
409	152	N/A	152	-5.61	152	-10.47	152	-15.32
410	133	N/A	133	-7.97	133	-13.49	133	-19.02

411	126	N/A	126	-7.68	126	-13.15	126	-18.59
412	301	N/A	301	7.34	301	5.40	301	3.46
413	278	N/A	278	3.38	278	0.65	278	-2.09
414	N/A	N/A	223	2.91	223	-0.06	223	-3.04
415	277	N/A	277	3.08	277	0.30	277	-2.47
419	175	N/A	175	13.01	175	12.21	175	11.40
420	N/A	N/A	247	14.11	247	13.57	247	13.03
424	N/A	N/A	101	5.37	101	2.87	101	0.39
425	150	-12.84	155	4.18	155	1.48	155	-1.22
426	574	N/A	574	11.05	574	10.08	574	9.11
429	79	N/A	147	5.40	147	2.78	147	0.16
430	125	-8.40	125	8.45	125	6.61	125	4.77
432	N/A	N/A	226	6.10	226	3.90	226	1.70
433	273	N/A	748	-0.14	748	-3.33	748	-6.51
434	N/A	N/A	657	4.35	657	1.85	657	-0.65
435	300	5.25	300	13.88	300	13.26	300	12.64
436	691	N/A	691	14.13	691	13.66	691	13.19
438	500	N/A	500	11.12	500	10.07	500	9.02
439	N/A	N/A	300	11.66	300	10.68	300	9.69
440	2,700	-15.00	418	4.91	418	2.48	418	0.06
441	341	-15.00	341	1.10	341	-1.94	341	-4.97
442	385	N/A	385	4.87	385	2.45	385	0.03
443	N/A	-6.90	1098	1.86	1098	-1.03	1098	-3.92
444	756	N/A	756	2.43	756	-0.48	756	-3.39
445	N/A	N/A	290	2.54	290	-0.26	290	-3.07
447	431	N/A	431	5.03	431	2.61	431	0.18
448	140	-19.00	140	-5.81	140	-10.82	140	-15.82
449	625	-15.22	625	6.54	625	4.63	625	2.72
450	471	-22.51	471	-6.83	471	-12.04	471	-17.24
454	926	-6.44	926	10.89	926	9.75	926	8.61
456	N/A	N/A	185	12.07	185	11.14	185	10.21
457	N/A	N/A	71	2.31	71	-0.55	71	-3.39
461	488	-0.95	152	7.46	152	5.45	152	3.45
462	N/A	N/A	600	13.80	600	13.19	600	12.57
463	214	N/A	214	10.51	214	9.22	214	7.94
465	97	0.78	97	11.96	97	10.98	97	10.00
467	461	N/A	461	7.31	461	5.49	461	3.67
470	N/A	N/A	173	1.18	173	-2.18	173	-5.55
471	216	N/A	216	3.55	216	0.87	216	-1.81
472	N/A	N/A	195	2.41	195	-0.38	195	-3.16
473	N/A	N/A	249	2.50	249	-0.28	249	-3.06
474	N/A	N/A	147	10.56	147	9.24	147	7.94
476	N/A	N/A	301	1.83	301	-1.48	301	-4.79
477	494	N/A	494	5.05	494	2.62	494	0.17
478	N/A	N/A	88	7.32	88	5.35	88	3.38
480	N/A	N/A	172	14.21	172	13.66	172	13.09

481	N/A	N/A	59	12.37	59	11.37	59	10.38
482	N/A	N/A	83	14.36	83	13.82	83	13.27
483	429	N/A	429	4.44	429	1.60	429	-1.24
492	N/A	N/A	270	6.97	270	4.93	270	2.87
495	N/A	2.81	433	15.37	433	15.10	433	14.83
499	72	N/A	219	15.27	219	15.00	219	14.72
506	184	N/A	184	4.73	184	2.19	184	-0.35
511	N/A	N/A	331	3.86	331	1.10	331	-1.66
512	58	N/A	30	13.38	30	12.75	30	12.13
513	458	-5.97	458	5.06	458	2.76	458	0.46
514	N/A	N/A	96	9.60	96	8.01	96	6.43
516	97	N/A	181	3.24	181	0.40	181	-2.45
518	859	N/A	1784	6.69	1784	4.65	1784	2.61
520	460	N/A	460	13.30	460	12.69	460	12.09
521	1,264	-8.34	1264	7.47	1264	5.55	1264	3.63
524	935	5.91	935	5.69	935	3.63	935	1.56
548	428	N/A	428	12.25	428	11.38	428	10.51
549	N/A	N/A	381	10.73	381	9.51	381	8.29
550	280	N/A	280	10.80	280	9.63	280	8.46
652	380	N/A	380	6.27	380	4.07	380	1.88
653	460	N/A	460	6.24	460	4.10	460	1.96
682	761	N/A	761	4.33	761	1.81	761	-0.69
740	N/A	N/A	171	6.38	171	4.33	171	2.29
1400	N/A	N/A	28	-3.41	28	-7.69	28	-11.95
1401	N/A	N/A	41	-8.61	41	-14.11	41	-19.60
1406	N/A	N/A	42	-31.70	42	-42.91	42	-54.11
1407	N/A	N/A	41	-22.40	41	-31.17	41	-39.94
1410	N/A	N/A	41	-16.40	41	-23.82	41	-31.23
1411	N/A	N/A	28	-10.88	28	-17.00	28	-23.10
1412	N/A	N/A	16	6.67	16	4.56	16	2.46
3671	211	N/A	609	8.69	609	7.03	609	5.37
3672	953	8.40	953	7.60	953	5.86	953	4.12
4461	589	6.86	589	12.03	589	11.10	589	10.16
4462	341	2.60	730	11.70	730	10.74	730	9.78
4531	339	3.00	339	13.16	339	12.48	339	11.78
4532	226	6.25	226	13.25	226	12.54	226	11.82
4681	N/A	N/A	1485	-0.64	1485	-4.35	1485	-8.06
4682	N/A	N/A	1218	-2.34	1218	-6.30	1218	-10.26
4683	704	N/A	704	3.94	704	1.31	704	-1.30
4841	N/A	N/A	861	6.89	861	4.93	861	2.99
4842	N/A	N/A	1711	6.65	1711	4.72	1711	2.79
4901	N/A	N/A	198	10.17	198	8.85	198	7.53
4902	N/A	N/A	388	10.62	388	9.45	388	8.29

Table A - 6 Simulation Results of Sensitivity Study by Adjusting Demand Distribution

NODE #	Measured		Init. Sim.		Scenario 1		Scenario 2	
	Demands (GPM)	ΔP (Psi)	Demands (GPM)	ΔP (Psi)	Demands (GPM)	ΔP (Psi)	Demands (GPM)	ΔP (Psi)
290	343	N/A	343	-6.28	343	-6.26	343	-6.55
291	218	-27.61	314	-7.26	329	-7.30	331	-7.60
292	271	N/A	271	-7.20	271	-7.21	271	-7.51
293	406	N/A	406	-4.94	406	-4.87	406	-5.15
294	234	5.00	234	13.33	234	13.12	234	13.11
353	561	4.18	561	8.00	561	8.16	561	8.14
361	N/A	9.43	475	13.19	497	13.00	485	12.98
369	542	0.40	542	8.55	542	8.33	542	8.33
376	N/A	N/A	1365	7.29	1429	7.46	1392	7.46
383	N/A	5.20	303	13.39	317	13.23	309	13.20
384	66	7.22	66	12.24	66	12.18	66	12.09
385	904	N/A	904	5.04	904	5.14	904	5.16
386	1,635	-9.76	1635	4.51	1635	4.62	1635	4.63
387	N/A	N/A	665	8.03	696	8.11	678	8.14
391	842	N/A	842	7.76	842	7.87	842	7.87
394	349	N/A	349	-4.73	349	-4.65	349	-4.94
398	528	-4.30	528	4.87	528	5.09	528	5.05
400	241	-14.00	241	1.84	241	1.98	200	1.13
401	182	N/A	182	2.05	182	2.19	200	1.17
402	119	-14.34	119	-4.26	119	-4.17	200	-8.88
403	170	N/A	170	-4.18	170	-4.09	200	-7.83
404	198	N/A	198	-5.47	198	-5.40	200	-9.30
405	175	N/A	175	-8.98	175	-8.97	200	-13.68
406	95	N/A	193	-8.45	202	-8.75	200	-12.26
407	171	N/A	171	-6.56	171	-6.55	200	-10.63
408	167	N/A	167	-5.68	167	-5.64	200	-9.77
409	152	N/A	152	-5.61	152	-5.56	200	-9.72
410	133	N/A	133	-7.97	133	-7.88	200	-15.10
411	126	N/A	126	-7.68	126	-7.60	200	-15.06
412	301	N/A	301	7.34	301	7.06	301	7.05
413	278	N/A	278	3.38	278	2.95	278	2.91
414	N/A	N/A	223	2.91	233	2.38	235	2.32
415	277	N/A	277	3.08	277	2.71	277	2.67
419	175	N/A	175	13.01	175	13.17	175	13.19
420	N/A	N/A	247	14.11	258	13.83	260	13.80
424	N/A	N/A	101	5.37	106	4.98	107	4.97
425	150	-12.84	155	4.18	155	3.98	155	3.96
426	574	N/A	574	11.05	574	10.84	574	10.84
429	79	N/A	147	5.40	154	4.56	155	4.45
430	125	-8.40	125	8.45	125	8.26	125	8.24

432	N/A	N/A	226	6.10	237	6.28	231	6.28
433	273	N/A	748	-0.14	783	-0.28	788	-0.54
434	N/A	N/A	657	4.35	688	4.11	670	4.32
435	300	5.25	300	13.88	300	14.06	300	14.06
436	691	N/A	691	14.13	691	14.15	691	14.15
438	500	N/A	500	11.12	500	11.64	500	11.66
439	N/A	N/A	300	11.66	314	11.43	306	11.45
440	2,700	-15.00	418	4.91	437	5.13	426	4.89
441	341	-15.00	341	1.10	341	1.12	341	0.90
442	385	N/A	385	4.87	385	5.11	385	4.85
443	N/A	-6.90	1098	1.86	1148	1.78	1119	1.88
444	756	N/A	756	2.43	756	3.56	756	3.40
445	N/A	N/A	290	2.54	304	2.53	296	2.59
447	431	N/A	431	5.03	431	5.27	431	5.01
448	140	-19.00	140	-5.81	140	-5.79	140	-9.58
449	625	-15.22	625	6.54	625	6.62	625	6.58
450	471	-22.51	471	-6.83	471	-6.81	471	-10.61
454	926	-6.44	926	10.89	926	10.70	926	10.70
456	N/A	N/A	185	12.07	193	12.02	188	11.96
457	N/A	N/A	71	2.31	74	2.28	72	2.36
461	488	-0.95	152	7.46	159	6.72	155	7.04
462	N/A	N/A	600	13.80	600	13.97	600	13.98
463	214	N/A	214	10.51	214	10.56	214	10.52
465	97	0.78	97	11.96	97	11.94	97	11.88
467	461	N/A	461	7.31	461	7.38	461	7.34
470	N/A	N/A	173	1.18	181	3.37	177	3.66
471	216	N/A	216	3.55	216	4.25	216	4.10
472	N/A	N/A	195	2.41	204	2.39	199	2.45
473	N/A	N/A	249	2.50	249	2.57	249	2.58
474	N/A	N/A	147	10.56	154	10.08	150	10.24
476	N/A	N/A	301	1.83	315	1.98	307	2.43
477	494	N/A	494	5.05	494	5.33	494	5.30
478	N/A	N/A	88	7.32	88	7.58	88	7.54
480	N/A	N/A	172	14.21	180	14.36	176	14.38
481	N/A	N/A	59	12.37	62	12.36	61	12.47
482	N/A	N/A	83	14.36	87	14.45	84	14.48
483	429	N/A	429	4.44	429	4.54	429	4.54
492	N/A	N/A	270	6.97	270	7.09	270	7.09
495	N/A	2.81	433	15.37	900	13.94	900	13.94
499	72	N/A	219	15.27	230	15.29	224	15.29
506	184	N/A	184	4.73	184	4.79	184	4.75
511	N/A	N/A	331	3.86	346	3.98	337	3.94
512	58	N/A	30	13.38	32	13.17	31	13.17
513	458	-5.97	458	5.06	458	5.15	458	5.17
514	N/A	N/A	96	9.60	101	9.35	98	9.39
516	97	N/A	181	3.24	189	3.30	185	3.28

518	859	N/A	1784	6.69	1866	6.65	1819	6.74
520	460	N/A	460	13.30	460	13.12	460	13.11
521	1,264	-8.34	1264	7.47	1264	7.55	1264	7.51
524	935	5.91	935	5.69	935	5.75	935	5.75
548	428	N/A	428	12.25	428	12.06	428	12.04
549	N/A	N/A	381	10.73	398	10.36	401	10.33
550	280	N/A	280	10.80	280	10.48	280	10.45
652	380	N/A	380	6.27	380	6.02	380	6.04
653	460	N/A	460	6.24	460	6.01	460	6.02
682	761	N/A	761	4.33	761	4.41	761	4.43
740	N/A	N/A	171	6.38	179	6.44	174	6.47
1400	N/A	N/A	28	-3.41	30	-3.74	29	-4.33
1401	N/A	N/A	41	-8.61	43	-9.41	42	-9.88
1406	N/A	N/A	42	-31.70	44	-34.11	43	-36.48
1407	N/A	N/A	41	-22.40	43	-23.88	42	-26.81
1410	N/A	N/A	41	-16.40	43	-17.31	42	-20.89
1411	N/A	N/A	28	-10.88	30	-11.29	29	-15.18
1412	N/A	N/A	16	6.67	17	6.32	16	6.35
3671	211	N/A	609	8.69	637	8.31	621	8.40
3672	953	8.40	953	7.60	953	7.37	953	7.38
4461	589	6.86	589	12.03	589	11.86	589	11.84
4462	341	2.60	730	11.70	764	11.38	745	11.44
4531	339	3.00	339	13.16	339	13.03	339	12.98
4532	226	6.25	226	13.25	226	13.11	226	13.06
4681	N/A	N/A	1485	-0.64	906	6.04	906	6.09
4682	N/A	N/A	1218	-2.34	850	1.31	850	1.15
4683	704	N/A	704	3.94	704	4.64	704	4.48
4841	N/A	N/A	861	6.89	901	7.11	878	7.12
4842	N/A	N/A	1711	6.65	1492	8.15	1454	8.29
4901	N/A	N/A	198	10.17	207	10.21	202	10.23
4902	N/A	N/A	388	10.62	388	10.69	388	10.69

VITA

Name: Chen Xu

Address: 200 Charles Haltom Ave. Apt. 1H
College Station, TX 77840

Education: Shanghai Jiao Tong University
Shanghai, People's Republic of China
B. S., 1999, Mechanical Engineering

Texas A&M University
College Station, Texas, United States
M. S., 2006, Mechanical Engineering

Present Employment: Texas Engineering Experiment Station, Energy Systems Laboratory, Texas A&M University, College Station